

UC San Diego

UC San Diego Electronic Theses and Dissertations

Title

Dynamic regulation of proteasome function by neuronal activity

Permalink

<https://escholarship.org/uc/item/8786p0z8>

Author

Djakovic, Stevan Nicholas

Publication Date

2010

Peer reviewed|Thesis/dissertation

UNIVERSITY OF CALIFORNIA, SAN DIEGO

Dynamic Regulation of Proteasome Function by Neuronal Activity

A dissertation submitted in partial satisfaction of the
requirements for the degree Doctor of Philosophy

in

Biology

by

Stevan Nicholas Djakovic

Committee in charge:

Professor Gentry N Patrick, Chair
Professor Randy Hampton
Professor Alexander Hoffmann
Professor Claudio A Joazeiro
Professor Edward H Koo
Professor Yimin Zou

2010

Copyright

Stevan Nicholas Djakovic, 2010

All rights reserved.

The Dissertation of Stevan N Djakovic is approved, and it is acceptable in quality and form for publication on microfilm and electronically:

Chair

University of California, San Diego

DEDICATION

This work is dedicated to my parents for always making education a priority,
my friends for keeping me sane,
and my amazing wife Meghan for her unending love and support.

EPIGRAPH

“Laughter and tears are both responses to frustration and exhaustion. I myself prefer to laugh, since there is less cleaning up to do afterward.”

~Kurt Vonnegut

TABLE OF CONTENTS

Signature Page	iii
Dedication	iv
Epigraph	v
Table of Contents	vi
List of Figures	ix
List of Tables	xi
List of Abbreviations	xii
Acknowledgements	xiv
Vita	xviii
Abstract of the Dissertation	xx
Chapter I Introduction	1
Introduction	2
The ubiquitin proteasome system (UPS).....	2
The Proteasome	4
Regulation of the proteasome	6
UPS and neurons	7
UPS and synaptic plasticity	8
UPS and neurodegenerative disease	12
Significance and Rationale	15

Chapter II Regulation of the proteasome by neuronal activity and CaMKII ...	21
Introduction	22
Results	24
Characterization of proteasome reporters.....	24
Action potential blockade and up-regulation produce rapid and opposite effects on proteasome activity in hippocampal dendrites	25
Regulation of proteasome activity by external calcium	28
Regulation of proteasome activity by CaMKII	29
Phosphorylation of the proteasome by CaMKII.....	32
Discussion	35
Materials and methods.....	37
Acknowledgments	46
Chapter III Phosphorylation of Rpt6 regulates proteasome function and synaptic strength.....	68
Introduction	69
Results	70
Rpt6 is phosphorylated at serine 120 by CaMKII.....	70
Phosphorylation of Rpt6 regulates proteasome function	72
Phosphorylation of Rpt6 regulates synaptic strength	74
Discussion	76

Materials and methods.....	79
Acknowledgments.....	84
Chapter IV Conclusion	94
Summary	95
Regulation of the proteasome.....	97
UPS and synaptic plasticity.....	98
UPS and neurodegenerative disease.....	99
Synaptic substrates of the UPS.....	101
References	104

LIST OF FIGURES

Chapter I

Figure 1-1: The ubiquitin proteasome system	18
Figure 1-2: The 26S proteasome	19
Figure 1-3: Neuronal activity regulates the ubiquitin proteasome system	20

Chapter II

Figure 2-1: paGFPu proteasome reporter	48
Figure 2-2: Characterization of paGFPu proteasome reporter in COS7 cells	49
Figure 2-3: Expression of paGFPu in hippocampal neurons	50
Figure 2-4: Action potential blockade and up-regulation produce opposite effects on proteasome activity in hippocampal neurons.	51
Figure 2-5: Neuronal activity induces paGFPu degradation in dendritic spines.....	52
Figure 2-6: Action potential blockade and up-regulation produce opposite effects on proteasome activity in hippocampal neurons as monitored by our ubiquitin-independent proteasome reporter	53
Figure 2-7: Proteasome inhibition or action potential blockade rapidly increase ubiquitin conjugate levels in hippocampal neurons	54
Figure 2-8: TTX-mediated proteasome inhibition requires mini EPSCs	55
Figure 2-9: CaMKII is required for activity-dependent proteasome function in hippocampal neurons.....	56
Figure 2-10: CaMKII regulates <i>in vivo</i> proteasome function	57
Figure 2-11: CaMKII T286D stimulates degradation of GFPu.....	58
Figure 2-12: CaMKII regulates <i>in vitro</i> proteasome function	59
Figure 2-13: CaMKII α phosphorylates 19S/PA700	60

Figure 2-14: CaMKII α phosphorylates Rpt6, a specific subunit of 19S/PA700	61
Figure 2-15: Phosphorylation of 19S by CaMKII does not regulate proteasome function <i>in vitro</i>	62
Figure 2-16: CaMKII dependent phosphorylation of proteasome or proteasome interacting proteins <i>in vivo</i>	63
Figure 2-17: Neuronal activity induces phosphorylation of Rpt6	64

Chapter III

Figure 3-1: Rpt6 is predicted to be phosphorylated by CaMKII at serine 120	86
Figure 3-2: Rpt6 phospho-mutants incorporate into the proteasome	87
Figure 3-3: CaMKII phosphorylates S120 of Rpt6 <i>in vivo</i>	88
Figure 3-4: Phosphorylation of Rpt6 S120 is necessary for CaMKII-dependent stimulation of the proteasome	89
Figure 3-5: Localization of Rpt6 phospho-mutants in hippocampal neurons	90
Figure 3-6: Phosphorylation of S120 regulates Rpt6 triton resistance.....	91
Figure 3-7: Phosphorylation of Rpt6 S120 regulates synaptic strength.....	92
Figure 3-8: UPS activity is regulated during homeostatic plasticity.....	93

Chapter IV

Figure 4-1: Model of CaMKII-dependent regulation of the proteasome	103
--	-----

LIST OF TABLES

Chapter II

Table 2-1: paGFPu mean rates of degradation	65
Table 2-2: paGFP-odc mean rates of degradation	66
Table 2-3: Identification of Rpt6 by mass spectrometry	67

LIST OF ABBREVIATIONS

Abbreviation	Definition
'	minutes
~	approximately
³² P	Radioactive phosphorous isotope
AD	Alzheimer's Disease
AIP	autocamtide-2-related inhibitory peptide
AMPA	(+/-)- α -amino-3-hydroxy-5-methyl-4-isoxazolepropionic acid
AP	action potential
APV	2-amino-5-phosphonopentanoic acid
ATP	adenosine-5'-triphosphate
AU	arbitrary units
BHK	baby hamster kidney cell line
BIC	bicuculline
Ca ²⁺	calcium
CaMKII	calcium/calmodulin-dependent protein kinase II
CNQX	6-cyano-7-nitroquinoxaline-2,3-dione
CP	core particle (20S proteasome)
DIV	days <i>in vitro</i>
DUB	de-ubiquitinating enzyme
E3	ubiquitin-protein isopeptide ligase
IRES	internal ribosomal entry site
GFP	green fluorescent protein
HA	hemagglutinin protein tag
HEK293T	Human embryonic kidney cell line
HBS	hepes buffered saline solution
IRES	internal ribosomal entry site
LTD	long term depression
LTP	long term potentiation
LTF	long term facilitation
mCherry	monomeric cherry-red fluorescent protein
mEPSC	miniature excitatory postsynaptic current
NMDA	<i>N</i> -methyl-D-aspartate
odc	ornithine decarboxylase
pa-	photoactivatable
PD	Parkinson's Disease
PKA	Protein Kinase A
PSD	postsynaptic density
pSG	Sindbis subgenomic promoter
RP	regulatory particle (19S proteasome)
S120	Serine 120 of Rpt6
suc-LLVY-AMC	succinimyl-Leu-Leu-Val-Tyr-amidomethylcoumarin
TTX	tetrodotoxin

UPS	ubiquitin proteasome system
VGCC	voltage-gated calcium channels
vinyl sulfone	adamantane-acetyl-(6-aminohexanoyl)(3)-(leucinyl)(3)-vinyl (methyl)-sulfone;
WT	wild type

ACKNOWLEDGEMENTS

I would like to thank Gentry Patrick for being my mentor throughout my graduate career. He has been exceptionally supportive, with late nights writing ImageJ macros, to early mornings working with millimoles of radioactivity. When I started graduate school I switched from plant biology to neurobiology. Gentry was instrumental in teaching me the basics in neuroscience and mammalian cell biology techniques. He has also been instrumental in my scientific development. I truly feel honored to be Gentry's first graduate student.

I would also like to thank the members of my thesis committee, both past and present. Dr. Randy Hampton, Dr. Alexander Hoffman, Dr. Claudio Joazeiro, Dr. Edward Koo, Dr. Yimin Zou and Dr. Lisa Boulanger all provided me with invaluable discussions, direction and advice which helped me to maintain focus, learn and progress throughout my graduate career. Dr. Laurie Smith, Dr. Mary Frank and the entire Smith lab also provided me with a great research experience, teaching me valuable techniques, skills, tips and tricks. Most importantly they helped foster my love for science and research.

The Patrick lab, a small but solid core of researchers, has also been a tremendously supportive and positive environment for me during the past six years. When I first arrived we had a strong foundation. Oscar Bravo and Diana Immenhausen were instrumental in getting the lab up and running. Not only were they friendly and truly genuine people but also hard workers and solid researchers. Soon after, the “franchise players” of the lab arrived. Jeff Keil, my partner in crime, arrived

a few months after I did. Jeff has been a supporter, collaborator, advisor and friend. Despite his bad luck with experiments he was always willing to help me troubleshoot or discuss problems. Our long therapeutic walks to price center were one of the few things that helped keep me sane during my last year of graduate school. A year later, Lindsay Schwarz, another graduate student and my current office mate joined the lab. Lindsay has been a key collaborator, whose ubiquitin conjugate studies helped provide a foundation for my thesis work. Lindsay has been a great friend and a pleasure to work with. Her work ethic has also been a substantial motivation for me. I would also like to acknowledge Anna Cartier, a post-doctoral researcher who worked in the lab for two years. Her experience and expertise were a valuable resource. Additionally it was a pleasure to collaborate with her on her UCHL1 studies.

I have also been lucky enough to work with and mentor many high school, undergraduate and graduate students. Not only did they provide me with mentorship and leadership experience, teaching them helped me solidify my understanding of my own research. It was a pleasure to watch my high school students David Pardo and Ryan Ghosh grow up and develop a love of science. I would also like to thank undergraduates Lilly Flores for help with Amyloid Beta experiments, Martin Edwards for cloning help and Tania Manchenkov for help with GFPu experiments. Graduate rotation students Shamim Sinnar and Alysia Birkholz also performed key proteasome phosphorylation experiments. I also had the pleasure of mentoring a Danish graduate student Benedicte Mengel on a project that aimed to observe dynamics of ubiquitination in NF κ B signaling. Although the experiments didn't work her

optimism and friendly demeanor never wavered. Lastly I would like to thank an undergraduate, Carissa Chu whom I mentored Carissa for her undergraduate honors thesis. Carissa was instrumental in experiments studying the distribution of Rpt6 phospho-mutants in neurons. She was an excellent researcher and hard worker, and truly enjoyable to work with.

Most importantly I would like to thank my parents for raising me to be kind, honest and hardworking. My brothers Michael, Robert and Benny Lopez for being my friends through good times and bad. My mother in law Brenda for her support and wise words (and dog sitting!). NaCl for providing me with hundreds of miles of fun. My dogs for all their affection, even though they have been neglected for quite some time. Lastly, I would like to thank my wife Meghan Morris. For eight and a half years she has been my rock. In addition to wife she has taken on multiple roles: best friend, number one fan, therapist, supporter, editor, presentation critic, advisor and life coach. The list goes on, but the take home message is that, without a doubt, I couldn't have done this without her.

Chapter Two, in full, consists of the following publication:

Djakovic SN, Schwarz LA, Barylko B, DeMartino GN, Patrick GN. "Regulation of the proteasome by neuronal activity and calcium/calmodulin-dependent protein kinase II". *J Biol Chem*. 2009 Sep 25;284(39):26655-65.

I was the primary researcher of these studies and Gentry Patrick directed and supervised the research. Lindsay Schwarz assisted with ubiquitin conjugate

experiments. Barbara Barylko assisted in determining the proteasome subunit phosphorylated by CaMKII in the laboratory of George DeMartino.

Chapter Three, in full, consists of the following manuscript in preparation for submission to the *Journal of Neuroscience*:

Djakovic SN, Jakawich S, DeMartino GN, Sutton M, Patrick GN. “Phosphorylation of Rpt6 regulates the proteasome and synaptic function”.

I was the primary researcher and author under the supervision and direction of Gentry Patrick. Sonya Jakawich performed all electrophysiology, under the direction of Michael Sutton. George DeMartino assisted with proteasome work. I also wish to thank Carissa Chu for assistance with experiments.

VITA

EDUCATION

- 2010 Ph.D., Biology, University of California, San Diego
- 2003 B.S., Biology: Biochemistry and Cell Biology,
University of California, San Diego
- 1999 High school diploma, with Honors, Chino High School

WORK EXPERIENCE

- 2009 Graduate Student Advocate, STARS Summer Program
- 2001-2004 Research Assistant, University of California, San Diego

PUBLICATIONS

Djakovic SN, Jakawich S, DeMartino GN, Sutton M, Patrick GN. Phosphorylation of Rpt6 regulates the proteasome and synaptic function. (In preparation for *Journal of Neuroscience*).

Jakawich S, Nealy R, **Djakovic SN**, Patrick GN, Sutton M. The Ubiquitin Proteasome System mediates slow homeostatic changes in synaptic strength. (In review at *Journal of Neuroscience*)

Djakovic SN, Schwarz L, Barylko B, DeMartino GN, Patrick GN. Regulation of the Proteasome by CaMKII and Neuronal Activity. *Journal of Biological Chemistry*. 2009 Jul 28.

Cartier A, **Djakovic SN**, Salehi A, Wilson S, Masliah E, Patrick GN. Regulation of Synaptic Structure by the Ubiquitin C-terminal Hydrolase UCH-L1. *Journal of Neuroscience*. 2009 June 17

Kerjan G, Han E, Dube C, **Djakovic SN**, Patrick G, Baram T, Heinemann S, Gleeson J. Mice lacking doublecortin and doublecortin-like kinase 2 display altered hippocampal neuronal maturation and spontaneous seizures. *Proc Natl Acad Sci U S A*. 2009 Apr 2.

Dyachok J, Shao MR, Vaughn K, Bowling A, Facette M, **Djakovic S**, Clark L, Smith LG. Plasma membrane-associated SCAR complex subunits promote cortical F-actin accumulation and normal growth characteristics in Arabidopsis roots. *Molecular Plant*. 2008 Oct. 8

Djakovic S, Dyachok J, Burke M, Frank MJ, Smith LG. BRICK1/HSPC300 functions with SCAR and the ARP2/3 complex to regulate epidermal cell shape in Arabidopsis. *Development*. 2006 Mar;

Frank M, Egile C, Dyachok J, **Djakovic S**, Nolasco M, Li R, Smith LG. Activation of Arp2/3 complex-dependent actin polymerization by plant proteins distantly related to Scar/WAVE. *Proc Natl Acad Sci U S A*. 2004 Nov 16

TEACHING AND MENTORSHIP

Teaching Assistant, BIMM 110, Molecular Basis of Disease,
Professor William McGinnis, University of California, San Diego, 2008

Teaching Assistant, BICD 136, AIDS and Society,
Professor Cathy Gustafson-Brown, University of California, San Diego, 2007

Teaching Assistant, BIMM 101, Recombinant DNA Techniques Laboratory,
Professor Mandy Butler, University of California, San Diego, 2006

Mentor to Carissa Chu, Undergraduate Honors Thesis, 2009-2010

Mentor to David Pardo, Exploratory Work Experience Internship Program,
2004-2008

FIELDS OF STUDY

Major Field: Biology

Studies in Molecular and Cellular Neurobiology
Professor Gentry N. Patrick
University of California, San Diego

Studies in Plant Biology – Cell Biology and Genetics
Professor Laurie G. Smith
University of California, San Diego

ABSTRACT OF THE DISSERTATION

Dynamic Regulation of Proteasome Function by Neuronal Activity

by

Stevan Nicholas Djakovic

Doctor of Philosophy in Biology

University of California, San Diego, 2010

Professor Gentry N Patrick, Chair

Protein degradation via the ubiquitin proteasome system (UPS) has been shown to regulate changes in synaptic strength that underlie multiple forms of synaptic plasticity. It is plausible, therefore, that the UPS is itself regulated by synaptic activity. By utilizing live-cell imaging strategies we report the rapid and dynamic regulation of the proteasome in hippocampal neurons by neuronal activity. We find that the blockade of action potentials (APs) with tetrodotoxin (TTX) inhibited the activity of the proteasome, while the up-regulation of APs with bicuculline (BIC) dramatically increased the activity of the proteasome. In addition the regulation of the proteasome is dependent upon external calcium entry, in part through N-methyl-D-aspartate (NMDA) receptors and L-type voltage gated calcium channels (VGCCs),

and requires the activity of calcium/calmodulin-dependent protein kinase II (CaMKII). Using *in vitro* and *in vivo* assays we find that CaMKII stimulates proteasome activity and directly phosphorylates Rpt6, a subunit of the 19S (PA700) subcomplex of the 26S proteasome. Our data provide a novel mechanism whereby CaMKII may regulate the proteasome in neurons to facilitate remodeling of synaptic connections through protein degradation.

We next aimed to further elucidate how phosphorylation of Rpt6 regulates proteasome function in neurons. Using a phospho-specific antibody we showed that Rpt6 is phosphorylated at Serine 120 (S120) in a CaMKII-dependent fashion. While phosphorylation of this site is not sufficient to regulate proteasome activity, it is necessary for CaMKII-dependent stimulation of the proteasome. Interestingly we find that phosphorylation of S120 promotes detergent resistance of Rpt6, presumably by tethering the proteasome to the actin cytoskeleton at postsynaptic compartments. Additionally, electrophysiology experiments suggest that this phosphorylation event is important for proteasome dependent synaptic remodeling. Specifically, a phospho-mimetic Rpt6 S120 mutant leads to a decrease in miniature excitatory postsynaptic current (mEPSC) amplitude, while a phospho-dead mutant causes an increase in mEPSC amplitude. Together this data suggests that CaMKII-dependent phosphorylation of Rpt6 at S120 is an important regulator of proteasome function and UPS dependent synaptic remodeling.

Chapter I

Introduction

Introduction

The selective strengthening or weakening of synaptic connections in the central nervous system (CNS), commonly known as synaptic plasticity, is a fundamental mechanism for the storage and processing of information in the brain. This process is accompanied by the dramatic structural remodeling of the postsynaptic density (PSD), a specialized biochemical compartment consisting of neurotransmitter receptors, scaffold proteins and signaling molecules. Such plasticity is thought to be controlled by activity-dependent modifications of the molecular composition and signaling properties of the PSD [1]. Indeed, the incorporation of newly synthesized proteins is required for long lasting changes in synaptic efficacy [2,3]. Protein degradation, on the other hand, provides an additional mechanism to modify the stoichiometry of synaptic proteins to promote, limit, or restrict plasticity. It has become increasingly evident that the ubiquitin proteasome system (UPS) plays an integral role in the formation, maintenance, and remodeling of synaptic connections in the nervous system. Moreover, protein degradation via the UPS has been shown to regulate changes in synaptic strength which underlie multiple forms of synaptic plasticity [4]. While it is known that many UPS components are present at synapses and play important roles in synaptic function, information of how the UPS may respond to and be regulated by neuronal activity is not well understood.

The ubiquitin proteasome system (UPS)

The UPS is a major pathway for protein turnover in eukaryotic cells. The selective degradation of proteins via the UPS involves three steps: recognition of the target protein via specific signals, marking of the target protein with ubiquitin chains, and delivery of the target protein to the 26S proteasome, a multi-subunit protein complex that degrades the ubiquitinated proteins. Protein modification via the covalent attachment of ubiquitin is one of the most common regulatory processes in mammalian cells. Ubiquitination is a process whereby target proteins can be marked for degradation by the proteasome. It is a multi-step enzymatic process, using three classes of enzymes (E1s, E2s, and E3s), and involves the sequential transfer of ubiquitin from these enzymes to a lysine residue on the target protein (Figure 1-1). Ubiquitin, a 76 amino acid protein, is first activated. This activation is catalyzed by the ubiquitin-activating enzyme (E1) in an ATP-dependent reaction in which the C terminal glycine residue of ubiquitin binds to the active-site cysteine of an E1 in a thioester linkage. The activated ubiquitin is then transferred to a ubiquitin-conjugating enzyme (E2). Finally, a ubiquitin ligase (E3) catalyzes the attachment of ubiquitin to a lysine of the specified substrate [5]. While there are many known E2s (~100), there is an exceptionally large amount of E3s (~1000), which are essential for conferring substrate specificity [6]. Each E3 pairs up with one or more E2 to recognize a set of substrates that share one or more signals for ubiquitination [5].

Similar to how phosphatases make the phosphorylation reaction reversible, deubiquitinating enzymes (DUBs) can reverse the ubiquitination reaction. DUBs are cysteine proteases that generate free usable ubiquitin from a number of sources

including ubiquitin-protein conjugates, ubiquitin-adducts, and ubiquitin precursors. DUBs have multiple functions, including maintenance of the free ubiquitin pool and preventing protein degradation. DUBs also trim down ubiquitin chains from poly- to mono-ubiquitin, a process also known as chain editing, to ensure that the proper ubiquitin-dependent signal is activated. Interestingly, ubiquitination and phosphorylation have commonalities: both occur rapidly, often in response to extracellular signals, and both are quickly reversed, and often cooperate in mobilizing a particular cellular pathway [7]. Ubiquitination is most commonly associated with protein degradation by the 26S proteasome; however, it is also known that ubiquitination is involved in non-degradative and proteasome-independent pathways such as the endocytosis of integral membrane proteins. Additionally ubiquitination has been shown to regulate protein location, interactions and activity [8].

The proteasome

Degradation of poly-ubiquitinated protein substrates is carried out by the 26S proteasome. The 26S proteasome is a large energy-dependent protease consisting of two multi-protein subcomplexes: the 20S core and 19S cap (also known as PA700). The 20S core particle (CP) consists of 28 α and β subunits. 19S regulatory cap particle (RP) consists of Rpt (ATPase) and Rpn (non-ATPase) regulatory subunits (Figure 1-2)[9]. The 20S CP, consisting of 28 subunits (α and β), is a barrel-like structure that contains the proteolytic components of the proteasome. The barrel of the CP is formed by four stacked heptameric rings. The inner two rings each consist

of β 1- β 7 subunits, while the outer two rings each contain α 1- α 7 subunits. Only the β subunits have peptidase activity, including: chymotrypsin-like, trypsin-like, and caspase-like activities [10].

The 19S RP is a multi-functional protein complex essential for the degradation of ubiquitinated proteins. The 19S has two distinct functional components: the “base” consisting mainly of Rpt6 ATPase subunits, and the “lid” consisting mainly of Rpn non-ATPase subunits [11]. The base consists of a hetero-hexameric ring of Rpt (1-6) subunits. All six Rpt proteins have the same two functional domains: an N-terminus coiled-coil domain important for complex formation, and a C-terminus ATPase domain which is involved in ATP-dependent substrate unfolding. In addition to protein unfolding, the Rpt proteins are critical for opening of the CP, and translocation of the unfolded substrates into the CP to be degraded [12]. Recent evidence also suggests that Rpt subunits initiate 26S assembly by binding 20S CP and recruiting the remaining 19S subunits for full complex formation [13,14]. The main functions of the 19S lid components are binding of ubiquitinated substrates and removal of the ubiquitin from the substrate. Initial targeting of the substrates to the proteasome is accomplished through the recognition of the polyubiquitin chain by the non-ATPase Rpn subunits of the 19S cap. Ubiquitin chain binding is mediated by the ubiquitin-interaction motifs (UIM). Rpn10 is a specific subunit with two UIMs that binds ubiquitin chains of four or more [15]. The 19S lid also has several DUB activities. Some of these DUBs have been shown to be involved in chain editing, acting as a checkpoint to prevent degradation of substrates that should only be mono-

ubiquitinated [16]. Additionally, some DUBs are critical for removing all ubiquitin proteins from substrates, returning the ubiquitin to the free-ubiquitin pool. This is critical for maintaining cellular ubiquitin homeostasis [7].

Regulation of the proteasome

Despite the extensive studies on its structure and function [17], relatively little is known about the regulation of the proteasome. Most studies relating to regulation have focused on the interaction of regulatory proteins with the proteasome. Indeed, multiple chaperone proteins have been shown to be critical for regulating the assembly of 19S and 20S subcomplexes, and the 26S complex [18,19]. The proteasome has also been shown to be regulated by non-19S protein subcomplexes. The 11S regulator (REG) complex binds in place of the 19S, and activates the cleavage of non-ubiquitinated antigen peptides [20]. This complex regulates cleavage of antigen peptides, aiding the cell in presentation of antigens for immune system detection [21]. The PA200 activator complex, which can also replace the 19S, activates hydrolysis of unfolded peptides and has been shown to be involved in DNA repair [22]. Interestingly, the proteasome can form a hybrid complex, in which a 20S CP is capped at one end with a 19S RP, and at the other end with a PA200 or 11S complex [23,24].

Recent evidence has suggested an important role for post-translational modifications in regulation of the proteasome. Phosphorylation, a versatile method for dynamically regulating protein activity, has been shown to extensively regulate ubiquitination of substrates by mediating interaction with, or activity of E3 ligases

[25]. It is therefore likely that the activity of the proteasome may also be regulated in tandem by phosphorylation. Several studies have reported phosphorylation of both 20S and 19S proteasome subunits [26,27,28,29,30,31,32,33]. These modifications have been implicated in regulation of assembly [26,31] and proteolytic activity [33,34] of the proteasome. Protein Kinase A (PKA) has been reported to be a main regulator of proteasome function by phosphorylation of both 19S and 20S subunits [32,34,35]. PKA is a cAMP activated kinase that is involved in many cellular processes including synaptic plasticity [36]. In addition to phosphorylation, the proteasome has also been shown to be extensively modified by glycosylation [37]. Addition of O-GlcNAc to the 19S has been shown to inhibit activity of the proteasome [38]. Together, these modifications allow for the dynamic regulation of protein turnover by the proteasome.

UPS and neurons

The UPS plays a major role in many biological processes, including the regulation of the cell cycle; cancer and cell survival; DNA repair, growth, and differentiation; inflammatory and immune responses; and misfolded protein and ER-associated degradation. In neurons, most studies of UPS function have focused on impairment of the UPS in neurodegenerative disease such as Alzheimer's disease (AD) and Parkinson's disease (PD). In some cases, such as seen in AD and PD, genetic abnormalities of the UPS can be directly linked to these diseases [39]. The implications for disease suggest that the UPS is essential for normal neuronal function.

Indeed, the UPS is involved in multiple neuronal functions including brain development, axon outgrowth, synaptic development, and synaptic plasticity [4]. Spatially and temporally regulated degradation of substrates is critical for the directed growth of neurons and their axons [40,41]. Extensive work has been studying the role of the UPS in the formation, growth and elimination of synapses. *Fat facets*, a DUB, and *Highwire*, an E3, act antagonistically in their control of the growth of synapses at the neuromuscular junction of *Drosophila* [42].

UPS and synaptic plasticity

One of the first connections between UPS function and synaptic plasticity came from studies in Aplysia. Sensory-to-motor neuron synapses in Aplysia undergo a form of plasticity known as facilitation. This facilitation is presynaptic in nature and requires the action of a cAMP-dependent protein kinase (PKA) for both short-term and long-term facilitation (LTF). LTF is completely blocked by inhibitors of the proteasome [43]. The UPS regulates LTF by controlling the ratio of catalytic (C) and regulatory (R) subunits of PKA. The C subunits remain constant but the R subunits are decreased during LTF due to UPS-mediated degradation of the R subunit [44]. In addition, a neuronal specific ubiquitin C-terminal hydrolase (Ap-Uch) was identified as an immediate-early gene product essential for LTF in Aplysia. This protein associates with the proteasome to increase proteasome activity, presumably by de-ubiquitinating proteins prior to their delivery to the proteasome barrel. Disruption of Ap-Uch function substantially impairs LTF in Aplysia [45]. Therefore, activity-

dependent transcription is coupled to increased proteasome function in order to ensure the degradation of protein substrates that block the formation of long-term memory storage.

Long-term potentiation (LTP), and its opposing process, long-term depression (LTD), are considered the major cellular mechanisms which underlie learning and memory [46]. This process is accompanied by modifications in synaptic strength, controlled in part by the insertion or removal of alpha-amino-3-hydroxy-5-methyl-4-isoxazolepropionic acid (AMPA) receptors from the postsynaptic membrane [47]. Both LTP and LTD are significantly impaired by pharmacological inhibition of the proteasome. This suggests that either ongoing or activated protein degradation required for plasticity is blocked by proteasome inactivation. For instance, the activity of the proteasome is required for induction and maintenance of LTP in hippocampal slices [48,49]. Interestingly, there appears to be a strict balance between new protein synthesis and protein degradation via the proteasome. While the application of protein synthesis inhibitors or proteasome inhibitors alone block LTP, the application of these drugs together, occludes the affect of each other as LTP is unaltered [48]. These studies highlight the idea that the relative concentration of key synaptic proteins can be rate-limiting for long-lasting changes in synaptic efficacy. Proteasome inhibition was also found to block N-methyl-D-aspartate (NMDA) and mGluR-dependent synaptic depression [50,51,52]. Interestingly, Colledge et al., 2003 found that the PDZ binding domain protein, PSD-95, is rapidly ubiquitinated in response to NMDA

receptor activation, and mutations in PSD-95 which attenuates its degradation also block NMDA-induced AMPA receptor internalization [50].

The UPS is critical for presynaptic and postsynaptic function, as demonstrated by studies showing the significant defects caused by pharmacological inhibition of the proteasome. In *Aplysia*, synaptic strength has been shown to be locally regulated by the UPS. Proteasome inhibition increased the number of synaptic contacts, neurite length, and the amplitude of glutamate-evoked postsynaptic potentials [53]. In cultured hippocampal neurons, the size of the recycling vesicle pool at the presynaptic terminal is dramatically increased after 2 hours of proteasomal blockade [54]. In hippocampal slices, proteasome inhibition increases the frequency of miniature excitatory postsynaptic currents (mEPSCs). Interestingly, this increase is largely abolished in animals that lack SCRAPPER, an E3 enzyme that is localized to the presynaptic membrane. SCRAPPER was found to degrade RIM1, a Ca²⁺-dependent vesicle priming factor which highlights a key role for the UPS in presynaptic function [55].

In *C. elegans* both ubiquitination of glutamate receptors and proteasomal degradation of other synaptic proteins have been shown to regulate the glutamate receptor internalization and synaptic abundance [56,57,58]. It was demonstrated that proteasomal inhibition blocked the internalization of both GluR1 and GluR2 (two subunits of mammalian AMPA receptors) in hippocampal neurons. In addition, expression of an ubiquitin chain-elongation mutant (ubiquitin K48R) also blocked GluR1 and GluR2 endocytosis [59]. One hypothesis drawn from this data is that

proteasomal degradation of components of the AMPA receptor complex or other closely associated proteins is acutely required for GluR endocytosis. Indeed, Colledge et al. (2003), described such a proteasomal/target model, where the PDZ binding domain protein, PSD-95, is rapidly ubiquitinated in response to NMDA receptor activation, and mutations in PSD-95 which attenuates its degradation also block NMDA-induced AMPA receptor internalization [50].

The first E3 ligase to be implicated in synaptic plasticity in mammals is Ube3A (also referred to as E6-AP). E6-AP was the first member of the ubiquitin ligase HECT domain E3 family to be identified [60]. Mutations in the *Ube3A* gene are the cause of Angelman's Syndrome (AS), a human hereditary disease that results in mental retardation, seizures, abnormal gut, tremor and ataxia [61]. The E6-AP knockout mouse has reduced LTP and context dependent learning, similar to defects also seen in AS patients [62]. It has been recently reported that E6-AP regulates activity-dependent synapse development by controlling degradation of Arc, and important synaptic signaling molecule. Disruption of E6-AP function leads to overexpression of Arc and a downregulation of synaptic AMPA receptor levels, an event thought to contribute to the cognitive dysfunction observed in AS [63].

It has been well documented that the modifications in synaptic efficacy is accompanied by changes in the protein composition of synapses. These changes could arise by the incorporation of newly synthesized proteins or by the selective destabilization and removal of existing proteins. Indeed, some of the earliest work has shown that protein synthesis inhibitors cause memory impairment [64]. Interestingly,

it is the retention of memory that is most affected by protein synthesis inhibitors. For instance, the retrieval of fear memory in mice is blocked injection of protein synthesis inhibitors in the hippocampus [65,66,67]. Strikingly, however, it was recently shown that co-injection of lactacystin (a potent proteasome inhibitor) completely rescued the anisomycin-induced fear memory impairments [68]. This highlights the importance UPS-mediated protein degradation in the maintenance of new memories.

Furthermore, it indicates that a finely-tuned balance between protein synthesis and protein degradation must be engaged to facilitate the remodeling of synapses which underlies synaptic plasticity.

UPS and neurodegenerative disease

Although UPS dysfunction has been linked to neurodegenerative disease for years, many questions still remain. The molecular mechanisms underlying UPS dysfunction are still unclear, and it is still unknown whether the dysfunction is causative for or a result of the disease. Dysfunction of the proteasome has been implicated, either as a primary cause or secondary consequence, in the pathogenesis of both inherited and acquired neurodegenerative disorders such as Parkinson's disease (PD), Alzheimer's disease (AD), Huntington's disease (HD), amyotrophic lateral sclerosis (ALS) and others[39]. Despite being quite distinct diseases, each of these clinically separate neurodegenerative disorders share common neuropathological features. Collectively, these diseases are now considered 'proteinopathies' of the nervous system, characterized by accumulation of misfolded protein aggregates that

are resistant to degradation. Ubiquitinated proteins are found in these pathological aggregates, which include plaques and tangles in AD, Lewy bodies in PD and polyQ inclusion bodies in HD [69,70,71]. Interestingly, proteasomes are commonly found in ubiquitin-positive aggregates in postmortem brains which suggest proteins in the aggregates are marked for degradation but not efficiently removed [71]. In dementia with Lewy Bodies (DLB) and PD patients, it was found that the ubiquitin chain length on α -synuclein was limited to between one and three ubiquitins [72], which suggest it is inefficiently targeted to the proteasome as ubiquitin chain lengths of four or more are required for recognition and degradation by the proteasome. Proteasome activity is substantially decreased in many of these disorders [73]. So UPS dysfunction may be due to an increased load of misfolded proteins and protein aggregates and inability to recognize and degrade them, although it is still unclear if this contributes to the disease pathogenesis.

A large majority of understanding about UPS dysfunction in neurodegenerative disease has come from the identification of genes linked to familial and sporadic forms of PD. PD is a movement disorder characterized by selective degeneration of dopaminergic neurons in the substantia nigra [74]. Ten genetic loci responsible for rare Mendelian forms of PD have been identified by linkage analysis [75]. Of the genes cloned, two are components of the UPS. *PARK2* encodes for Parkin, an E2-dependent E3 ligase [76,77]. There is limited knowledge about substrates for Parkin, although recent evidence suggests its activity may be involved in aggresome formation and autophagy [78]. *PARK2* mutations, which appear to be loss-of-function [76],

cause early onset PD with loss of dopaminergic neurons in the substantia nigra in the absence of Lewy bodies [79]. Genetic association of *PARK5* with familial and sporadic PD provides some additional clues about UPS dysfunction. *PARK5* encodes for UCH-L1, a DUB critical for maintaining neuronal mono-ubiquitin levels which has been found in Lewy bodies [80]. A spontaneous mutation in UCH-L1 is also found in mice with neurodegenerative ataxia. These mice, called *gracile axonal dystrophy (gad)*, exhibit retrograde accumulation of β -amyloid aggregates but not α -synuclein aggregates in the gracile tract axons [81,82]. Since UCH-L1 is thought to help maintain monomeric ubiquitin levels in neurons, the deposition of aggregate-prone proteins could be a secondary effect [83,84].

Inhibition of the proteasome has also been associated with many neurodegenerative disorders, including AD, PD, HD and ALS. AD is commonly characterized by progressive memory loss and accumulation of neurofibrillary tangles (NFT) and extracellular senile plaques mainly consisting of $A\beta$ peptides [85]. These plaques are thought to contribute to the neuronal loss seen in late stages of AD. However, an emerging view is that synaptic dysfunction is an earlier event and is a key pathogenic factor in AD [86,87]. The molecular mechanisms underlying $A\beta$ induced synaptic dysfunction still remain unclear though. Inhibition of the proteasome has been observed both in brains of transgenic AD disease models and in hippocampal cultures treated with $A\beta$ peptides [88,89]. Recent evidence has shown that inhibition of the proteasome leads to dramatic defects in synaptic plasticity

[48,49,50]. It is predicted that inhibition of the proteasome may be involved in the synaptic defects commonly found in AD.

The big question, however, is how UPS dysfunction is related to the pathogenesis of these neurodegenerative diseases. Is the etiology of these diseases a consequence of altered UPS function? Ubiquitin positive protein aggregate formation is a hallmark of many of these diseases. It is still unclear whether formation of these aggregates is a result or cause of alterations in UPS function. Indeed, data suggest that aggregated proteins are detrimental to the neuron and inhibit the UPS, while consolidation of aggregates into inclusion bodies may be protective [90,91]. UPS dysfunction may also be unrelated to protein aggregates. Key components of the UPS are themselves regulated by synaptic activity which suggests that altered neuronal signaling during pathogenesis may directly contribute to global UPS dysfunction. Therefore neuronal activity and UPS function are likely dynamically intertwined to control the protein stoichiometry of synapses in normal neuronal physiology and neurodegenerative disease.

Significance and rationale

In vertebrates, changes in the composition of the postsynaptic density (PSD) are regulated by synaptic activity. These changes are bidirectional and require the activity of the UPS [92,93]. It is quite plausible that neuronal activity regulates UPS function to dynamically control synaptic protein composition. Regulated proteolysis by the UPS has been typically studied at the level of the ubiquitination. However,

there are hundreds of ubiquitin ligases identified, and thousands predicted in the mammalian genome. Therefore, mapping E3–substrate relationships remains a difficult task in all cell types. This is even more evident in neurons, as the distribution of UPS components in functionally distinct compartments is likely regulatory for their function. For instance, subcellular regulation a SCF-type E3 complex in flies contributes to precise synaptic connectivity through selective synapse elimination [94]. However, the proteasome itself is also dynamic in nature. For instance, subunit composition, core association with regulatory cap complexes, and interactions with accessory proteins have all been shown to control the specificity and activity of the proteasome [95,96,97,98]. Furthermore, there is a growing body of literature that indicates proteasomes to be modified by post-translational events such as phosphorylation [28,32]. Recently, it was shown that proteasomes rapidly redistribute from dendritic shaft to dendritic spine compartments in response to synaptic stimulation. This redistribution was found to be dependent upon NMDA receptor activation and CaMKII activity [99,100]. A subsequent report showed that NAC1, a cocaine regulated transcriptional protein that interacts with the proteasome, regulates the trafficking of the proteasome in an activity-dependent manner [101]. These data suggest that synaptic activity can promote the recruitment and sequestration of proteasomes to locally remodel the protein composition of synapses. However, a clear understanding of the synaptic molecular mechanisms involved to regulate proteasome trafficking and activity is far from understood.

As shown in Figure 1-3, neuronal activity may provide synaptic cues to regulate the ubiquitination and targeting of substrates to the proteasome, or by potentially regulating both the substrate ubiquitination and proteasome function. Activity-dependent regulation of ubiquitination [63,94](Figure 1-3B), and de-ubiquitination [102,103] (Figure 1-3A), are proven scenarios shown to dynamically control the turnover of proteins in neurons. Interestingly, the existence of cis-related proteasome regulatory mechanisms adds another potential layer of control over the degradation of synaptic proteins. Synchronization may facilitate greater spatial and temporal control in response to one or more synaptic cues, while antagonizing effects may fine-tune the rate of substrate degradation. Therefore we hypothesize that the proteasome complex may be regulated in tandem with ubiquitination, to enable the activity-dependent degradation of substrates in neurons (Figure 1-3C). In chapter two we investigated the activity-dependent regulation of proteasome function in neurons. In chapter three we further elucidated the underlying molecular mechanisms of proteasome regulation in neurons. Together our findings

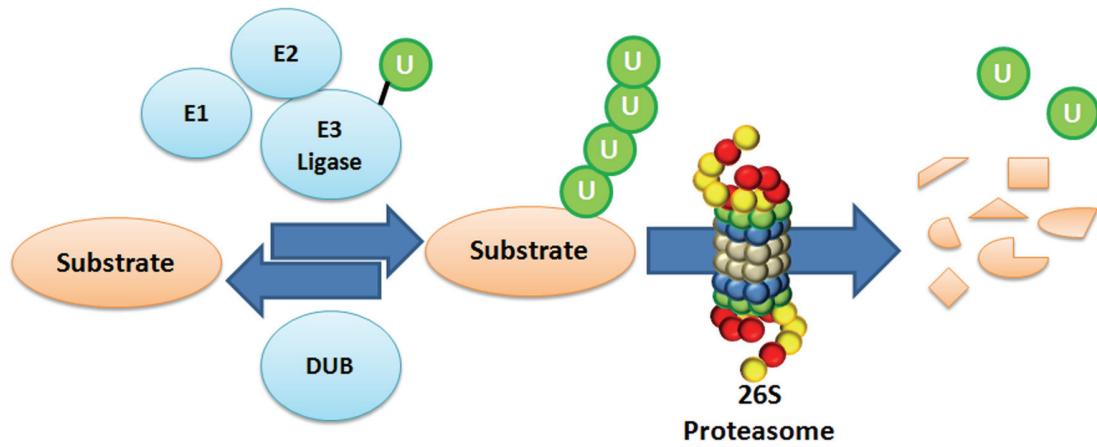


Figure 1-1: The ubiquitin proteasome system

Substrates are targeted for degradation by addition of a ubiquitin moiety. Dub enzymes can reverse this reaction. Substrates tagged with multiple ubiquitins are recognized and then degraded by the 26S proteasome.

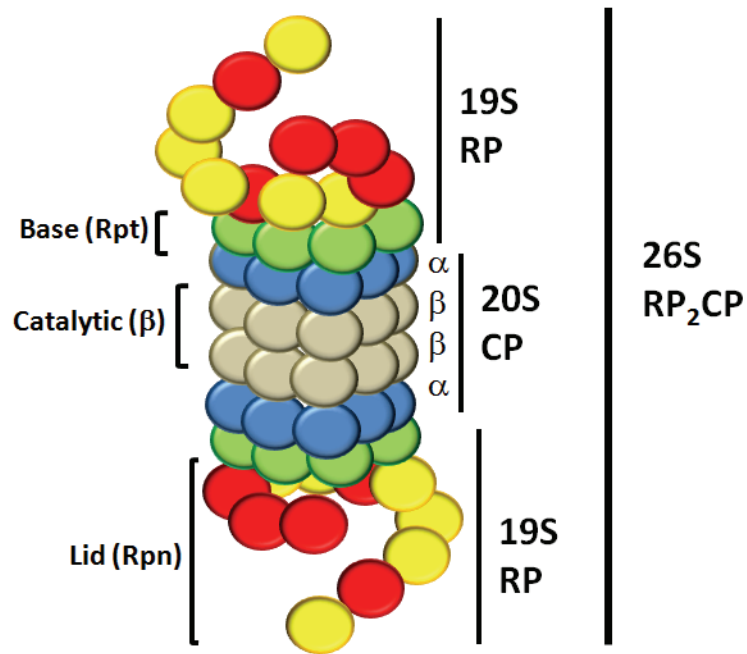


Figure 1-2: The 26S proteasome

The 26S proteasome consists of two subcomplexes: the 19S regulatory particle (RP) and 20S core particle (CP). Two 19S particles cap the ends of the barrel like 20S to form the 26S complex (RP₂CP). The 20S consists of alpha and beta (catalytic) subunits. The 19S consist of the base (Rpt proteins) and the lid (Rpn proteins).

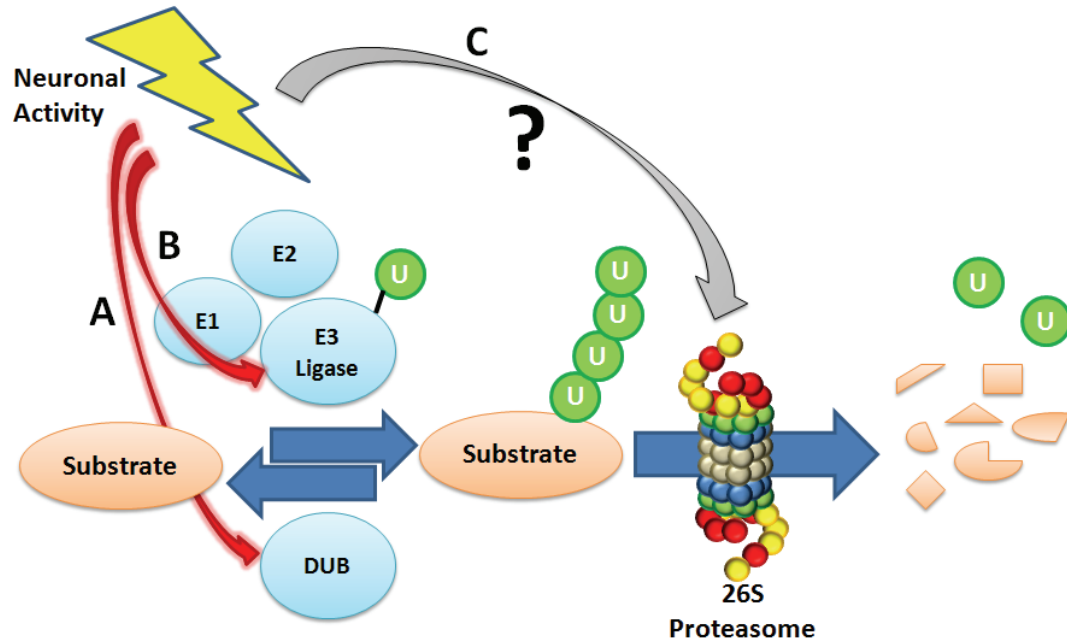


Figure 1-3: Neuronal activity regulates the ubiquitin proteasome system

A,B, Both the ubiquitination (B) and de-ubiquitination (A) processes have been shown to be regulated by neuronal activity. *C*, It is still unclear whether the proteasome is directly regulated by neuronal activity.

Chapter II

Regulation of the Proteasome by Neuronal Activity and CaMKII

INTRODUCTION

Synaptic plasticity is a complex process that requires the selective remodeling of synaptic connections. A majority of this remodeling occurs postsynaptically, where neurotransmitter receptors, scaffold proteins and signaling molecules are modified in response to neuronal activity [1]. The incorporation of newly synthesized proteins is required for long lasting changes in synaptic efficacy [2,3]. Protein degradation, on the other hand, provides an additional mechanism to modify the stoichiometry of synaptic proteins to promote, limit, or restrict plasticity.

The ubiquitin proteasome system (UPS) is a major pathway for protein turnover in eukaryotic cells. The selective degradation of proteins via the UPS involves three steps: recognition of the target protein via specific signals, marking of the target protein with ubiquitin chains by ubiquitin ligases, and delivery of the target protein to the 26S proteasome for degradation [5]. The 26S proteasome is a large energy-dependent protease consisting of two multi-protein subcomplexes: the 20S proteolytic core and 19S cap (PA700). The 20S consists of 28 subunits (α and β , six of which are catalytic, while the 19S consists of Rpt (ATPase) and Rpn (non-ATPase) regulatory subunits [9].

The UPS plays a crucial role in the development, maintenance, and remodeling of synaptic connections [4,104,105,106]. Additionally, pharmacological inhibition of the proteasome inhibits various forms of synaptic plasticity [48,49,50,53,54,68,107,108]. Several studies have identified key synaptic proteins such as PSD-95, Shank, GKAP, AKAP, SPAR, RIM-1 and GRIP1 that are regulated

by UPS dependent protein turnover [50,55,92,109,110]. In addition, it appears that cohorts of synaptic proteins are degraded in response to chronic activity blockade or up-regulation [92,93].

While ubiquitination has been widely studied, much less is known about regulation of the proteasome itself. There is increasing evidence that the proteasome may be regulated by interacting proteins or posttranslational modifications such as glycosylation or phosphorylation [30,95,111,112]. Here, we set out to determine how the proteasome is regulated in neurons. We utilized live-cell imaging strategies to uncover dynamics of proteasome activity in cultured hippocampal neurons. We found that both the blockade of action potentials (APs) with tetrodotoxin (TTX) and the up-regulation of APs with bicuculline (BIC) had rapid and opposing effects on proteasome activity. In addition, increased proteasome activity was found to be dependent upon external calcium entry in part through *N*-methyl-D-aspartate (NMDA) receptors and L-type voltage gated calcium channels (VGCCs), and required the activity of calcium/calmodulin-dependent protein kinase II (CaMKII). To investigate the involvement of CaMKII in proteasome regulation we overexpressed the constitutively active CaMKII (T286D) in HEK293T cells. CaMKII robustly stimulated the activity of the proteasome. Additionally, CaMKII α directly phosphorylated Rpt6, a 19S proteasome subunit, *in vitro*. Together, our data indicate proteasome function can be rapidly controlled by neuronal activity, with CaMKII as a key regulator.

RESULTS

Characterization of proteasome reporters

To determine the effects of neuronal activity on proteasome function, we utilized a GFP-based reporter imaging strategy to monitor the rate of proteasome activity in the dendrites of cultured hippocampal neurons. GFPu is a fusion of the CL1 degron, a 16 amino acid hydrophobic sequence first identified in yeast [113], with the carboxyl terminus of GFP [91]. It has a very short half-life (< 30 minutes) in mammalian cells, and is constitutively ubiquitinated and degraded by the proteasome [91,113,114]. We modified GFPu by replacing GFP with a photoactivatable (pa) variant [115] (Figure 2-1), in order to monitor the fluorescence decay of an isolated population of reporter proteins after photoactivation. mCherry, a monomeric variant of red fluorescent protein [116], was simultaneously expressed by an internal ribosomal entry site (IRES) sequence to identify transfected cells prior to photoactivation of paGFPu (Figure 2-1). After photoactivation, paGFPu fluorescence decay was monitored by confocal time-lapse imaging. paGFP (control reporter that lacks the CL1 degron) was utilized to account for effects of diffusion and photobleaching. paGFPu was first expressed in cos7 cells to verify its half life. Nearly 30% of the population of paGFPu was degraded in 30 minutes in a proteasome dependent manner (Figure 2-2). Degradation was blocked by addition of MG132, a proteasome inhibitor, indicating that our reporter is degraded by the proteasome (Figure 2-2).

Action potential blockade and up-regulation produce rapid and opposite effects on proteasome activity in hippocampal dendrites

Our experiments in cos7 cells indicated that our proteasome reporter would be a valuable tool for dynamically monitoring the activity of the proteasome in live neurons. paGFPu was next expressed in mature hippocampal neurons (>21 DIV) for 12-14 hours by Sindbis viral delivery. We found that paGFPu was rapidly degraded (as monitored by its fluorescence decay) in hippocampal neuron dendrites (Figure 2-3 and Figure 2-4), which is consistent with our findings of paGFPu degradation in mammalian non-neuronal cells (Figure 2-2). When paGFPu expressing cells were treated with three different proteasome inhibitors (MG132 - 25uM, Vinyl Sulfone - 1uM, and Epoxomicin - 1uM), the degradation rate of paGFPu was significantly blocked to levels of paGFP, which lacked the CL1 degron (Mean rates of degradation \pm SEM relative to control: MG132, $23.9 \pm 16.1\%$; Vinyl Sulfone, $22.6 \pm 11.9\%$; Epoxomicin, $35.8 \pm 7.4\%$; paGFP, $10.3 \pm 10.3\%$; Figure 2-3 and Figure 2-4, Table 2-1).

We next asked what the effect of blocking APs with TTX or up-regulating APs with BIC would be on proteasome activity. After monitoring paGFPu degradation in hippocampal dendrites for a 10 minute control period, BIC (40uM final) or TTX (2uM final) was added to the bath solution. paGFPu expressing dendrites were then imaged for an additional 20 minutes (2 minute intervals). Relative to control treated neurons, BIC significantly increased paGFPu rate of degradation ($167 \pm 15.2\%$ relative to control; Figure 2-4, Table 2-1). The rate of paGFPu degradation in BIC treated

neurons was most pronounced within the first 10 minutes after the addition of BIC ($233 \pm 15.2\%$ relative to control; Figure 2-4, Table 2-1). This effect was specific to proteasome-mediated turnover of paGFPu as the BIC-induced increase in paGFPu degradation was blocked in cells that were pre-treated with the proteasome inhibitor MG132 (25uM), but not with a specific calpain inhibitor, calpeptin (10uM) (Relative to BIC: MG132 + BIC, $37.9 \pm 7.6\%$; Calpeptin + BIC, $96.6 \pm 9.9\%$; Figure 2-4, Table 2-1). Furthermore, minimal effects of BIC were observed on the fluorescence decay of the paGFP control reporter ($31.3 \pm 3.0\%$ relative to BIC; Table 2-1). Interestingly, we also observed in the majority of BIC-treated neurons that the highest rates of paGFPu degradation initiated and persisted in spines for more than 10 minutes (Figure 2-5). In contrast, we observed opposite effects on paGFPu degradation by AP blockade. We found the rate of paGFPu degradation to be significantly attenuated in cells that were treated with TTX ($46.5 \pm 4.1\%$ relative to control; Figure 2-4, Table 2-1).

To confirm these results, we utilized an additional GFP-based degradation reporter. Ornithine decarboxylase (ODC) is a well-characterized cellular protein subject to ubiquitin-independent proteasomal degradation [117,118,119]. Fusion of amino acids 422-461 of the degradation domain of mouse ornithine decarboxylase to the C-terminal end of GFP promotes its degradation by the proteasome [120]. As with paGFPu, we modified the GFP-odc proteasome reporter with the photoactivatable (pa) variant of GFP [115] (Figure 2-6A). Degradation of paGFP-odc is independent of the ubiquitination cascade, allowing us to monitor the activity of the proteasome

exclusively. We found paGFP-odc to be degraded in hippocampal dendrites in a proteasome-dependent manner (Figure 2-6, Table 2-2). We then examined the effect of blocking or up-regulating APs on proteasome activity by monitoring the degradation of paGFP-odc. As observed with paGFPu, we found that BIC increased the rate of paGFP-odc degradation, while TTX significantly attenuated its degradation (BIC, $149 \pm 15.6\%$ relative to control; TTX, $11.9 \pm 9.2\%$ relative to control; Figure 2-6, Table 2-2). The largest increase in the rate of paGFP-odc degradation occurred immediately after the addition of BIC ($679 \pm 70.6\%$ relative to control; Figure 2-6D, Table 2-2).

The activity of the proteasome is often assessed by monitoring buildups of ubiquitin conjugates. Indeed, a brief ten minute treatment of neurons with proteasome inhibitors leads to a two-fold increase in ubiquitin conjugates (Figure 2-7). As expected, application of TTX rapidly increased ubiquitin conjugate levels in neurons in a manner similar to cells treated with proteasome inhibitors (Figure 2-7). Co-application of TTX with proteasome inhibitors did not lead to an additive increase in ubiquitin conjugates suggesting that neuronal activity blockade inhibits the proteasome (Figure 2-7E).

Action potential blockade with TTX does not remove all traces of activity. Indeed, during TTX treatment, miniature postsynaptic currents (mEPSCs) occur from spontaneous presynaptic vesicle fusions. It has been previously shown that mEPSCs regulate dendritic protein synthesis [121]. We therefore hypothesized that mEPSCs may regulate the TTX-dependent proteasome inhibition. Neurons expressing paGFPu

were first treated with TTX for ten minutes to allow for proteasome inhibition. mEPSCs were then blocked by addition of α -amino-3-hydroxy-5-methylisoxazole-4-propionic acid (AMPA) receptor antagonist, 6-cyano-7-nitroquinoxaline-2,3-dione (CNQX). Interestingly, paGFPu degradation increased over three-fold after addition of CNQX (Figure 2-8B). Indeed proteasome activity recovered immediately after mEPSC blockade (Figure 2-8A). This suggests that proteasome inhibition resulting from neuronal activity blockade may depend on mEPSCs. Together, these results indicate that the activity of the proteasome is rapidly tuned to increased or decreased neuronal activity.

Regulation of proteasome activity by external calcium

Due to the rapid and dynamic nature of proteasome regulation by neuronal activity, we hypothesized that calcium (Ca^{2+}) might be a regulator of proteasome function in neurons. During action potentials, extracellular Ca^{2+} enters postsynaptic dendritic and spine compartments largely through NMDA receptors and L-type voltage gated calcium channels (VGCC) [122,123]. Furthermore, the influx of Ca^{2+} into postsynaptic compartments regulates many biochemical signaling pathways that are involved in controlling synaptic strength [124]. To determine if proteasome activity required the influx of external Ca^{2+} , we monitored the degradation rate of our reporters in neurons incubated with Ca^{2+} -free media for 15 minutes. The rates of paGFPu and paGFP-odc degradation were attenuated to levels comparable to neurons treated with proteasome inhibitors (Relative to Control: paGFPu, $27.6 \pm 7.8\%$; paGFP-

odc, 20.2 ± 21.1 %; Table 2-1 and Table 2-2). This suggests that external Ca^{2+} entry into dendrites is required for proteasome activity.

To determine the mode of Ca^{2+} entry that was involved in regulation of the proteasome, we monitored paGFPu degradation in neurons treated with NMDA receptor antagonist (2*R*)-amino-5-phosphonovaleric acid (APV) or L-type VGCC antagonist Nimodipine. Application of APV or Nimodipine slightly attenuated the rate of paGFPu degradation when compared to the control paGFPu degradation rate (Relative to Control: APV, 55.1 ± 11.1 %; Nimodipine, 70 ± 2.1 %; Table 2-1). However, both APV and Nimodipine significantly attenuated BIC-stimulated degradation of paGFPu (Relative to BIC: APV, 46.8 ± 6.4 %; Nimodipine, 41.1 ± 7.4 %; Table 2-1). This suggests that NMDA receptors and L-type VGCCs are required for the BIC-induced increase in proteasome activity. Furthermore, we also found that blocking synaptic activity with the competitive AMPA receptor antagonist CNQX, also significantly attenuated BIC-stimulated paGFPu degradation (30.1 ± 3.9 % relative to BIC; Table 2-1). Indeed it has been previously reported that post-synaptic activity-dependent Ca^{2+} influx is highly sensitive to AMPA receptor blockade [125,126]. Taken together, these results suggest that external calcium influx through postsynaptic NMDA receptors and L-type VGCCs is important for activity-dependent proteasome function in neurons.

Regulation of proteasome activity by CaMKII

Ca²⁺ influx through postsynaptic compartments leads to a subsequent activation of Ca²⁺-dependent kinases, such as Ca²⁺/calmodulin dependent protein kinase II (CaMKII), to modulate changes in synaptic strength [127]. Phosphorylation of substrates can regulate targeting of these proteins for ubiquitination and proteasomal degradation [25]. Additionally, the proteasome itself has been shown to be phosphorylated [111]. We wondered if CaMKII, a key plasticity kinase, regulates proteasome function in neurons. We found that the BIC-stimulated degradation of paGFPu was significantly attenuated in hippocampal neurons when pre-treated for 10 minutes with a CaMKII inhibitor, KN-93 (10 uM, 38.9 ± 2.7% relative to BIC; Table 2-1). Additionally, KN-93 blocked BIC-stimulated degradation of paGFP-odc, especially 8 minutes after stimulation (19.7 ± 4.6% relative to BIC at 8 min; Table 2-2). Treatment with KN-93 alone only slightly attenuated the degradation of paGFPu or paGFP-odc (Relative to Control: paGFPu, 57.2 ± 4.9%; paGFP-odc, 80.7 ± 3.7%; Table 2-1 and Table 2-2). One potential caveat to these results is that KN-93 has also been shown to inhibit other CaM-kinase family members [128]. To obtain specificity we treated neurons with myristolated-Autocamtide-2-related inhibitory peptide (myr-AIP), a cell permeable, highly specific and potent inhibitor of CaMKII [129]. BIC-stimulated degradation of paGFPu was significantly blocked in neurons pre-treated with myr-AIP (5 uM) for 30 minutes (40.1 ± 8.6% relative to BIC; Figure 2-9). These results suggest that CaMKII regulates proteasome activity in response to increased AP's.

Since inhibition of CaMKII blocked increased neuronal activity dependent proteasome function, we next asked if the activation of CaMKII could increase proteasome activity. To accomplish this we overexpressed a constitutively active form of CaMKII (T286D mutation, [130,131]) in HEK293T cells and performed *in vitro* and *in vivo* proteasome activity assays. To test *in vivo* proteasome activity we co-transfected our proteasome reporter GFPu along with either CaMKII T286D or a control vector in HEK293T cells. GFPu protein levels were significantly decreased in cells expressing CaMKII T286D after two hours of protein synthesis inhibition (GFPu protein levels at t120: Control, $63.1 \pm 1.6\%$; CaMKII T286D, 31.1 ± 7.5 ; Figure 2-10). Steady state levels of GFPu were also dramatically lower in CaMKII T286D transfected cells (GFPu fluorescence relative to control: $45.6 \pm 2.5\%$; Figure 2-11A and Figure 2-11B). This is likely due to increased proteasome activity, and not an impairment of protein synthesis, as the addition of proteasome inhibitor MG132 increases the levels of GFPu in both control and CaMKII expressing cells (Figure 2-11A and Figure 2-11C). To determine if this was a direct effect on proteasome function by CaMKII we assayed lysates for *in vitro* proteasome activity with the fluorogenic proteasome substrate Suc-LLVY-AMC. Lysates from HEK293T cells transfected with CaMKII T286D had significantly increased proteasome activity as measured by AMC hydrolysis ($153 \pm 12\%$ relative to control; Figure 2-12A). This was not merely due to an increase in total proteasome levels, as western blot analysis showed similar amounts of core and cap proteasome subunit levels (Figure 2-12B). Furthermore, hippocampal neurons infected with CaMKII T286D Sindbis virion also

had a slight but significant increase in proteasome activity as measured by Suc-LLVY-AMC cleavage ($114 \pm 3.2\%$ relative to control; Figure 2-12C), despite less than 50% viral infection. Together these results suggest CaMKII is a regulator of proteasome function.

Phosphorylation of proteasome by CaMKII

Since inhibition of CaMKII blocked activity-dependent proteasome activity and overexpression of a catalytically active CaMKII increased proteasome activity, we hypothesized that phosphorylation of the proteasome may regulate its function. Phosphorylation of proteasomes has been reported in non-neuronal cell types by both Casein Kinase 2 (CK2) and Protein Kinase A (PKA) [26,29,30,32,132]. This phosphorylation is believed to regulate proteasome function by affecting assembly, activity or interactions [30,32,111]. To test if proteasomes are directly phosphorylated by CaMKII, we performed *in vitro* kinase assays using highly purified 19S (PA700) and 19S subcomplexes (PS-1 and PS-2) as substrates [133]. CaMKII catalyzed the incorporation of ^{32}P phosphate from ATP into a single band of both 19S and PS-1, a subcomplex of 19S that contains only two of the six Rpt subunits found in intact 19S. This band had an approximate molecular weight of about 45 kDa and was indistinguishable between 19S and PS-1 (Figure 2-13). After long incubations a second, minor band appeared in some experiments. The sizes of both the major and minor labeled proteins were similar to those of subunits Rpt3, Rpn9 or Rpt6. Kinase reactions with PS-2 and PS-3, two additional 19S subcomplexes that do not contain

Rpt3, Rpn9 or Rpt6 subunits produced no labeled proteins (Figure 2-14A and data not shown). Interestingly, Rpt3 and Rpt6 previously have been reported to be phosphorylated [27,32]. To determine the identity of the labeled protein we performed western blotting with antibodies against Rpt3, Rpn9 and Rpt6 as well as other 19S subunits with this approximate size. The ^{32}P labeled protein co-migrated with Rpt6 (Figure 2-14A). To further demonstrate the identity of the labeled protein in 19S, we excised the band from the SDS gel, solubilized the protein and subjected it to a second round of SDS-PAGE. The recovered labeled protein was detected only by antibodies against Rpt6 (Figure 2-14B). Moreover, mass spectrometric analysis of tryptic peptides identified the protein as Rpt6 (Table 2-3). Together, these data strongly indicate that Rpt6 is the proteasome subunit phosphorylated by CaMKII.

We next asked whether this *in vitro* phosphorylation had a direct effect on proteasome function. Purified proteasomes were mixed with purified CaMKII α and then tested for activity by fluorogenic peptidase assay. While CaMKII phosphorylated both the control MBP (myelin basic protein) substrate and proteasomes *in vitro*, no significant changes in proteasome activity were observed (Figure 2-15A and Figure 2-15B). Additionally we measured 26S proteasome assembly from isolated 20S proteasome and 19S subcomplexes and again observed no effect after CaMKII phosphorylation (Figure 2-15C). This suggests that CaMKII phosphorylation of proteasomes likely affects proteasome activity via regulation of interactions of additional factors not present in our highly purified *in vitro* system.

We next asked whether CaMKII phosphorylates Rpt6 *in vivo*. HEK293T cells transfected with CaMKII T286D were labeled with ^{32}P orthophosphate. Proteasomes were immunoprecipitated with an antibody to the $\alpha 2$ subunit previously shown to effectively pull down human proteasomes [134]. We observed a CaMKII dependent phosphorylation of a protein with the approximate molecular weight of 45 kDa, similar to that of Rpt6 (Figure 2-16). Indeed, we also observed highly phosphorylated proteins that migrated at approximately 45 kDa in Rpt6 immunoprecipitates from ^{32}P live labeled rat cortical neurons (Figure 2-14C). Together, with our *in vitro* phosphorylation experiments, this data indicates that Rpt6 is phosphorylated by CaMKII.

We hypothesized that phosphorylation of the proteasome could be modulated by synaptic activity. To test this we stimulated cortical neurons for 15 minutes with AMPA, an AMPA receptor agonist that robustly stimulates paGFPu degradation (Table 2-1), after ^{32}P orthophosphate labeling. Membrane depolarization by AMPA receptor activation has been shown to facilitate and induce influx of calcium through NMDA receptors and L-type VGCCs [135,136]. We observed a modest increase (~9%) in phosphorylation of Rpt6 in response to AMPA stimulation (Figure 2-17). Western blot analysis of the immunoprecipitates with an antibody to Rpt6 indicates that the observed phosphorylation increase was not due to increased protein levels (Figure 2-17). Together, these results indicate proteasomes may be phosphorylated in response to synaptic activity.

DISCUSSION

In our current study we report the rapid and dynamic regulation of proteasome function by neuronal activity. Action potential blockade or upregulation produced rapid and opposite effects on the activity of the proteasome as monitored by our fluorescent proteasome reporters. The activation of proteasome by increased action potentials required external calcium influx through NMDA receptors and L-type VGCCs. UPS components may be regulated directly by Ca^{2+} [103,137,138,139] and it has been reported that the release of Ca^{2+} from intracellular stores transiently activates the 26S proteasome [140]. Our findings are in line with these studies and they provide evidence for Ca^{2+} signaling in the regulation of the proteasome activity in neurons.

To further explore the role of calcium signaling in regulation of the proteasome we investigated the involvement of calcium activated kinase cascades. We identified CaMKII as a novel regulator of proteasome activity in neurons. CaMKII is a calcium dependent protein kinase that plays a key role in neuronal behavior, development and plasticity [128]. We found that BIC-stimulated activation of the proteasome to require the activity of CaMKII. Additionally, overexpression of a constitutively active form of CaMKII robustly stimulated the proteolytic activity of the proteasome. We have identified Rpt6, a 19S regulatory subunit of the proteasome, to be phosphorylated by CaMKII. This is the first time, to our knowledge, that CaMKII has been shown to phosphorylate the proteasome. Interestingly, Rpt6 has also been shown to be phosphorylated by Protein Kinase A (PKA) in non-excitabile cells [32]. We therefore

cannot rule out a role for PKA in regulation of proteasome in neurons. CaMKII and PKA both phosphorylate targets at similar substrate recognition motifs [141].

Furthermore, CaMKII has been shown to be activated in neurons stimulated with the PKA agonist forskolin [142,143]. However, both Zhang et al. (2007) and our findings identify the phosphorylation of Rpt6 in the regulation of proteasome function. This is significant because components of the 19S complex have been shown to be important regulators of 26S proteasome assembly and activation [144].

Since CaMKII-dependent phosphorylation of Rpt6 did not directly regulate proteasome activity *in vitro*, we hypothesize that other regulatory factors, not present in our reconstituted and highly purified *in vitro* assay, may be required. Associated proteins have previously been found to regulate various aspects of proteasome function [95,101,145]. Interestingly, both proteasome and CaMKII translocate from dendritic shaft to dendritic spine compartments in response to neuronal activity in a similar timeframe [99,146,147]. This indicates that the phosphorylation of the proteasome by CaMKII may regulate its trafficking in neurons, as suggested by recent evidence that CaMKII acts as a scaffold to recruit proteasome to synapses [100].

Proteasome function has been shown to be required for various learning and memory and behavior related paradigms such as long term potentiation (LTP) [48,49,68,148,149]. Our findings support a role for the direct modulation of proteasome activity in neurons to be important for synaptic plasticity. This is substantiated by our findings that CaMKII regulates proteasome activity which provides a mechanistic link for the regulation of proteasome function by neuronal

activity. Phosphorylation of proteasomes by CaMKII may directly affect the interactions of regulatory proteins to modulate the assembly, activity or localization of the proteasome. This in turn can facilitate protein degradation and alterations in the stoichiometry of synaptic proteins to promote, limit or restrict synaptic plasticity. We predict neurons to utilize this mechanism to synergize tunable proteasome activity with the dynamic ubiquitination of substrates for degradation. Moreover, since both UPS dysfunction and aberrant Ca²⁺ signaling have been attributed to several neurodegenerative diseases such as AD and Huntington's disease (HD), it will be interesting to determine if misregulation of proteasome phosphorylation is involved in the pathogenesis of these diseases [39,150].

MATERIALS AND METHODS

Antibodies and reagents

α 2 proteasome (MCP21, mAb), $\alpha\beta$ core proteasome (pAb) and Rpt6 (mAb) antibodies were purchased from Biomol. GFP antibody (FL, pAb) from Santa Cruz Biotechnology. FK2 (mAb mono and poly-ubiquitin conjugate) antibody was purchased from Biomol (Plymouth Meeting, PA). Anti-synapsin antibody (pAb) was purchased from Chemicon (Temecula, CA). The following pharmacological reagents were used: 2-amino-5-phosphonopentanoic acid (APV), bicuculline (BIC), Nimodipine, tetrodotoxin (TTX) and 6-cyano-7-nitroquinoxaline-2,3-dione (CNQX) from Tocris Bioscience. MG132 from Peptide Institute. Cycloheximide (CHX) from MP Biomedicals. Adamantane-acetyl-(6-aminohexanoyl)(3)-(leucinyl)(3)-vinyl-

(methyl)-sulfone (Vinyl Sulfone - VS), Epoxomicin (Epox), (\pm)- α -Amino-3-hydroxy-5-methyl-4-isoxazolepropionic acid (AMPA), KN-93, and myristolated-Autocamtide-2-related inhibitory peptide (myr-AIP) from Biomol. Calpeptin from EMD Biosciences. Suc-LLVY-AMC fluorogenic substrate from Biomol. Purified Calmodulin (human, recombinant) and CaMKII α (full-length human recombinant) from Biomol.

DNA and Sindbis constructs

RSV-CaMKII T286D was a kind gift from Anirvan Ghosh (UC San Diego, La Jolla, CA). CaMKII T286D was amplified by PCR with primers containing XbaI and StuI with 5' and 3' overhangs, respectively. The PCR products were ligated into the XbaI and StuI sites of SinRep5 (Invitrogen, Carlsbad, CA). GFPu (in EGFP-C1 plasmid backbone – Clontech, Palo Alto, CA), a fusion of the CL1 degron (degradation signal) on the carboxyl terminus of GFP, was kindly provided by Ron Kopito (Stanford University, Palo Alto, CA). GFPu is ubiquitinated and specifically degraded by the proteasome [91,113,114]. GFP-odc (in EGFP-C1 plasmid backbone – Clontech), a fusion of the ornithine decarboxylase (odc) degron on the carboxyl terminus of GFP, was also kindly provided by Ron Kopito. GFP-odc is targeted directly to the proteasome for degradation, in an ubiquitin-independent manner [117,120]. The AgeI-BsrGI fragment from photoactivatable (pa) GFP (a kind gift provided by Jennifer Lipponcott-Schwartz – National Institutes of Health, Bethesda, MD) was subcloned into the AgeI-BsrGI sites of the GFP, GFPu and GFP-odc

plasmids. paGFPu, paGFP-odc and the paGFP (no degron control) open reading frames were amplified by PCR with primers containing NheI and BamHI 5' and 3' overhangs, respectively. The PCR products were ligated into the NheI – BamHI sites of pCMV-IRES-mCherry. pCMV-IRES-mCherry was created by subcloning mCherry (pRSETB-mCherry - a kind gift from Roger Tsien – University of California San Diego, La Jolla, CA) into IRES2-EGFP (Clontech). This was done by ligating the BamHI (blunted)-BsrGI mCherry containing fragment into BstXI (blunted)-BsrGI sites. For Sindbis virus construction, the NheI-XbaI reporter-IRES-mCherry containing fragment from pCMV-paGFP, paGFPu, and paGFP-odc plasmids were subcloned into the XbaI site of SinRep5. All constructs were confirmed by DNA sequencing. For production of recombinant Sindbis virions, RNA was transcribed using the SP6 mMessage mMachine Kit (Ambion, Austin, TX), and electroporated into BHK cells using a BTX ECM 600 at 220V, 129 Ω , and 1050 μ F. Virion were collected after 24-32 hours and stored at -80°C until use.

Neuronal cultures

Rat dissociated hippocampal neurons from postnatal day 1 or 2 were plated at a density of 45,000 cells/cm² onto poly-D-lysine coated coverslips or glass bottom 35 mm dishes (Mattek, Ashland, MA) and maintained in B27 supplemented Neurobasal media (Invitrogen) until 17 days or more as previously described [59]. High density rat cortical or hippocampal neurons from postnatal day 1 were plated onto poly-D-

lysine coated 6-well dishes (~500,000 cells per well) and maintained in B27 supplemented Neurobasal media.

Confocal microscopy

For all imaging purposes, we used a Leica (Wetzlar, Germany) DMI6000 inverted microscope outfitted with a Yokogawa (Tokyo, Japan) Spinning disk confocal head, a Orca ER High Resolution B&W Cooled CCD camera (6.45 $\mu\text{m}/\text{pixel}$ at 1X) (Hamamatsu, Sewickley, PA), Plan Apochromat 40x/1.25 na and 63x/1.4 na objective, and a Melles Griot (Carlsbad, CA) Argon/Krypton 100 mW air-cooled laser for 488/568/647 nm excitations. Confocal z-stacks were acquired in all experiments. Photoactivation of reporter constructs was achieved with 100 W Hg²⁺ lamp and a D405/40X with 440 DCLP dichroic filter set (Chroma, Rockingham, VT) (10 to 15 sec exposure times for photoactivation).

Drug treatment and imaging of fixed cells

Mature hippocampal neuron cultures (>17 DIV) were treated with various drugs or vehicle (DMSO) in conditioned growth media. Cells were then fixed in 4% paraformaldehyde/4% sucrose for 10 minutes, and blocked and permeabilized in PBS-MC (phosphate buffered saline with 1 mM MgCl₂ and 0.1 CaCl₂) with Triton X-100 (0.2%) and BSA (2%). Cells were incubated overnight with anti-ubiquitin conjugate specific (FK2 mAb, 1:1000) and anti-synapsin (pAb, 1:1000) antibodies diluted in PBS-MC plus 2% BSA. Cells were washed and incubated with goat anti-mouse Alexa

488 and goat anti-rabbit Alexa 568 secondary antibodies (1:1000) diluted in PBS-MC plus 2% BSA. Cells were then washed and coverslips were mounted in Aqua Poly/Mount (Polysciences, Warrington, PA). For proteasome perturbation experiments in Supplementary Figure 1, cultures were treated with MG132 (5 μ M), vinyl sulfone (1 μ M), epoxomicin (1 μ M) or calpeptin (10 μ M). For quantitation of FK2 (ubiquitin conjugate) immunofluorescence, max projected confocal z-stacks were analyzed with NIH ImageJ. FK2 images were thresholded to a level at least 1.5-2x times background (minimum gray values). The mean FK2 fluorescence intensity integrated from 63X fields of neurons is plotted relative to control treated neurons. Three separate experiments were performed for each condition, with each experiment normalized to its own control.

Live imaging

For Sindbis virus infection of mature hippocampal neurons (>21 DIV) on glass bottom 35 mm dishes, paGFPu, paGFP-odc or paGFP reporter virion were added directly to culture media. Expression was allowed to continue for only 12-14 hours to prevent cytotoxicity. The media was then replaced with HEPES based saline (HBS) solution containing in mM: 119 NaCl, 5 KCl, 2 CaCl₂, 2 MgCl₂, 30 Glucose, 10 HEPES with the appropriate pharmacological treatments. To determine basal rates of reporter degradation, cells were pre-incubated for 20 minutes in HBS with either vehicle (DMSO) or proteasome inhibitors (MG132 25 μ M, VS 1 μ M or Epox 1 μ M) at ~35°C using a ceramic heat lamp (ZooMed, San Luis Obispo, CA). The bath

temperature was continually monitored by a digital probe thermometer. Infected neurons (identified by mCherry expression) were then photoactivated for 10-15 seconds with 100 W Hg²⁺ lamp and a D405/40X with 440 DCLP dichroic filter set (Chroma). For live imaging of neurons, the primary dendrites from pyramidal-like neurons were selected. Confocal Z-stack images (with 0.5 μm sections) were acquired with a 63X objective every 2, 3 or 4 minutes (as indicated) for the duration of the time lapse experiment. In some experiments (as indicated) both GFP (excitation 488 nm) and mCherry (568 nm) images were acquired. In others, GFP was acquired every time point while pre and post mCherry time lapse images were acquired. For treatment of neurons with APV (50 μM), CNQX (40 μM), calpeptin (10 μM), KN-93 (10 μM), AIP (5 μM) or Ca²⁺-free containing HBS, cells were similarly pre-incubated, selected by mCherry expression, photoactivated and imaged by time-lapse microscopy. All pre-treatments were 15 minutes except for AIP (30 minutes). For treatment of neurons with TTX or BIC alone or with various combinations of other pharmacological treatments in HBS; TTX or BIC was added to the bath after an initial 10 imaging minute period (12 minutes for paGFP-odc). Time lapse imaging followed for an additional 20 minutes period (48 minutes for paGFP-odc). Imaging of control and BIC-treated cells were interspersed between different treatments to verify that the degradation rates of our reporters under control and BIC-stimulated conditions in individual dendrites performed throughout the study did not vary significantly from the grouped data.

Florescence intensity quantitation

All imaging was acquired in the dynamic range of 8 bit or 12 bit acquisition (0-255 and 0-1024 pixel intensity units, respectively) with Simple PCI (Hamamatsu) imaging software. For quantitation of reporter degradation, straightened dendrites from maximum projected confocal z-stacks were analyzed with NIH ImageJ. Images were thresholded above background. Total integrated fluorescence intensity was measured from entire (proximal and distal regions) dendrites at each time interval and expressed as the percent change from time zero. Grouped analysis of dendritic fluorescence decay over time from each treatment group is plotted as line graphs (mean \pm SEM). The degradation rate of reporter fluorescence decay is obtained by taking the difference of total fluorescence loss (arbitrary units – AU) over time ($F_i - F_n/\text{time}_n$) from individual experiments. The mean degradation rate \pm SEM per treated group is then divided by the control rate to obtain the “relative to control” value. In some cases the degradation rate was extracted from smaller defined time windows after the addition of activity altering pharmacological drugs to highlight and compare dynamic changes in reporter degradation. For statistical analysis, degradation rates were compared using student’s t-tests. P values are listed in Table 1 and S1.

26S Proteasome fluorogenic peptidase assays

In vitro assay of 26S proteasome chymotryptic activity was performed as previously described [151] with slight modifications. HEK293T cells were transfected with RSV-CaMKII T286D for 24-36 hours. Neuronal cultures were transduced with

CaMKII T286D by Sindbis virus. Cells were lysed in proteasome activity assay buffer (50 mM Tris-HCl (pH 7.5), 250 mM Sucrose, 5 mM MgCl₂, 0.5 mM EDTA, 2 mM ATP, 1 mM DTT and 0.025% Digitonin). 100 μM of the fluorogenic substrate Suc-LLVY-AMC was then added to lysates in a 96-well microtiter plate. Fluorescence (380 nm excitation, 460 nm emission) was monitored on a microplate fluorometer (HTS 7000 Plus, Perkin Elmer) every 4 min for 2 hours at room temperature.

³²P Orthophosphate Live Labeling and Immunoprecipitation

HEK293T cells were transfected with CaMKII (T286D) for 24-36 hours. Cultured cortical neurons or HEK293T cells were live labeled for 2 hours in a low-phosphate HEPES buffered solution [152] (5.6 mM KCl, 0.2 mM KH₂P₀₄, 137.6 mM NaCl, 2.4 mM NaHCO₃, 5.6 mM glucose, 0.4 mM MgSO₄, 0.5 mM MgCl₂, 1.26 mM CaCl₂, 20 mM HEPES, pH 7.4) with 0.40 mCi/mL ³²P orthophosphate added to each well (of a 6-well culture dish). Cells were lysed in proteasome IP buffer (25 mM Tris (pH 7.5), 15% Glycerol, 2.5 mM MgCl₂, 5 mM ATP, 5 mM Na pyrophosphate, 50 mM Na Fluoride, 1 mM Na Vandadate, 1 mM DTT, 0.5% NP40). Lysates were immunoprecipitated with indicated antibodies, and resolved by SDS-PAGE. ³²P labeling was detected with a Typhoon Scanner (GE Healthcare Life Sciences) and analyzed using ImageQuant TL (Amersham Biosciences).

In vitro phosphorylation of PA700, the 19S regulator of the 26S proteasome

19S proteasome was purified from bovine red blood cells as described previously [153]. PS-1 and PS-2, subcomplexes of the 19S were purified as described previously [133]. Phosphorylation reactions were conducted with autoactivated CaMKII α . CaMKII α was activated in reactions containing 100 μ M ATP, 1.2 μ M calmodulin, 10 mM MgCl₂ and 2 mM CaCl₂. After incubation for 10 mins at 30°C, activated kinase was incubated with 19S. Assays contained 5 μ M CaMKII α , 45 μ M 19S, 100 μ M [γ -³²P] ATP (500 mCi/ m mol), 50 mM Tris-HCl (pH 7.6), 2 mM DTT, and 10% glycerol in a final volume of 50 μ l. Control reactions contained either no kinase or no 19S. After various times of incubation at 30°C samples were treated with SDS sample buffer and subjected to SDS-PAGE and autoradiography.

Evaluation of CaMKII α on 26S proteasome activity

The effect of CaMKII α on 26S proteasome activity was evaluated by measuring rates of Suc-LLVY-AMC hydrolysis. 26S proteasome was purified from bovine red cells as described previously [154]. 26S proteasome was pre-incubated in the presence or absence of activated CaMKII α as described for 19S. 10 nM 26S proteasome samples were assayed for peptidase activity as described previously [155].

Evaluation of CaMKII α on 19S-dependent activation of 20S proteasome activity

The effect of CaMKII α on 19S-dependent activation of 20S proteasome activity was evaluated as described previously [153,155]. Purified 19S was pre-

incubated in the presence or absence of activated CaMKII α prior to incubation with 20S proteasome and assay of peptidase activity.

Mass spectrometry

Protein identification by mass spectrometry was conducted by the Protein Chemistry Core Research Facility at UT Southwestern Medical Center.

ACKNOWLEDGEMENTS

We thank M. Scanziani and R. Hampton for advice and critical review of the manuscript; A. Ghosh, M. Sutton and D. Berg for helpful discussion; A. Hoffmann and S. Werner for help with ^{32}P experiments. D. Immenhausen for hippocampal cultures and the rest of the Patrick lab for support. We also thank R. Kopito (Stanford) for GFPu and GFP-odc constructs, J. Lipponcott-Schwartz (NIH) for the paGFP construct, A. Ghosh for the CaMKII construct and R. Tsien for the mCherry construct. Some of the impetus for these experiments was conceived in the laboratory of Erin Schuman (CalTech).

Chapter Two, in full, consists of the following publication:

Djakovic SN, Schwarz LA, Barylko B, DeMartino GN, Patrick GN. "Regulation of the proteasome by neuronal activity and calcium/calmodulin-dependent protein kinase II". *J Biol Chem*. 2009 Sep 25;284(39):26655-65.

I was the primary researcher of these studies and Gentry Patrick directed and supervised the research. Lindsay Schwarz assisted with ubiquitin conjugate

experiments. Barbara Barylko assisted in determining the proteasome subunit phosphorylated by CaMKII in the laboratory of George DeMartino.

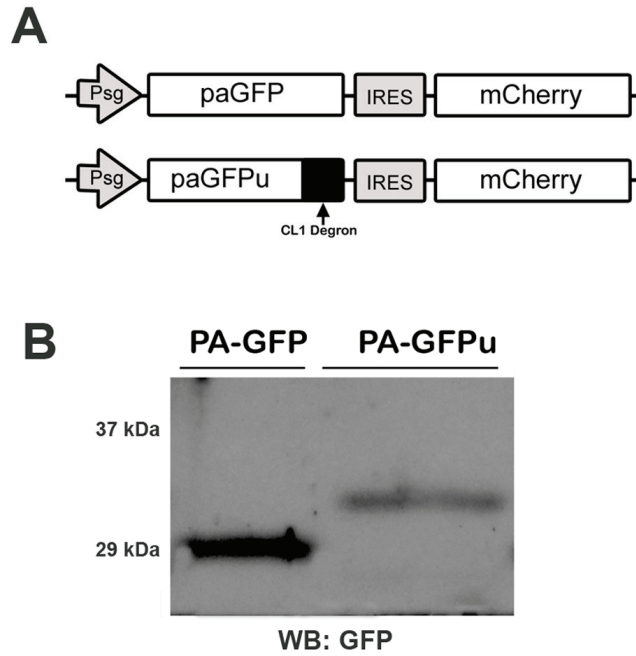


Figure 2-1: paGFPu proteasome reporter

A, Schematic of the photoactivatable (pa) UPS reporter Sindbis constructs. The CL1 degradation signal (degron) is fused to the carboxyl terminus of paGFP (non CL1 containing control reporter), converting it into an ubiquitin-dependent proteasomal degradation reporter (paGFPu). mCherry is co-expressed using an IRES signal. *B*, COS7 cells were transfected for 12hrs with paGFPu or paGFP no degron control vector. Lysates were probed with anti-GFP antibody.

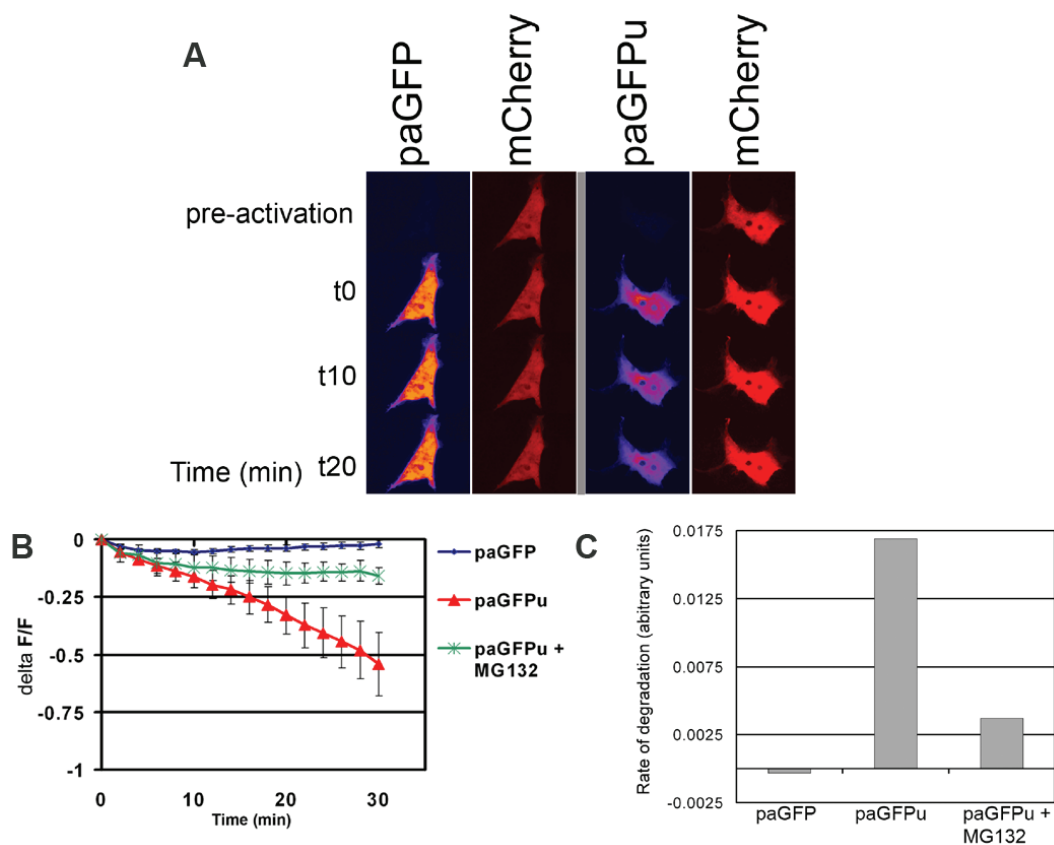


Figure 2-2: Characterization of paGFPu proteasome reporter in COS7 cells

A, COS7 cells were transfected for 12hrs with paGFPu-IRES-mCherry and paGFP-IRES-mCherry. Representative images of pre-activation, 0, 10, and 20 minutes are shown. *B*, The change of fluorescence from time 0 divided by each time point – delta F/F is shown in the combined line graph. *C*, The difference in rates of degradation is depicted in the bar graph. Rates of degradation were extrapolated from the slope of the line using linear fit analysis. N = 20, 25, and 13 cells for paGFP, paGFPu, and paGFPu + MG312, respectively.

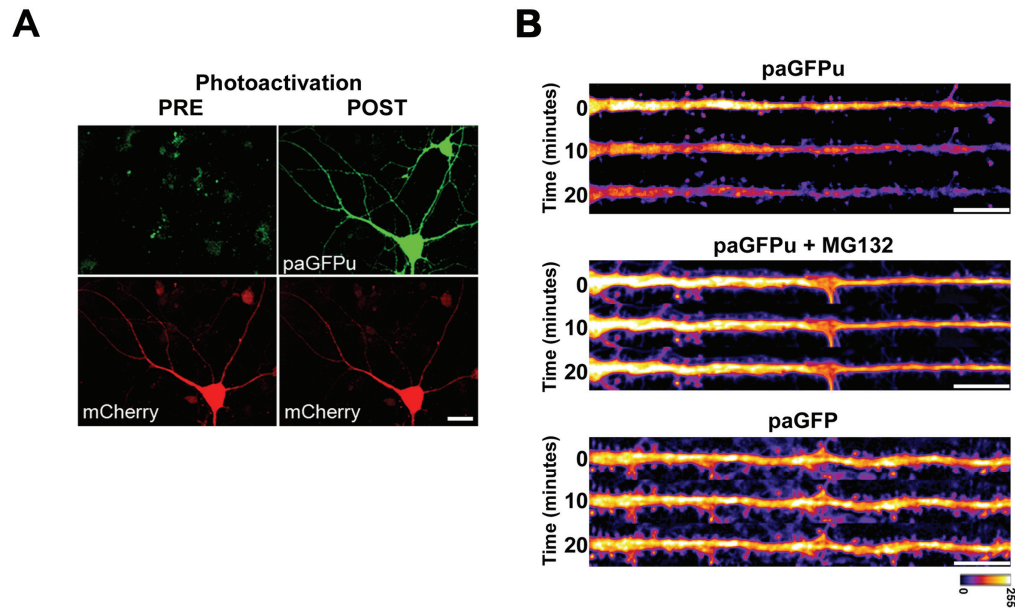


Figure 2-3: Expression of paGFPu in hippocampal neurons

A, Representative image of a hippocampal neuron infected with paGFPu before (PRE) and after (POST) photoactivation. mCherry is expressed to locate infected cells before photoactivation. *B*, CL1 degron promotes degradation of paGFPu. Straightened dendrites from representative time-lapse experiments of cultured hippocampal neurons expressing paGFPu alone, paGFPu plus MG132 (25 μ M), or paGFP. paGFPu fluorescence decay is observed in dendrites, and is blocked by addition of the proteasome inhibitor MG132. No significant fluorescence loss is observed in paGFP (no degron control) expressing dendrites.

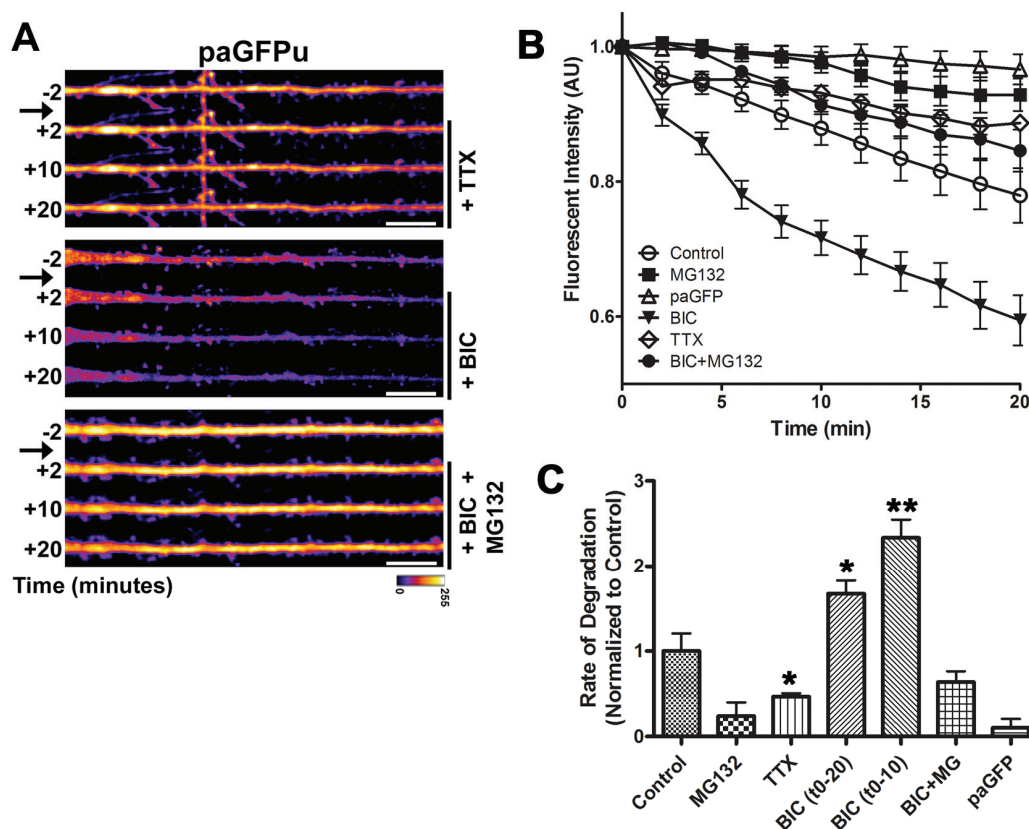


Figure 2-4: Action potential blockade and up-regulation produce opposite effects on proteasome activity in hippocampal neurons

A, Representative straightened dendrites from time-lapse experiments in which cultured hippocampal neurons expressing paGFPu were treated with TTX (2 μ M), BIC (40 μ M), or BIC plus MG132 (25 μ M) and imaged every 2 minutes for 20 minutes. Time of treatment indicated by black arrow. *B*, Grouped analysis (plotted as line graphs - mean \pm SEM) of dendritic Fluorescent intensity normalized to time zero for control (paGFPu alone), MG132, TTX, BIC, BIC plus MG132 treated neurons, or paGFP (no degraon). *C*, Bar graph depicting the mean degradation rate \pm SEM (AU) per treated group normalized to the control (paGFPu) rate of fluorescence decay. BIC dramatically increased paGFPu rate of degradation, most significantly in the first ten minutes, while TTX blocks paGFPu degradation (* - $P < 0.05$, ** - $P < 0.001$, relative to paGFPu (control)). See Table 2-1 for rates of degradation, and p and n values. Scale bar for all images is 10 μ m.

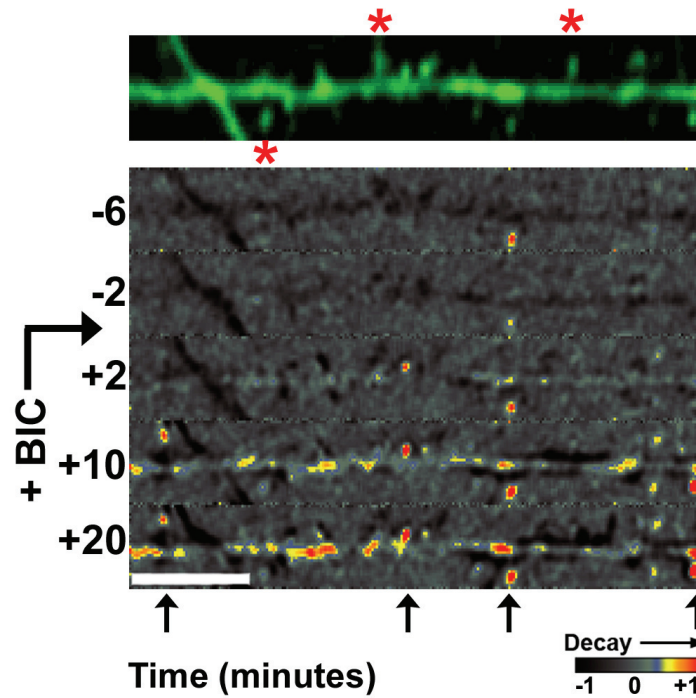


Figure 2-5: Neuronal activity induces paGFPu degradation in dendritic spines

A time-lapse image sequence of paGFPu degradation in a representative dendrite from a cell treated with BIC (shown as $F_n - F_{n-1}/F_{n-1}$ to highlight the highest rates of fluorescence decay between successive frames) showed significant paGFPu degradation that initiated and persisted in spines (black arrows denote spines with high rates of fluorescent decay, red asterisks denote spines with little or no fluorescent decay). Scale bar is 5 μm .

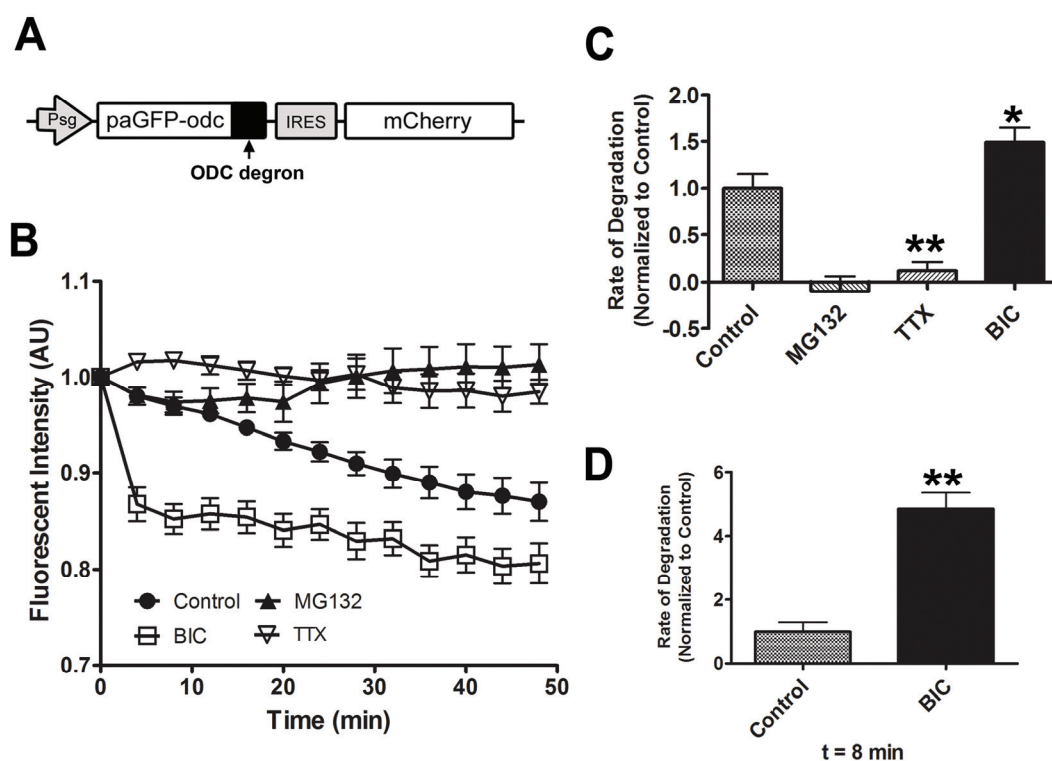


Figure 2-6: Action potential blockade and up-regulation produce opposite effects on proteasome activity in hippocampal neurons as monitored by our ubiquitin-independent proteasome reporter

A, Schematic of the paGFP-odc reporter Sindbis construct. The degradation sequence (degron) of ornithine decarboxylase (odc) is fused to the carboxyl terminus of paGFP, converting it into an ubiquitin-independent reporter of proteasome activity. mCherry is co-expressed using an IRES signal. *B*, Grouped analysis (plotted as line graphs \pm SEM) of dendritic paGFP-odc fluorescence intensity normalized to time zero. Cultured hippocampal neurons expressing paGFP-odc were treated with DMSO (Control), MG132 (25 μ M), BIC (40 μ M) or TTX (2 μ M) and imaged every 4 minutes for 48 minutes. *C*, Bar graph depicting the mean degradation rate \pm SEM (AU) per treated group relative to the control (paGFP-odc) rate of fluorescence intensity. TTX significantly blocks paGFP-odc degradation, while BIC significantly increases the rate of degradation. As expected, the rate of paGFP-odc degradation is blocked by MG132 (* - $P < 0.05$, ** - $P < 0.001$, relative to control). *D*, The BIC induced degradation was most dramatic in the first 8 minutes (** - $P < 0.001$, relative to control for 0 to 8 minute timepoint). See Table 2-2 for rates of degradation, and p and n values.

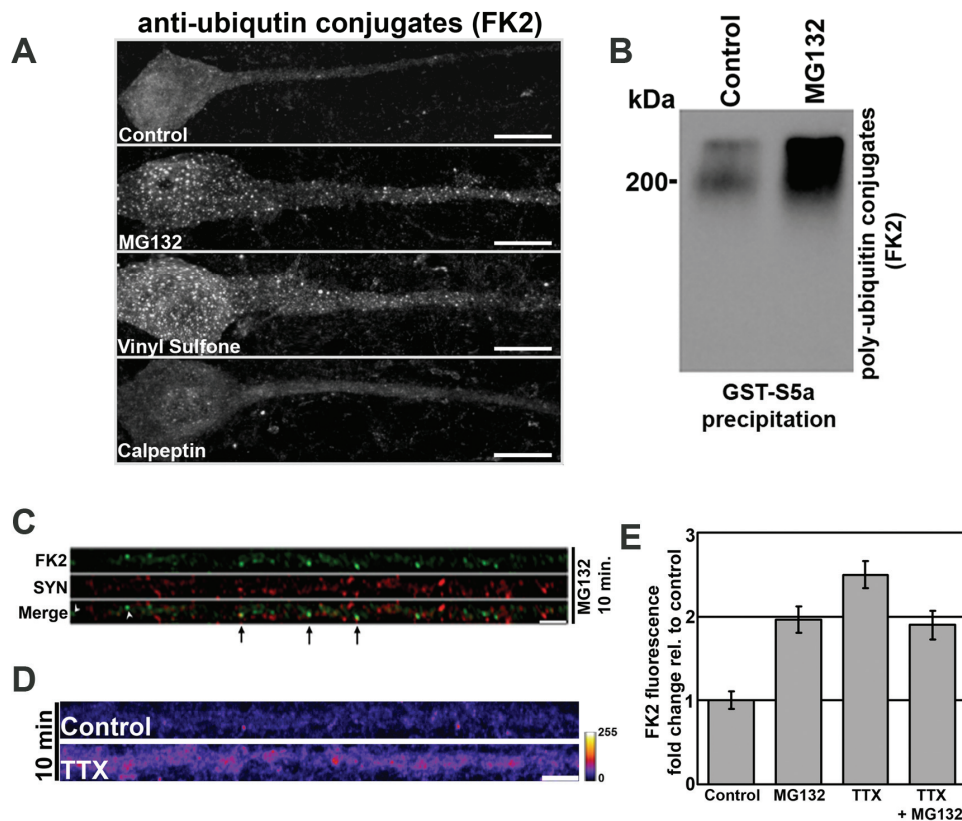


Figure 2-7: Proteasome inhibition or action potential blockade rapidly increase ubiquitin conjugate levels in hippocampal neurons

A, Hippocampal neurons were treated with either control (DMSO), MG132 (5 μ M), vinyl sulfone (1 μ M), epoxomicin (1 μ M) or calpeptin (10 μ M) for 10 minutes. Representative straightened dendrites with cell body are shown. As depicted proteasome inhibitors increase ubiquitin conjugate levels (FK2), while the calpain specific inhibitor, calpeptin, had no effect. Scale bar = 5 microns. *B*, Poly-ubiquitin conjugates from control and MG132 treated neurons are precipitated by GST-S5A, resolved on SDS-PAGE, and western blotted with FK2 antibody. *C*, Treatment of hippocampal neurons with MG132 (10 minutes) induces ubiquitin conjugate (FK2) positive puncta, many of which are juxtaposed with the pre-synaptic marker synapsin (SYN) (black arrows; FK2 - green, SYN - red). Scale bar is 10 microns. *D*, Action potential (AP) blockade with TTX rapidly increases ubiquitin conjugate levels in hippocampal neurons. Neurons were immunostained with FK2 after treatment with vehicle (DMSO) or TTX (2 μ M) for 10 minutes. Representative dendrites from each treatment are depicted. Scale bar = 5 microns. *E*, Co-application of the proteasome inhibitor MG132 with TTX for 10 minutes uncovers activity-regulated proteasome inhibition in hippocampal neurons. Relative to control treated neurons, TTX or MG132 rapidly increased ubiquitin conjugate levels at 10 minutes. The levels of ubiquitin conjugates induced by co-application of TTX and MG132 were not significantly different from either alone (*, $P < 0.001$). This suggests that action potential blockade with TTX mimics proteasome inhibition. Analysis of total FK2 fluorescence is depicted in bar graph (mean \pm SEM). Three separate experiments performed. $n = 30$ individual 63x fields (2-3 cells per field).

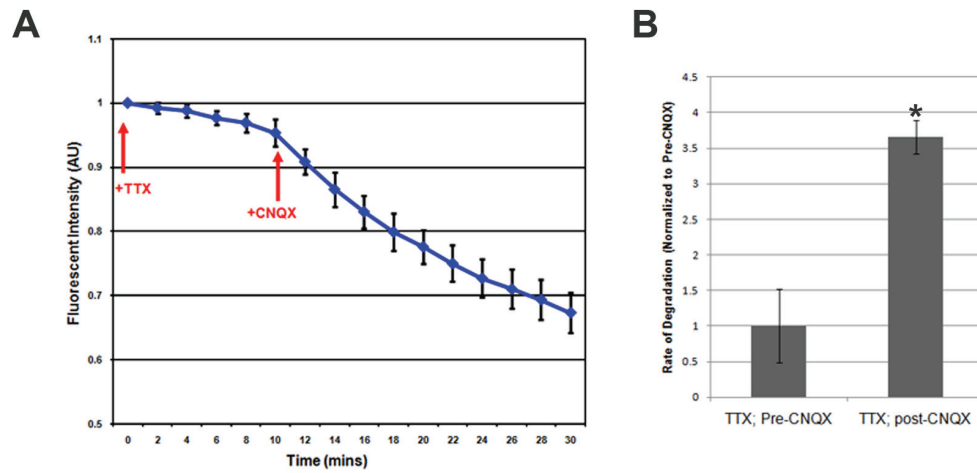


Figure 2-8: TTX-mediated proteasome inhibition requires mini EPSCs

A, Grouped analysis (plotted as line graphs \pm SEM) of dendritic paGFPu fluorescence intensity normalized to time zero. Cultured hippocampal neurons expressing paGFPu were treated with TTX for 10 minutes. CNQX was then added for 20 additional minutes to block all mini EPSCs. *B*, Bar graphs depict the mean degradation rate \pm SEM (AU) per treated group relative to the pre-CNQX rate of fluorescence intensity ($n=10$ imaged dendrites; * - $P < 0.001$).

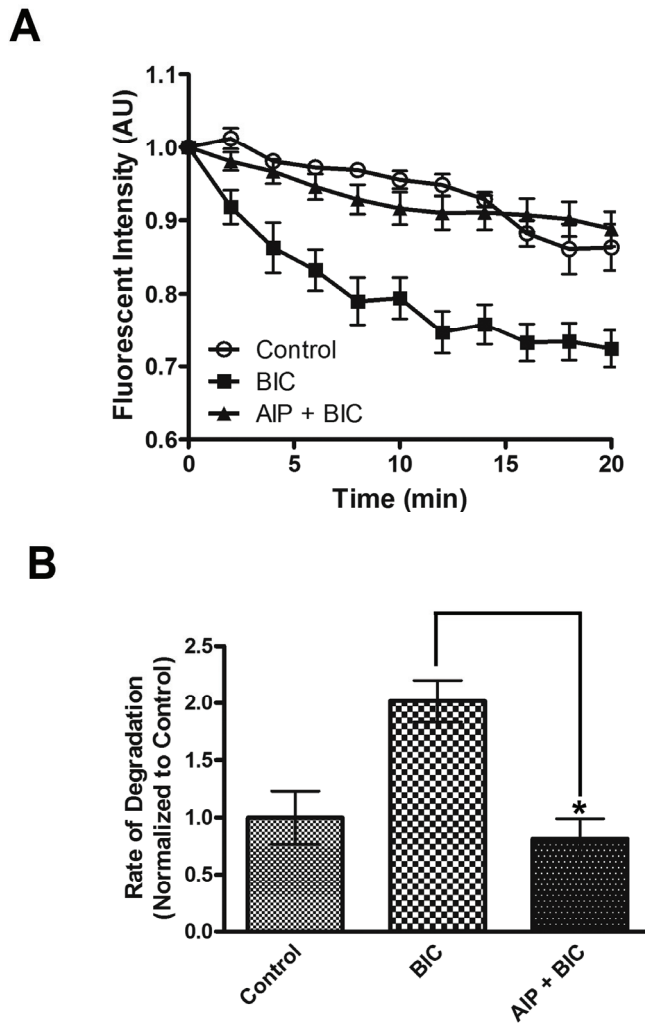


Figure 2-9: CaMKII is required for activity-dependent proteasome function in hippocampal neurons

A, The increased degradation of paGFPu induced by BIC is significantly blocked by CaMKII inhibitor myr-AIPII (AIP, 10 μ M). *A*, Line Graphs display grouped analysis (\pm SEM) of dendritic proteasome reporter fluorescence intensity normalized to time zero. *B*, Bar graphs depict the mean degradation rate \pm SEM (AU) per treated group relative to the control rate of fluorescence intensity ($n= 8, 19$ and 20 imaged dendrites for control, BIC and AIP + BIC respectively; * - $P < 0.01$).

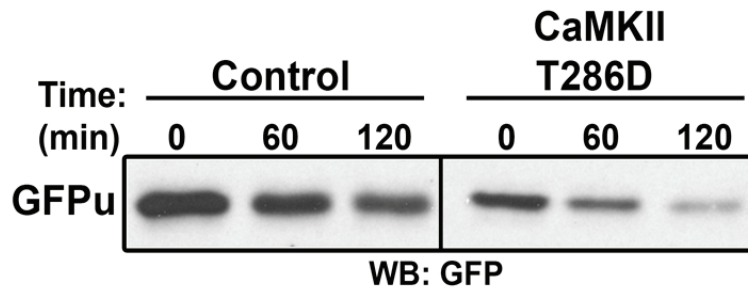
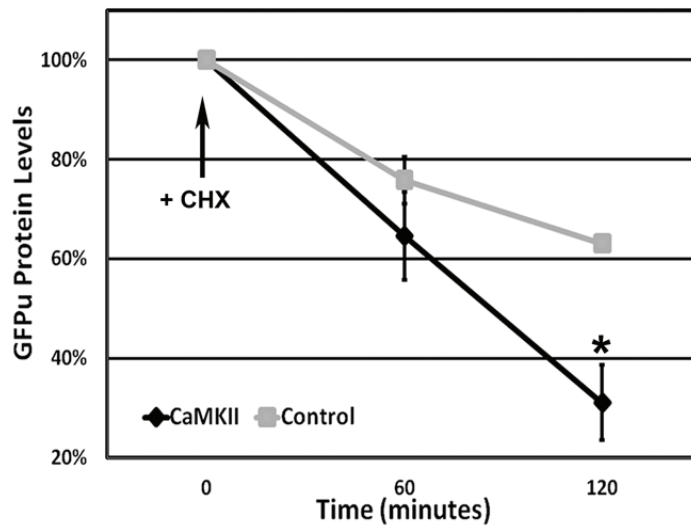
A**B**

Figure 2-10: CaMKII regulates *in vivo* proteasome function.

A, HEK293T cells were co-transfected with GFPu and either CaMKII T286D or control vector (β -gal). Cells were treated with protein synthesis inhibitor cycloheximide (CHX) for indicated time lengths, and equal amounts of protein were resolved by SDS-PAGE, and probed for total GFPu protein levels. *B*, Quantification of total GFPu protein levels in (A). CaMKII stimulates the rapid degradation of the GFPu proteasome reporter. (*, $p < 0.05$, t-test; $n = 3$).

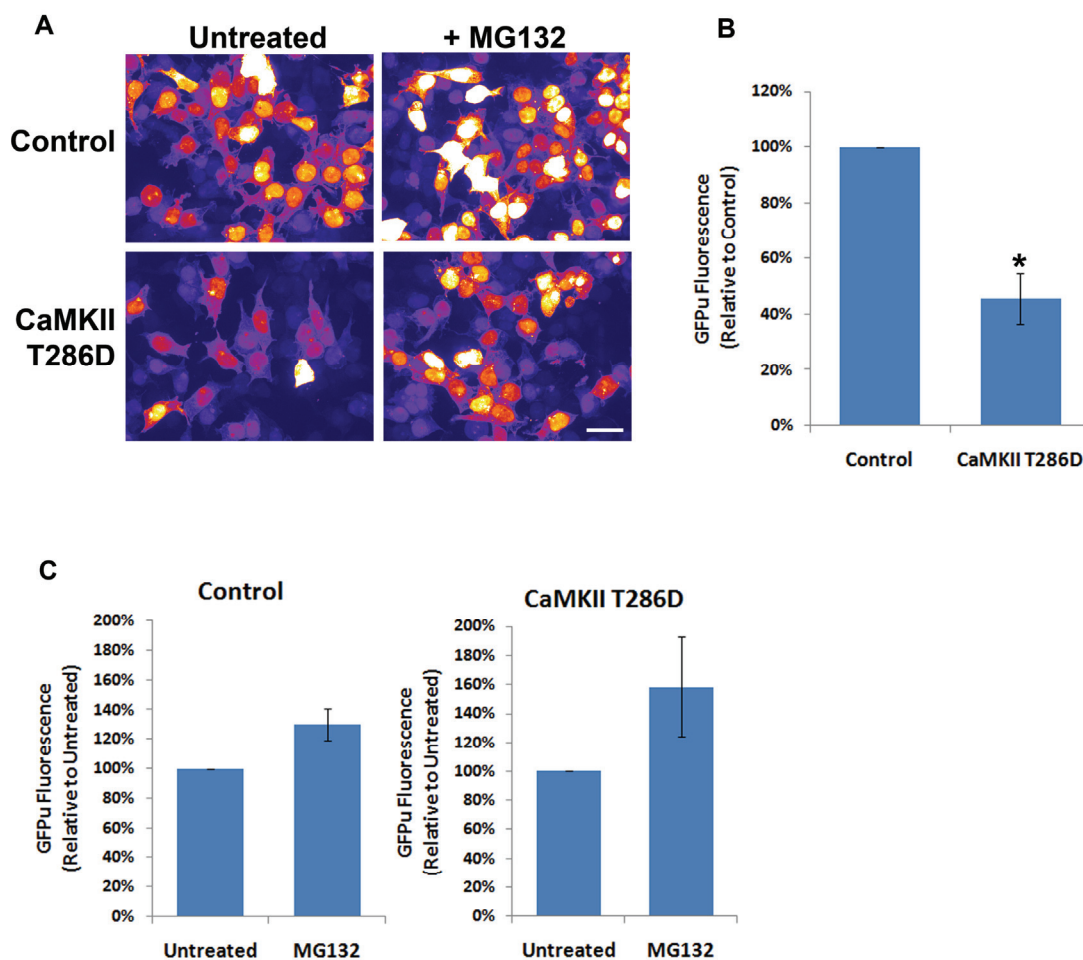


Figure 2-11: CaMKII T286D stimulates degradation of GFPu

A, Representative images of HEK293T cells co-transfected with GFPu degradation reporter and CaMKII T286D or empty vector (Control) for 20 hours, and then treated with MG132 (25 μ M) for 2 hours. (Scale bar = 25 micron; Color lookup is black to white, low to high fluorescence; $n=3$). *B*, Bar graph comparing total GFPu fluorescence in HEK293T cells after 20 hours. The steady state level of GFPu fluorescence is significantly lower in HEK293T cells transfected with CaMKII T286D (*, $p < 0.01$). *C*, Bar graph comparing total GFPu fluorescence of untreated and MG132 treated HEK293T cells. Incubation with MG132 for 2 hours increases GFPu fluorescence in both control and CaMKII T286D transfected cells.

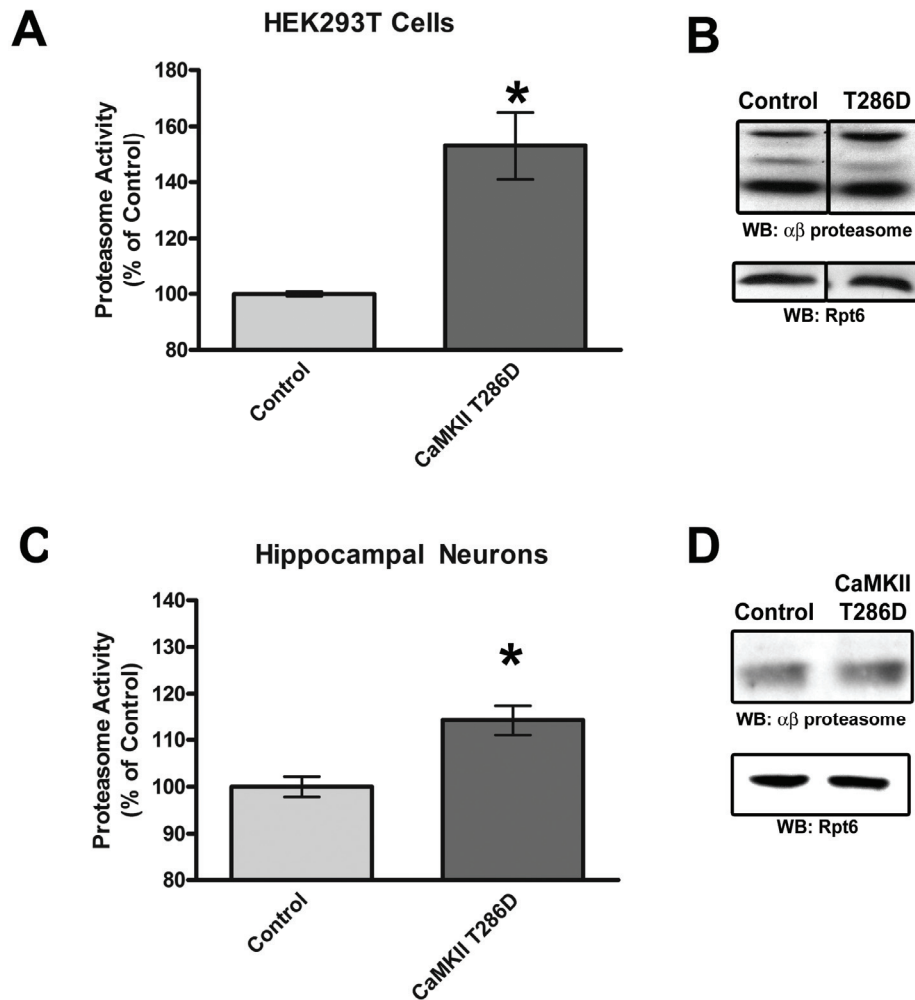


Figure 2-12: CaMKII regulates *in vitro* proteasome function.

A, HEK293T cells were transfected with either CaMKII T286D or control vector, and lysates were assayed for 26S proteasome activity with fluorogenic substrate Suc-LLVY-AMC. Bar graph depicting final fluorescent values (mean \pm SEM) relative to control. CaMKII significantly stimulates 26S proteasome activity *in vitro* (*, $p < 0.05$, t-test; $n=10$). *B*, Western blotting shows similar amount of total core ($\alpha\beta$ proteasome) and cap (Rpt6) proteasome subunits for HEK293T cells transfected with either CaMKII T286D or control vector. *C*, Cultured rat hippocampal neurons were infected with Control (GFP only) or CaMKII T286D (co-expressing GFP) Sindbis virion for 20 hours ($\sim 50\%$ infection rate). Proteasome activity was measured by Suc-LLVY-AMC hydrolysis. AMC fluorescence increased by $14.2 \pm 3.2\%$ in neurons overexpressing CaMKII T286D (*, $p < 0.01$, t-test; $n=15$). *D*, Western blotting similar equal amount of total core ($\alpha\beta$ proteasome) and cap (Rpt6) proteasome subunits for neurons infected with either CaMKII T286D or control virus.

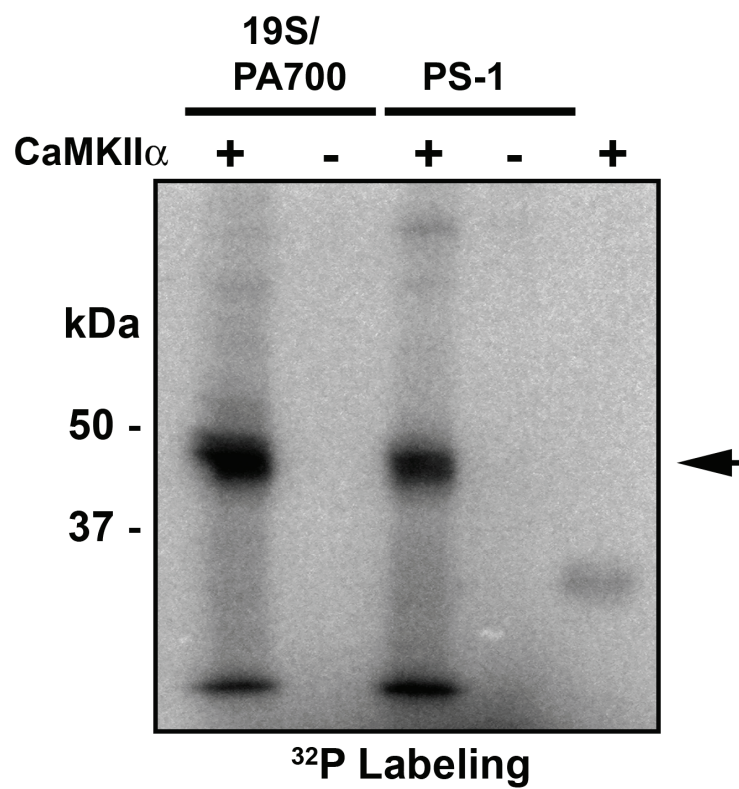


Figure 2-13: CaMKII α phosphorylates 19S/PA700

A, Equimolar amounts of 19S or PS-1 (19S subcomplex) were subjected to phosphorylation reactions with CaMKII α and ^{32}P -ATP under identical conditions and subjected to SDS-PAGE and autoradiography. CaMKII phosphorylates a 19S subunit of approximately 45 kDa (arrowhead).

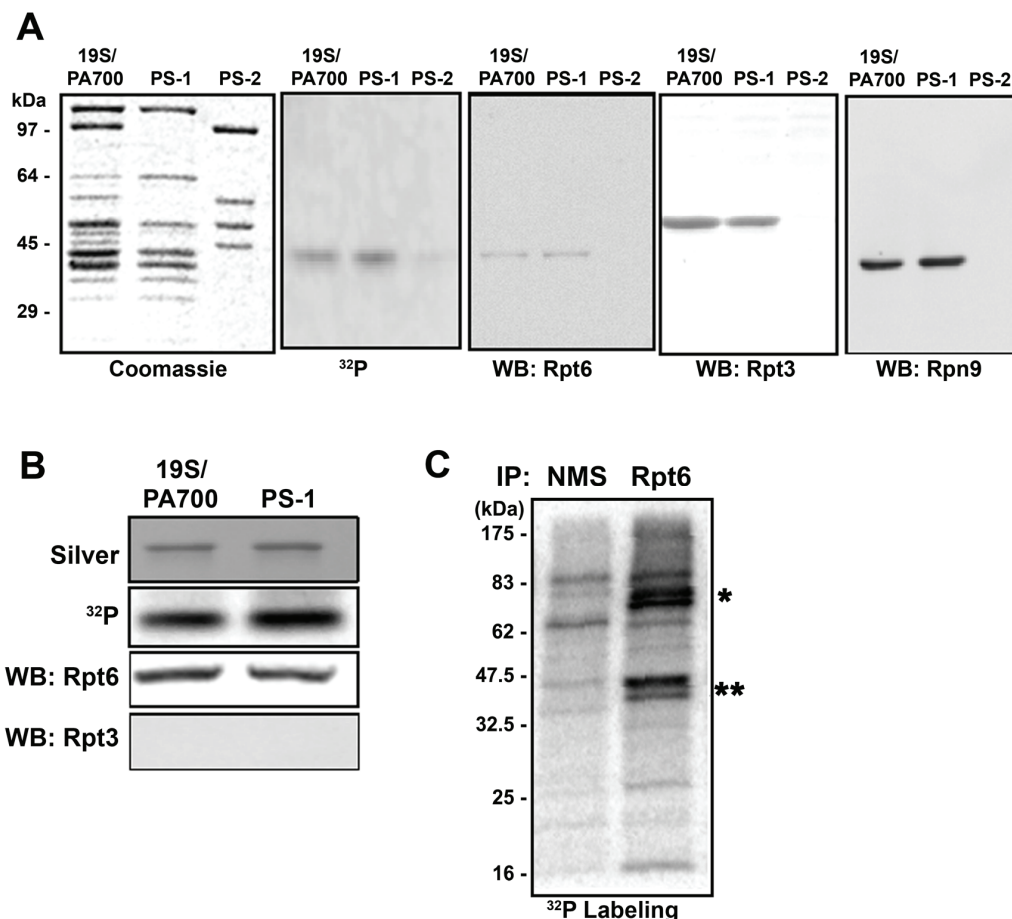


Figure 2-14: CaMKII α phosphorylates Rpt6, a specific subunit of 19S/PA700

A, Equimolar amounts of 19S or PS-1 (19S subcomplex) were subjected to phosphorylation reactions with CaMKII α and ^{32}P -ATP under identical conditions. Phosphorylated 19S, PS-1 or PS-2 (19S subcomplex that does not contain Rpt6) were subjected to SDS-PAGE and samples were analyzed by protein staining, autoradiography and western blotting for the indicated 19S subunits. Gels are aligned for direct comparison. *B*, The ^{32}P labeled proteins were excised from the gel, solubilized and re-subjected to SDS-PAGE. The gel was analyzed for labeled protein and subjected to western blotting for the indicated proteins. *C*, Representative autoradiogram of ^{32}P orthophosphate labeling for immunoprecipitations of Rpt6 from cortical neuron lysates. Normal mouse serum (NMS) served as a control IP. The two highly phosphorylated bands at 45-47 kDa (**) present in the RPT6 IP are likely Rpt6 and another 19S Rpt subunit. Two highly phosphorylated bands at 70-80 kDa (*) do not correspond to any proteasome subunits.

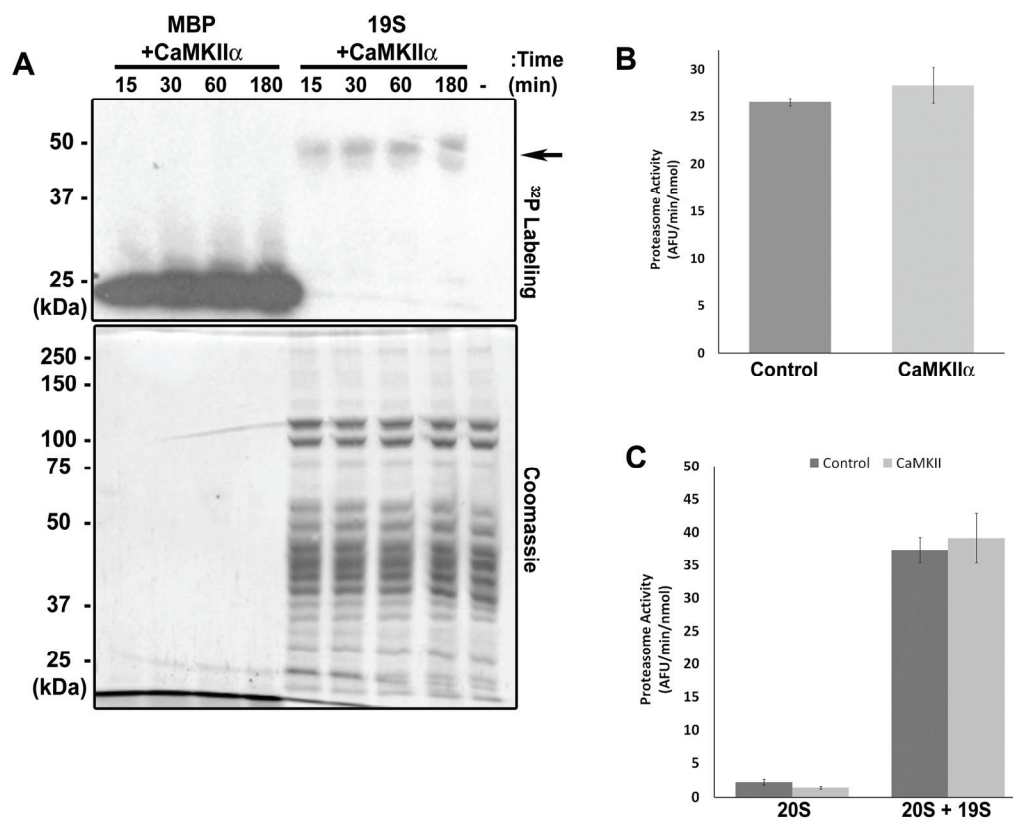


Figure 2-15: Phosphorylation of 19S by CaMKII does not regulate proteasome function *in vitro*

A, CaMKII α rapidly phosphorylated 19S proteasome. Purified CaMKII α was added to purified MBP (CaMKII α control substrate) or 19S complex for up to 180 minutes *in vitro*. Autoradiography shows 19S proteasome subunits of ~45-47 kDa (black arrow) 32 P labeled by CaMKII α within 15 minutes (top). Total protein stain by Coomassie (bottom) displays all 19S proteasome subunits. *B*, Purified CaMKII α was added to purified 26S proteasome and subsequently assayed for Suc-LLVY-AMC hydrolysis. Phosphorylation by CaMKII α had no effect on proteasome activity. No increase in proteasome activity (as measured by AMC fluorescence) over control (no kinase) was observed. *C*, Purified 20S (core) was added to purified 19S (cap) proteasome with or without addition of purified CaMKII α and subsequently assayed for Suc-LLVY-AMC hydrolysis. Phosphorylation by CaMKII α had no effect on proteasome core-cap assembly. An increase in assembly would lead to an increase in proteasome activity. No increase in AMC fluorescence was observed.

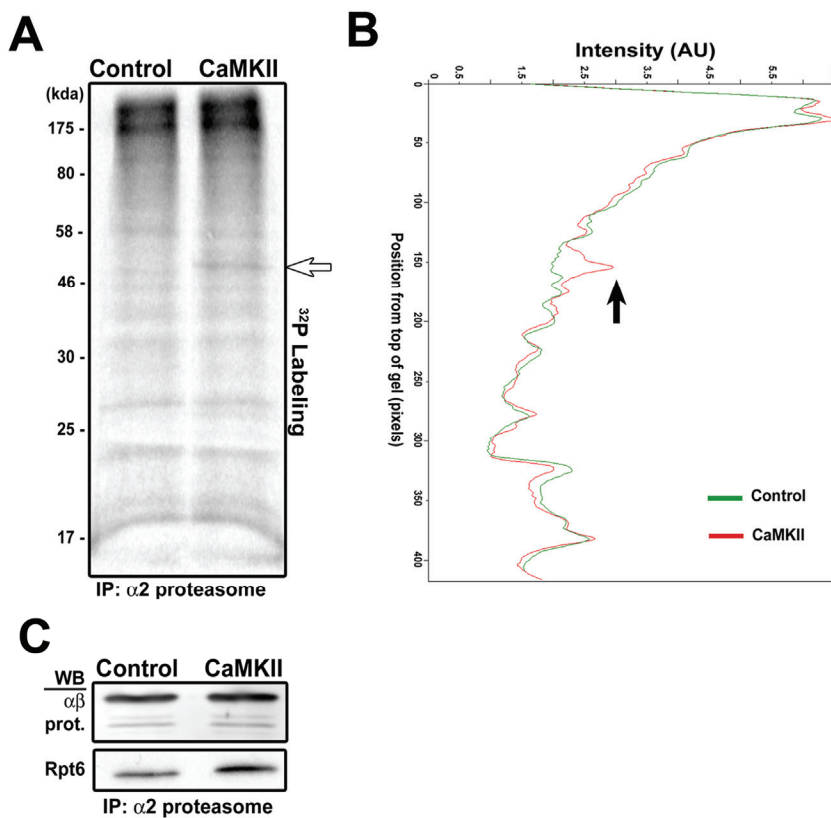


Figure 2-16: CaMKII dependent phosphorylation of proteasome or proteasome interacting proteins *in vivo*

HeK293T cells were transfected with either empty vector or constitutively active CaMKII (T286D) and labeled with ^{32}P orthophosphate. *A*, Representative autoradiogram for ^{32}P orthophosphate labeling of immunoprecipitated 26S proteasome (IP: $\alpha 2$ proteasome). White arrow denotes CaMKII stimulated phosphorylation. $n=3$. *B*, Line scan analysis of autoradiogram from (*A*) highlights the induction of a phosphorylated protein at around 45-47 kDa (black arrow) similar to the molecular weight of Rpt6. *C*, Western Blot analysis of immunoprecipitated core ($\alpha\beta$ prot) or 19S (Rpt6) proteasomes.

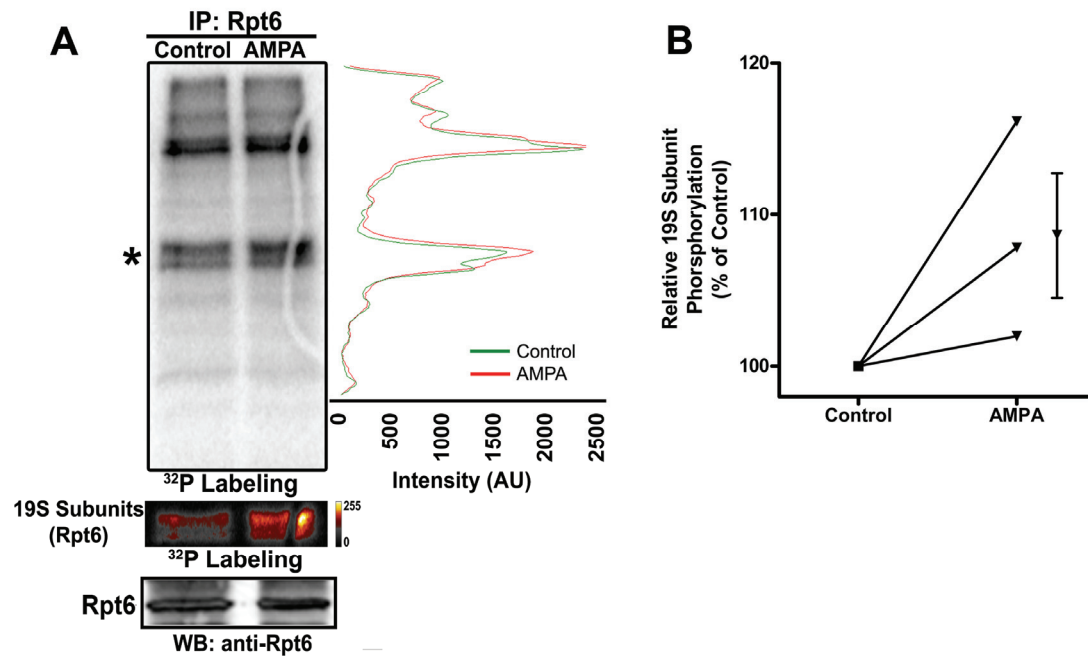


Figure 2-17: Neuronal Activity induces phosphorylation of Rpt6

A, Representative autoradiogram (left) and line-scan analysis (right) from ^{32}P orthophosphate labeling experiments where cultured cortical neurons were treated with AMPA receptor agonist (15 minutes, 100 μM AMPA). 19S regulatory cap of the proteasome was immunoprecipitated with an antibody to Rpt6. AMPA induces phosphorylation of two 19S subunit bands (*), where the top band aligns with Rpt6. Autoradiograph signal of 19S subunit bands are cropped and artificially colored to highlight the increase of phosphorylation upon AMPA stimulation (middle). Rpt6 immunoreactivity confirmed equal amount of immunoprecipitation of 19S proteasomes (bottom). *B*, Autoradiograph signal of 19S subunit bands from (A) are quantified from 3 independent orthophosphate labeling experiments and plotted as percent of control band intensity. Summary of values from AMPA treatments are plotted as mean \pm SEM (on right). ($p=0.17$, t-test; $n=3$).

Table 2-1: paGFPu mean rates of degradation

Rates are listed as percent fluorescent decay (\pm SEM) per 2 or 4 minute interval respectively. *P*-values listed are in comparison to the reference group using two-tailed unpaired students T-test. n = number of imaged dendrites.

paGFPu rates of degradation			
<i>Conditions</i>	<i>Rate of Degradation¹</i>	<i>p-value</i>	<i>Number of imaged dendrites</i>
Control ^a	2.43 +/- 0.50		21
MG132	0.58 +/- 0.39	0.009	16
Vinyl Sulfone	0.55 +/- 0.29	0.025	9
Epoxomicin	0.87 +/- 0.18	0.035	11
Calcium Free	0.67 +/- 0.19	0.012	13
APV	1.34 +/- 0.27	0.115	13
Nimodipine	1.70 +/- 0.05	0.418	7
CNQX	2.14 +/- 0.28	0.704	10
BIC, t:10 min	5.67 +/- 0.51	< 0.001	27
t:20 min	4.06 +/- 0.37	0.01	27
t:60 min	1.65 +/- 0.07	0.47	5
AMPA	5.90 +/- 0.34	< 0.001	11
TTX	1.13 +/- 0.10	0.02	19
KN-93	1.39 +/- 0.12	0.076	16
paGFP ^b	0.25 +/- 0.25	0.003	13
BIC ^a	4.06 +/- 0.37		27
MG132 + BIC	1.54 +/- 0.31	0.001	8
Calpeptin + BIC	3.92 +/- 0.40	0.814	15
paGFP ^b + BIC	1.27 +/- 0.12	< 0.001	12
APV + BIC	1.90 +/- 0.26	< 0.001	14
Nimodipine + BIC	1.67 +/- 0.30	0.001	10
CNQX + BIC	1.25 +/- 0.16	0.003	5
KN-93 + BIC	1.58 +/- 0.11	< 0.001	17

¹Percent fluorescence decay per 2 minute interval. ^aIndicates Reference Category. ^bpaGFP no-degron control reporter. BIC = Bicuculline. p-value determined by two-tailed unpaired student's t-test.

Table 2-2: paGFP-odc mean rates of degradation

Rates are listed as percent fluorescent decay (\pm SEM) per 2 or 4 minute interval respectively. *P*-values listed are in comparison to the reference group using two-tailed unpaired students T-test. n = number of imaged dendrites.

<i>Conditions</i>	<i>Rate of Degradation¹</i>	<i>p-value</i>	<i>Number of imaged dendrites</i>
Control^a	1.09 +/- 0.17		14
MG132	-0.11 +/- 0.18	< 0.001	14
Calcium Free	0.22 +/- 0.23	0.007	16
TTX	0.13 +/- 0.10	< 0.001	12
BIC	1.62 +/- 0.17	0.036	15
KN-93	0.88 +/- 0.04	0.274	12
BIC^a	1.62 +/- 0.17		15
KN-93 + BIC	1.03 +/- 0.16	0.021	12
BIC, t:8 min^a	7.40 +/- 0.77		15
Control, t:8 min	1.53 +/- 0.45	< 0.001	14
KN-93 + BIC, t:8 min	1.46 +/- 0.34	< 0.001	12
¹ Percent fluorescence decay per 4 minute interval. ^a Indicates Reference Category. BIC = Bicuculline. p-value determined by two-tailed unpaired student's t-test.			

Table 2-3: Identification of Rpt6 by mass spectrometry

Purified 19S/PA700 was incubated with CaMKII for phosphorylation with ^{32}P -ATP. The area of the gel containing the labeled subunit was excised; the protein was solubilized and rerun on SDS-PAGE. The area of label protein was excised, subjected to treatment with trypsin for identification of peptides by mass spectrometry. Only peptides corresponding to 19S subunit Rpt6 were identified (18.5% coverage).

Rpt6 tryptic peptides
R.VSGSELVQK
K.VIMATNR.I
K.GVLLYGPPGTGK
K.IEFPPNNEEAR
K.IAELMPGASGAEVK
R.VHVTQEDFEMAVAK
R.NDSYTLHK
R.HPELFEALGIAQPK
K.VDPLVSLMMVEK.V
R.LEGGSGGDSEVQR.T
R.TMLELLNQLDGFEATK.N
R.EHAPSIIFMDEIDSIGSSR.L
K.EVIELPVKHPELFEALGIAQPK.G

Chapter III

Phosphorylation of Rpt6 Regulates Proteasome Function and Synaptic Strength

INTRODUCTION

Synaptic plasticity is a complex process that requires the selective remodeling of synaptic connections. This remodeling requires dynamic alterations in the molecular composition of the synapse [1], which has been shown to depend on new protein synthesis [2,3]. Protein degradation, on the other hand, provides an additional mechanism to modify the stoichiometry of synaptic proteins to promote, limit, or restrict plasticity.

The ubiquitin proteasome system (UPS) is a major pathway for regulated protein turnover in eukaryotic cells. The selective degradation of proteins via the UPS involves three steps: recognition of the target protein, tagging the target protein with ubiquitin chains by ubiquitin ligases, and delivery of the target protein to the 26S proteasome for degradation [5]. The 26S proteasome is a large energy-dependent protease consisting of two multi-protein subcomplexes: the proteolytic 20S core particle (CP) and 19S regulatory particle (RP). The 20S CP consists of α and proteolytic β subunits. The 19S RP consists of two distinct functional components: the “base” consisting mainly of Rpt6 ATPase subunits, and the “lid” consisting mainly of Rpn non-ATPase subunits [9].

The UPS plays an essential role in the development, maintenance, and remodeling of synaptic connections [4,104,105,106]. Several studies have identified key synaptic proteins such as PSD-95, Shank, GKAP, AKAP, SPAR, RIM-1, Arc and GRIP1 whose stabilities are regulated by UPS dependent protein turnover [50,55,63,92,109,110]. Indeed, large cohorts of synaptic proteins can be degraded in

response to chronic activity blockade or up-regulation [92]. The signals that regulate this activity-dependent protein degradation remain elusive though.

The regulation of protein ubiquitination has been extensively studied. Although the structure and function of the proteasome has been well studied [17], relatively little is known about how it is regulated. There is increasing evidence that the proteasome may be regulated by interacting proteins or posttranslational modifications such as glycosylation or phosphorylation [30,95,111,112]. Indeed, we previously showed that CaMKII phosphorylates the proteasome and stimulates its activity [156]. In this study we aimed to determine how CaMKII-dependent phosphorylation regulates proteasome function. We identified Serine 120 (S120) of Rpt6 as the site of phosphorylation by CaMKII. We found that phosphorylation of Rpt6 S120 regulates activity-dependent stimulation and detergent resistance of the proteasome. Additionally, we provide evidence that regulation of proteasome function by phosphorylation of Rpt6 is sufficient to modify synaptic strength. This data uncovers a novel mechanism for regulation of proteasome in neurons. Additionally, it solidifies the importance of regulated protein degradation by the UPS in the plasticity of synaptic connections.

RESULTS

Rpt6 is phosphorylated at serine 120 by CaMKII

We previously showed that proteasome subunit Rpt6 is phosphorylated by CaMKII, a kinase that plays a key role in synaptic function [156]. Rpt6, also known

as *psmc5*, is a 45 kDa ATPase subunit in the 19S regulatory particle of the proteasome. Rpt6 binds Rpt1-5 to form a hexameric ring, known as the “base” of the 19S. All six Rpt proteins have two main functional domains: an N-terminus coiled-coil domain important for formation of the base, and a C-terminus ATPase domain which is involved in ATP-dependent substrate unfolding and 20S CP opening [10]. Studies on Archaea proteasomes have identified an additional functional domain in Rpt proteins, known as the OB fold, which has ATP-independent chaperone activity [157,158](Figure 3-1B).

For this study we aimed to gain further insight into molecular mechanisms of CaMKII-dependent proteasome regulation in neurons. First, we sought to identify the site of CaMKII phosphorylation on Rpt6. Using phosphorylation site prediction software [159], Serine 120 (S120) of Rpt6 was identified as a potential CaMKII phosphorylation site (Figure 3-1B). Recent mass spectrometry studies have also identified S120 as the site phosphorylated by CaMKII [100]. Interestingly, S120 has previously been shown to also be phosphorylated by PKA [32]. To determine the significance of this phosphorylation event, Rpt6 S120 phospho-mutants were created. Serine was mutated to Alanine (S120A) to create a phospho-dead mutant (Figure 3-2A). This prevents phosphorylation at that residue, although CaMKII may phosphorylate another residue as we cannot definitively say that S120 is the only phosphorylation site on Rpt6. Serine was also mutated to Aspartic Acid (S120D) to create a phosphor-mimetic mutant (Figure 3-2A). Our HA tagged phospho-mutants were expressed in HEK293 cells, and proteasomes were immunoprecipitated with an

antibody to the 20S CP subunits. S120A and S120D phospho-mutants, and wild-type (WT) Rpt6 immunoprecipitated with the 20S CP at similar levels (Figure 3-2B). This suggests that S120 phosphorylation is not required for incorporation of Rpt6 into the proteasome.

To directly determine if Rpt6 is phosphorylated by CaMKII *in vivo*, a phospho-specific-antibody against S120 was generated. The specificity of our antibody was verified as it recognized WT Rpt6 expressed in HEK293 cells, but not Rpt6 S120A phospho-dead mutant by western blot. Our antibody also slightly cross reacted with the S120D phospho-mimetic mutant (Figure 3-3A). Interestingly co-expression with a constitutively active form of CaMKII (T286D) lead to a significant increase in phosphorylation of WT Rpt6 *in vivo* as measured by our phospho-specific antibody (~3 Fold increase, Figure 3-3B). To show additional specificity of our antibody, the nitrocellulose membrane was treated with lambda phosphatase. Treatment with the phosphatase blocked the majority of antibody staining, suggesting that our antibody is specific to phosphorylated S120, with little cross-reactivity to the unphosphorylated residue (Figure 3-3D). Additionally, our phospho-specific antibody immunoprecipitated WT Rpt6 only after co-expression with CaMKII (Figure 3-3E). Together these results provide strong evidence that Rpt6 is phosphorylated at S120 by CaMKII.

Phosphorylation of Rpt6 regulates proteasome function

Rpt6 is a 19S base subunit that is an important regulator of many aspects of proteasome function, including assembly, protein unfolding and 20S CP activation [10,19,144]. We previously showed that CaMKII stimulates activity of the proteasome [156]. We hypothesized that CaMKII dependent activation of proteasome required S120. Overexpression of our S120A or S120D Rpt6 phospho-mutants had no significant effect on proteasome activity compared to WT Rpt6 in HEK293 cells or hippocampal neurons (Figure 3-4A and Figure 3-4B). Interestingly, overexpression of S120A was able to prevent CaMKII-dependent stimulation of the proteasome (CaMKII, $121 \pm 4.0\%$ relative to control; S120A + CaMKII, $89.6 \pm 2.1\%$ relative to control) (Figure 3-4C). This is supported by a previous study that showed that expression of Rpt6 S120 blocked activation of proteasome following addition of purified CaMKII to cell lysates [100]. Therefore, phosphorylation of S120 is likely to be necessary, but not sufficient for activation of the proteasome.

The 26S proteasome has been shown to translocate to synaptic spines following neuronal stimulation [99]. We were interested to see if our Rpt6 phospho-mutants would have distinct localization patterns. While S120D appeared to slightly enrich at synapses, there was no significant differences from WT Rpt6. Rpt6 S120A had less synaptic localization compared to WT, although again, the difference was not statistically significant. It was previously reported that sequestration of the proteasome in synaptic spines required association with the actin cytoskeleton [99]. We next asked whether phosphorylation of Rpt6 regulated association with the actin cytoskeleton. Synaptic proteins resistant to Triton X-100 extraction are tethered to the

postsynaptic density by association with the actin cytoskeleton [160]. We examined whether phosphorylation of Rpt6 was involved in the detergent resistance of the proteasome by both immunofluorescent and biochemical staining. Rpt6 S120D had significantly increased detergent resistance relative to WT (Figure 3-6). This result is similar to the increased triton resistance of the proteasome in response to NMDA stimulation [99]. In contrast, S120A was more readily extracted by triton X100 treatment (Figure 3-6). This suggests that phosphorylation regulates association of Rpt6, and possibly the entire proteasome complex, to the actin cytoskeleton.

Phosphorylation of Rpt6 regulates synaptic strength

The UPS has been shown to be essential for many aspects of synaptic function. Inhibition of the proteasome blocks activity-dependent changes in synaptic strength during both LTP and LTD [4]. We hypothesized that modifying proteasome function by Rpt6 phosphorylation would lead to changes in synaptic strength. Miniature EPSCs (mEPSCs) are spontaneous synaptic events that are commonly used as readouts of synaptic strength [161]. Our phospho-mutants were expressed in cultured hippocampal neurons for 20 hours, and mEPSC frequency and amplitude were measured. mEPSC amplitude, but not frequency was significantly affected by phospho-mutant expression (Figure 3-7). This implicates an effect on postsynaptic function. Interestingly the effects were bidirectional. Overexpression of Rpt6 S120D caused a significant decrease in mEPSC amplitude (11.37 ± 0.63 pA), while S120A lead to a significant increase in mEPSC amplitude (17.90 ± 0.76 pA) compared to WT

infected neurons (14.73 ± 1.16 pA) (Figure 3-7B). Similar effects on mEPSC amplitude are also observed during homeostatic plasticity in response to chronic activity upregulation or blockade [161]. Phosphorylation of Rpt6 S120 may be a key mechanism for activity dependent synaptic remodeling during homeostatic plasticity.

To determine if proteasome regulation is involved in homeostatic plasticity, we monitored the activity of the proteasome during chronic activity blockade or upregulation. In previous studies we showed that the activity of the proteasome is regulated immediately following neuronal activity blockade or upregulation. To accomplish this we utilized a paGFPu proteasome reporter to monitor dynamics of proteasome activity [156]. Here we asked whether degradation of paGFPu was altered following chronic upregulation or blockade. Following 10 hours of treatment of TTX (activity blockade) or Bicuculline (activity upregulation) neurons expressing paGFPu were fixed and imaged. Fluorescence of paGFPu was significantly higher in neurons treated with TTX, likely due to a block of the proteasome ($118 \pm 5.0\%$ relative to control). In contrast, paGFPu was efficiently degraded in neurons stimulated with Bicuculline, likely due to an activation of the proteasome ($50.0 \pm 3.7\%$ relative to control) (Figure 3-8A and Figure 3-8B). No changes in fluorescence were observed in our paGFP control expressing neurons (Figure 3-8C and Figure 3-8D), providing evidence that the observed results are dependent on proteasome activity. The changes in paGFPu degradation during chronic activity modification are likely due to regulations of proteasome function, possibly through phosphorylation of Rpt6 S120.

DISCUSSION

The remodeling of synaptic connections requires modifications of the molecular composition of the postsynaptic density [1]. This process is dependent on neuronal activity, is bi-directional, and requires activity of the UPS [92]. Therefore, it is quite plausible that neuronal activity regulates UPS function to control the stoichiometry of proteins at synapses.

Regulated proteolysis by the UPS has been typically studied at the level of the ubiquitination. Interestingly, neuronal activity has been shown to regulate activity of E3 ligases such as E6-AP and TRIM3 [63,162]. Additionally, neuronal activity also regulates the ubiquitination of multiple synaptic substrates such as, Arc, GKAP, Shank and AKAP [63,92]. Very little is known about the regulation of the proteasome in neurons. Recently data has shown that CaMKII mediates the translocation of proteasomes into synaptic spines in response to neuronal activity [99,100]. Furthermore, NAC1, a cocaine-regulated transcriptional protein interacts with the proteasome to regulate the trafficking of the proteasome in an activity-dependent manner [101]. These data suggest that neuronal activity can promote the redistribution of proteasomes into synapses to regulate protein degradation and remodeling of synaptic connections. However, a clear understanding of the synaptic molecular mechanisms involved to regulate proteasome trafficking and activity is far from understood.

Mechanisms of proteasome regulation remain elusive, even in non-neuronal cell types. Phosphorylation has been shown to extensively regulate ubiquitination of

substrates by mediating interaction with or activity of E3 ligases [25]. Recent evidence suggests that the proteasome may also be regulated by phosphorylation [112]. We previously showed that Rpt6 is the proteasome subunit phosphorylated by CaMKII, an important protein kinase involved in synaptic plasticity [156]. Here we show that Rpt6 is phosphorylated at S120 in a CaMKII-dependent fashion. Rpt6 has been previously shown to also be phosphorylated at S120 by PKA [32]. While phosphorylation of this site is not sufficient to regulate proteasome activity, it is necessary for CaMKII-dependent stimulation of the proteasome. Indeed, in Zhang et al. S120 was required for PKA dependent stimulation of proteasome activity [32]. Together, this suggests that phosphorylation of Rpt6 at S120 may be a key mechanism for regulating the function of the proteasome in response to neuronal activity.

The functional significance of S120 phosphorylation remains unclear though. Rpt6 has two main functional domains: an N-terminus coiled-coil domain important for formation of the 19S base, and a C-terminus ATPase domain which is involved in ATP-dependent substrate unfolding and 20S CP opening [10]. Studies on Archaea proteasomes have identified an additional functional domain in Rpt6, known as the OB fold, which contains S120. This domain has been shown to be involved in energy independent chaperone activity which is crucial for preventing aggregation of unfolded proteins and then funneling them into the 20S CP for degradation [157,158]. While phosphorylation is thought to regulate assembly or proteolytic activity [112], it is still unclear how S120 regulates proteasome function.

Interestingly we find that phosphorylation at S120 promotes detergent resistance of Rpt6. This is likely due to increased association with the actin cytoskeleton, presumably to tether the proteasome in postsynaptic compartments. NMDA stimulation was also shown to increase detergent resistance of the proteasome [99]. NMDA stimulation induces postsynaptic calcium influx, causing activation and synaptic translocation of CaMKII [163]. CaMKII also acts as a scaffold to recruit proteasomes into synaptic spines [100]. It is likely that phosphorylation of Rpt6 is required for the association with CaMKII and trafficking into spines. Alternatively, the phosphorylation may be required for tethering of the proteasomes to the postsynaptic compartment after trafficking by regulating association with PSD components.

Electrophysiology experiments suggest that phosphorylation of S120 is important for proteasome dependent synaptic remodeling. A phospho-mimetic Rpt6 S120 mutant leads to a decrease in mEPSC amplitude, while a phospho-dead mutant causes an increase in mEPSC amplitude. We previously showed that the proteasome is stimulated in response to neuronal activity. Specifically, Bicuculline stimulation increases proteasome activity [156], presumably by CaMKII-dependent phosphorylation of Rpt6. Indeed chronic Bicuculline stimulation also decreases synaptic strength [161], mimicking our results with phospho-mimicked Rpt6. Additionally, we showed that TTX inhibits the activity of the proteasome [156], possibly by blocking phosphorylation of Rpt6. Chronic inhibition of neuronal activity with TTX has been shown to increase synaptic strength [161], again mimicking our

results with phospho-dead Rpt6. This suggests that phosphorylation of Rpt6 may mediate protein degradation required for synaptic changes during periods of chronic activity stimulation or blockade.

Proteasome function has been shown to be required for various learning, memory and behavior related paradigms such as LTP, LTD and fear memory consolidation [48,49,68,148,149]. Our findings support a role for the direct modulation of proteasome activity in neurons to be important for synaptic plasticity. This is substantiated by our findings that CaMKII-dependent phosphorylation of Rpt6 regulates proteasome function. We predict neurons to utilize this mechanism to synergize tunable proteasome activity with the dynamic ubiquitination of substrates for degradation. This in turn facilitates protein degradation and alterations in the stoichiometry of synaptic proteins to promote the plasticity of synaptic connections.

MATERIALS AND METHODS

Antibodies and reagents

$\alpha 7$ proteasome (mAb), $\alpha\beta$ core proteasome (pAb) and Rpt6 (mAb) antibodies were purchased from Biomol. HA (mAb) antibody is from Covance. Actin (mAb) antibody from Abcam. We made a rabbit anti-Rpt6 pS120 antibody by custom commercial preparation (ProSci, Inc., Poway, CA) against a synthetic peptide that was phosphorylated at S120 [NH₂-ALRND(pS)YTLHK-OH]. The following pharmacological reagents were used: bicuculline (BIC) and tetrodotoxin (TTX) from Tocris Bioscience. Suc-LLVY-AMC fluorogenic substrate from Biomol. λ

phosphatase from New England Biolabs. Protease (complete EDTA-free) and phosphatase (Phostop) inhibitor cocktails from Roche.

DNA and Sindbis constructs

RSV-CaMKII T286D was a kind gift from Anirvan Ghosh (UC San Diego, La Jolla, CA). Rat Rpt6 was cloned into Prk5. An HA tag was attached to the N-terminus of Rpt6. Serine to Alanine (S120A) phospho-dead or Aspartic acid (S120D) phospho-mimetic mutants were created using quick change site directed mutagenesis. HA-Rpt6 (wild type, S120A and S120D) was then cloned into pSinrep5. Sinrep5 pSG promoter was duplicated and GFP was inserted downstream of the promoter for co-expression. paGFPu, a fusion of the CL1 degron (degradation signal) on the carboxyl terminus of paGFP, was a modified version of GFPu that was kindly provided by Ron Kopito (Stanford University, Palo Alto, CA). GFPu is ubiquitinated and specifically degraded by the proteasome [91,113,114]. Sindbis paGFP and paGFPu were constructed as previously described [156]. For production of recombinant Sindbis virions, RNA was transcribed using the SP6 mMessage mMachine Kit (Ambion, Austin, TX), and electroporated into BHK cells using a BTX ECM 600 at 220V, 129 Ω , and 1050 μ F. Virion were collected after 24-32 hours and stored at -80°C until use.

Immunoprecipitation

HEK293T cells were transfected for 24-36 hours. Cells were lysed in proteasome IP buffer (25 mM Tris (pH 7.5), 10% Glycerol, 2.5 mM MgCl₂, 5 mM

ATP, 1 mM DTT, 0.5% NP40, protease and phosphatase inhibitor cocktails. Lysates were immunoprecipitated for 24 hours with indicated antibodies and Protein A or G agarose beads, and resolved by SDS-PAGE.

Neuronal cultures

Rat dissociated hippocampal neurons from postnatal day 1 or 2 were plated at a density of 45,000 cells/cm² onto poly-D-lysine coated coverslips or glass bottom 35 mm dishes (Mattek, Ashland, MA) and maintained in B27 supplemented Neurobasal media (Invitrogen) until 17 days or more as previously described [59]. High density rat cortical or hippocampal neurons from postnatal day 1 were plated onto poly-D-lysine coated 6-well dishes (~500,000 cells per well) and maintained in B27 supplemented Neurobasal media.

26S Proteasome fluorogenic peptidase assays

In vitro assay of 26S proteasome chymotryptic activity was performed as previously described [151] with slight modifications. HEK293T cells were transfected with HA-Rpt6 (WT, S120A, or S120D) and RSV-CaMKII T286D for 24-36 hours. Neuronal cultures were transduced with HA-Rpt6 (WT, S120A, or S120D) by Sindbis virus. Cells were lysed in proteasome activity assay buffer (50 mM Tris-HCl (pH 7.5), 250 mM Sucrose, 5 mM MgCl₂, 0.5 mM EDTA, 2 mM ATP, 1 mM DTT and 0.025% Digitonin). 100 μM of the fluorogenic substrate Suc-LLVY-AMC was then added to lysates in a 96-well microtiter plate. Fluorescence (380 nm excitation, 460

nm emission) was monitored on a microplate fluorometer (HTS 7000 Plus, Perkin Elmer) every 4 min for 2 hours at room temperature.

Immunofluorescent Staining

Mature hippocampal neuron cultures (>17 DIV) were infected with Sindbis Rpt6 (WT/S120A/S120D) for 20 hours. Triton extraction was performed as previously described [160]. Briefly, neurons were treated with 1% Triton X-100 and 4% polyethylene glycol (PEG; molecular weight, 40,000) in BRB80 buffer (80 mM PIPES, 1 mM MgCl₂, and 1 mM EGTA) for 5 min and then rinsed in BRB80 buffer. Neurons were then either lysed in boiling sample buffer for western blot analysis, or fixed in paraformaldehyde for immunofluorescent staining. Cells were fixed in 4% paraformaldehyde/4% sucrose for 10 minutes, and blocked and permeabilized in PBS-MC (phosphate buffered saline with 1 mM MgCl₂ and 0.1 CaCl₂) with Triton X-100 (0.2%) and BSA (2%). Cells were incubated overnight with anti-HA (mAb, 1:2500) and anti-synapsin (pAb, 1:1000) antibodies diluted in PBS-MC plus 2% BSA. Cells were washed and incubated with goat anti-mouse Alexa secondary antibodies (1:1000) diluted in PBS-MC plus 2% BSA. Cells were then washed and coverslips were mounted in Aqua Poly/Mount (Polysciences, Warrington, PA). For paGFPu experiments, mature neurons were infected for 14-16 hours with Sindbis virion and treated for 10 hours with Bicuculline or TTX. Neurons were then fixed and mounted as described above.

Confocal microscopy

For all imaging purposes, we used a Leica (Wetzlar, Germany) DMI6000 inverted microscope outfitted with a Yokogawa (Tokyo, Japan) Spinning disk confocal head, a Orca ER High Resolution B&W Cooled CCD camera (6.45 $\mu\text{m}/\text{pixel}$ at 1X) (Hamamatsu, Sewickley, PA), Plan Achromat 40x/1.25 na and 63x/1.4 na objective, and a Melles Griot (Carlsbad, CA) Argon/Krypton 100 mW air-cooled laser for 488/568/647 nm excitations. Confocal z-stacks were acquired in all experiments. Photoactivation of reporter constructs was achieved with 100 W Hg²⁺ lamp and a D405/40X with 440 DCLP dichroic filter set (Chroma, Rockingham, VT) (10 to 15 sec exposure times for photoactivation). All imaging was acquired in the dynamic range of 8 bit or 12 bit acquisition (0-255 and 0-1024 pixel intensity units, respectively) with Simple PCI (Hamamatsu) imaging software. All quantitation was performed in NIH ImageJ.

Florescence intensity quantitation

Mean fluorescence of straightened dendrites from maximum projected confocal z-stacks was analyzed. Images were thresholded above background. For triton extraction experiments, dendrites from untreated and extracted neurons were imaged. Mean fluorescent intensity of extracted dendrites were divided by the average mean fluorescent intensity of untreated dendrites to determine the percentage of Rpt6 that was extracted. All values were normalized to control (wild type).

Electrophysiology

Whole-cell patch-clamp recordings were made from cultured hippocampal neurons bathed in HBS (containing 119 mM NaCl, 5 mM KCl, 2 mM CaCl₂, 2 mM MgCl₂, 30 mM glucose, and 10 mM HEPES [pH 7.4]), plus 1 μ M TTX and 10 μ M bicuculine, with an Axopatch 200B amplifier. Whole-cell pipette internal solutions contained 100 mM cesium gluconate, 0.2 mM EGTA, 5 mM MgCl₂, 2 mM adenosine triphosphate, 0.3 mM guanosine triphosphate, and 40 mM HEPES (pH 7.2), and had resistances ranging from 4–6 M Ω . Cultured neurons with a pyramidal-like morphology were voltage-clamped at -70 mV and series resistance was left uncompensated. mEPSCs were analyzed off-line using Synaptosoft mini analysis software. Statistical differences between experimental conditions were determined by ANOVA and post hoc Fisher's LSD test.

ACKNOWLEDGEMENTS

We thank Carissa Chu, Alysia Birkholz and Tania Manchenkov for help with experiments and A. Ghosh for the CaMKII construct.

Chapter Three, in full, consists of the following manuscript in preparation for submission to the *Journal of Neuroscience*:

Djakovic SN, Jakawich S, DeMartino GN, Sutton M, Patrick GN. “Phosphorylation of Rpt6 regulates the proteasome and synaptic function”.

I was the primary researcher and author under the supervision and direction of Gentry Patrick. Sonya Jakawich performed all electrophysiology, under the direction

of Michael Sutton. George DeMartino assisted with proteasome work.

A

Scansite				
Basophilic serine/threonine kinase group (Baso_ST_kin)				
Calmodulin dependent Kinase 2				
Gene Card CAMK2G				
Site	Score	Percentile	Sequence	SA
S120	<u>0.5528</u>	1.69%	<u>RVALRN</u> <u>DSYTLHK</u> <u>IL</u>	1.597

B



Figure 3-1: Rpt6 is predicted to be phosphorylated by CaMKII at Serine 120

A, Serine 120 is the predicted CaMKII phosphorylation site on Rpt6 using the Scansite algorithm. *B*, The Rpt6 protein has three distinct domains. The Coiled Coil (CC) domain, ATPase region, and OB fold where S120 is located.

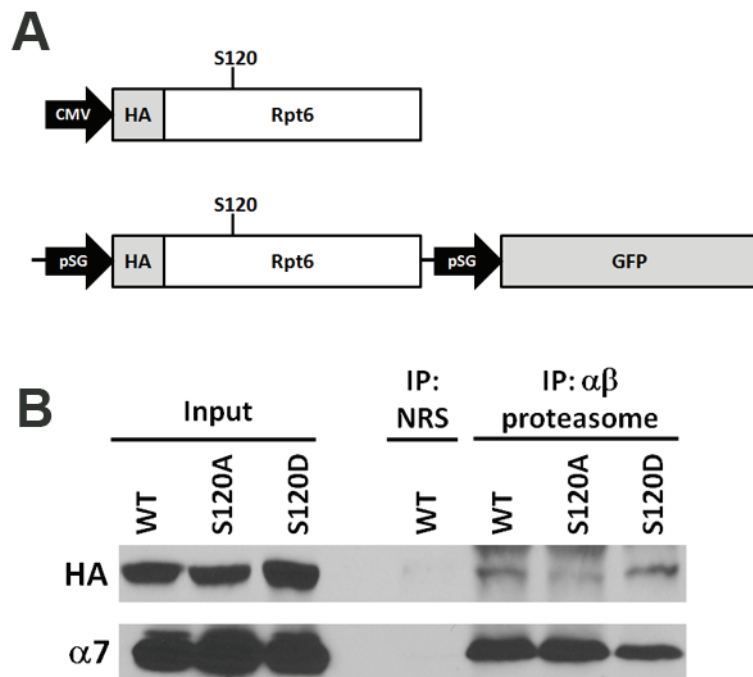


Figure 3-2: Rpt6 phospho-mutants incorporate into the proteasome

A, Rpt6 was tagged with HA and cloned into a CMV promoter vector and a Sindbis dual promoter vector that co-expressed GFP. In addition to the wild type (WT) Rpt6 two phospho-mutants were created: Serine to Alanine (S120A) phospho-dead mutant, and Serine to Aspartic Acid (S120D) phospho-mimetic mutant. *B*, CMV based Rpt6 constructs expressed in HEK293T cells incorporated into endogenous 26S proteasome. Proteasome was immunoprecipitated using an antibody to the core proteasome subunits ($\alpha\beta$ proteasome). Western blotting shows immunoprecipitated core proteasome ($\alpha 7$) and Rpt6 (HA). HA staining was used to identify the overexpressed Rpt6 subunits.

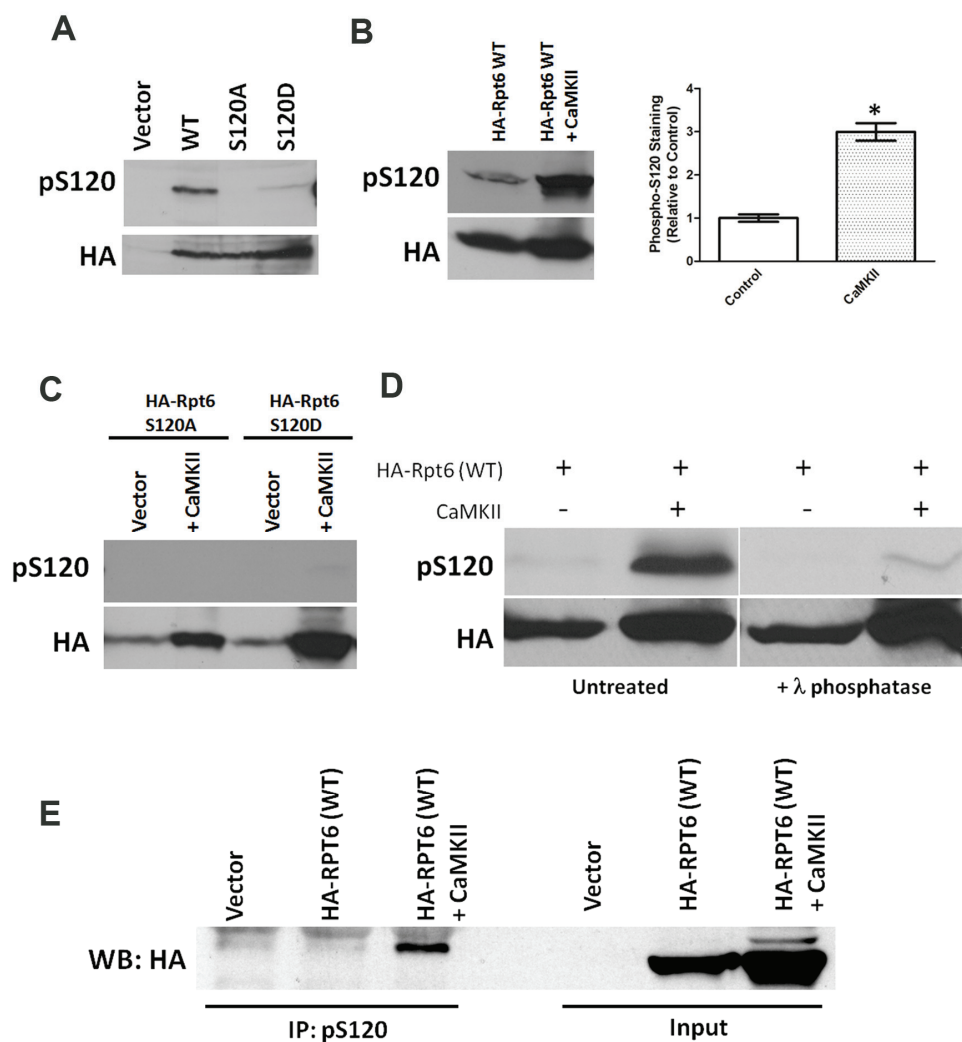


Figure 3-3: CaMKII phosphorylates S120 of Rpt6 *in vivo*

A, Lysates of HEK293T cell expressing HA-Rpt6 (WT, S120A and S120D) or empty vector were stained by Western blotting with a rabbit polyclonal antibody specific to the phosphorylated S120 site on rpt6 (pS120). HA staining showed total expressed protein. *B*, Lysates of HEK293T cells co-expressing the Wild type HA-Rpt6 and a constitutively active form of CaMKII (T286D) were stained with the pS120 antibody by Western blot. CaMKII induces ~3 fold increase in Rpt6 pS120 staining (n =4; p<0.001) as depicted in the bar graph (right). *C*, HEK293T cells co-expressed Rpt6 phospho-mutants and CaMKII. The phospho-mutants are not phosphorylated in a CaMKII-dependent fashion, as shown in Western blotting with the pS120 antibody. *D*, Western blotting was performed as in (A). Nitrocellulose membranes were either mock treated, or incubated with λ phosphatase overnight. λ phosphatase attenuated pS120 reactivity, suggesting that our antibody is phospho-specific. *D*, HEK293T cells expressed vector (control), HA-Rpt6 (WT), or CaMKII (T286D) with HA-Rpt6 (WT). Lysates were immunoprecipitated with phosphospecific antibody (pS120) and probed with an antibody to HA.

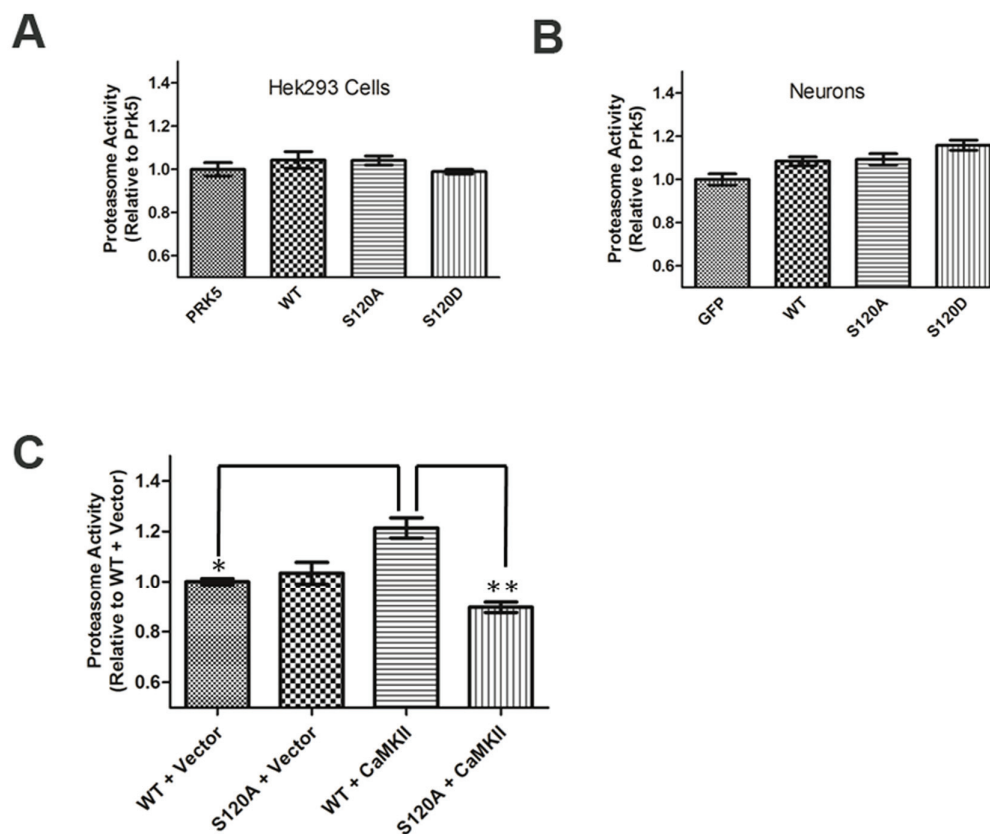


Figure 3-4: Phosphorylation of Rpt6 S120 is necessary for CaMKII-dependent stimulation of the proteasome

A, HEK293T cells were transfected with HA-Rpt6 (WT, S120A, S120D) or empty vector (PRK5). Lysates were assayed for 26S proteasome activity with fluorogenic substrate Suc-LLVY-AMC. Bar graph depicting final fluorescent values (mean \pm SEM) relative to control (PRK5). No significant changes to proteasome activity were observed ($n=9$). *B*, Cortical rat neurons were infected with Sindbis HA-Rpt6 (WT, S120A, S120D) or control virus (GFP). Lysates were assayed for 26S proteasome activity with fluorogenic substrate Suc-LLVY-AMC. Bar graph depicting final fluorescent values (mean \pm SEM) relative to control (GFP). No significant changes to proteasome activity were observed ($n=9$). *C*, HEK293T cells were co-transfected with HA-Rpt6 (WT or S120A) and CaMKII (or empty vector as a control). Lysates were assayed for 26S proteasome activity with fluorogenic substrate Suc-LLVY-AMC. Bar graph depicting final fluorescent values (mean \pm SEM) relative to control (WT + Vector). S120A phospho-dead mutant blocks the CaMKII-dependent increase in proteasome activity ($n=3$; *, $p<0.01$; **, $p<0.001$).

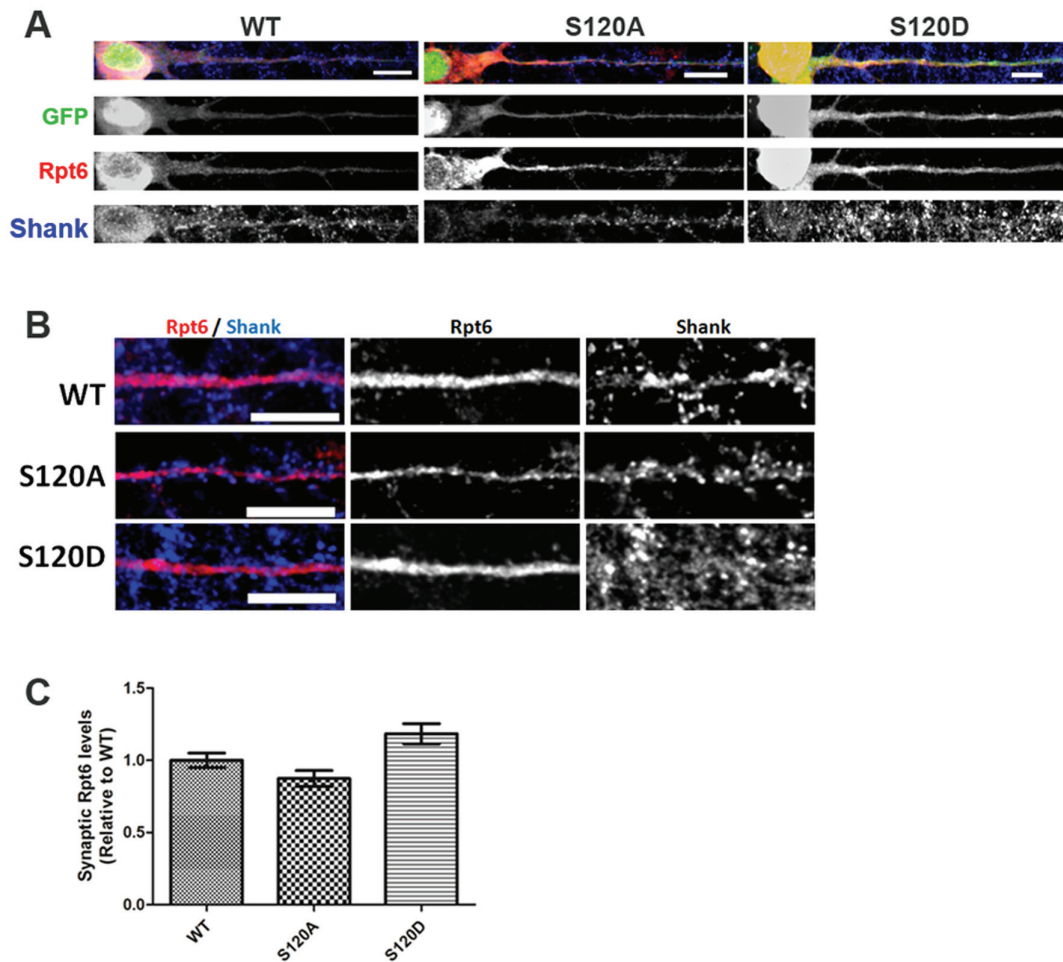


Figure 3-5: Localization of Rpt6 phospho-mutants in hippocampal neurons

A, Rat Hippocampal neurons were infected with Sindbis HA-Rpt6 (WT, S120A, S120D). Straightened dendrites (with cell bodies included) of neurons co-expressing HA-Rpt6 and GFP were stained for Rpt6 (HA antibody) and Shank (post-synaptic marker). *B*, Higher magnification of dendrites in (*A*) to highlight the dendritic and synaptic distribution of HA-Rpt6. *C*, While the S120D phospho-mimetic mutant had an increased synaptic distribution (as measured by percent overlap with Shank), no significant differences were observed ($n=30-40$ dendrites from 2 independent trials).

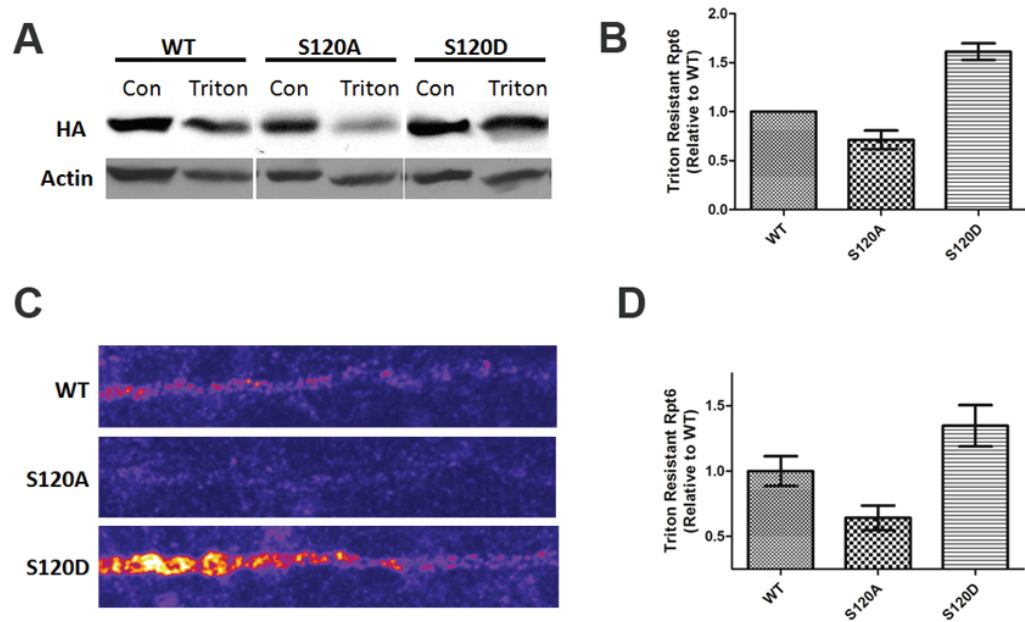


Figure 3-6: Phosphorylation of S120 regulates Rpt6 triton resistance

A, Rat Hippocampal neurons were infected with Sindbis HA-Rpt6 (WT, S120A, S120D). Neurons were triton-X extracted to isolate actin bound proteasome subunits and lysed for Western blot. Lysates were stained for Rpt6 (HA) or Actin. *B*, S120D Rpt6 was resistant to triton extraction, while S120A was easily extracted (n=4 from 2 independent experiments). *C*, Rat Hippocampal neurons were infected with Sindbis HA-Rpt6 (WT, S120A, S120D), triton extracted, and stained for immunofluorescence imaging. Straightened dendrites of neurons expressing HA-Rpt6 were stained for Rpt6 (HA antibody). *D*, Results mirrored those of the Western blotting analysis. S120D Rpt6 was resistant to triton extraction, while S120A was easily extracted (n=25 dendrites).

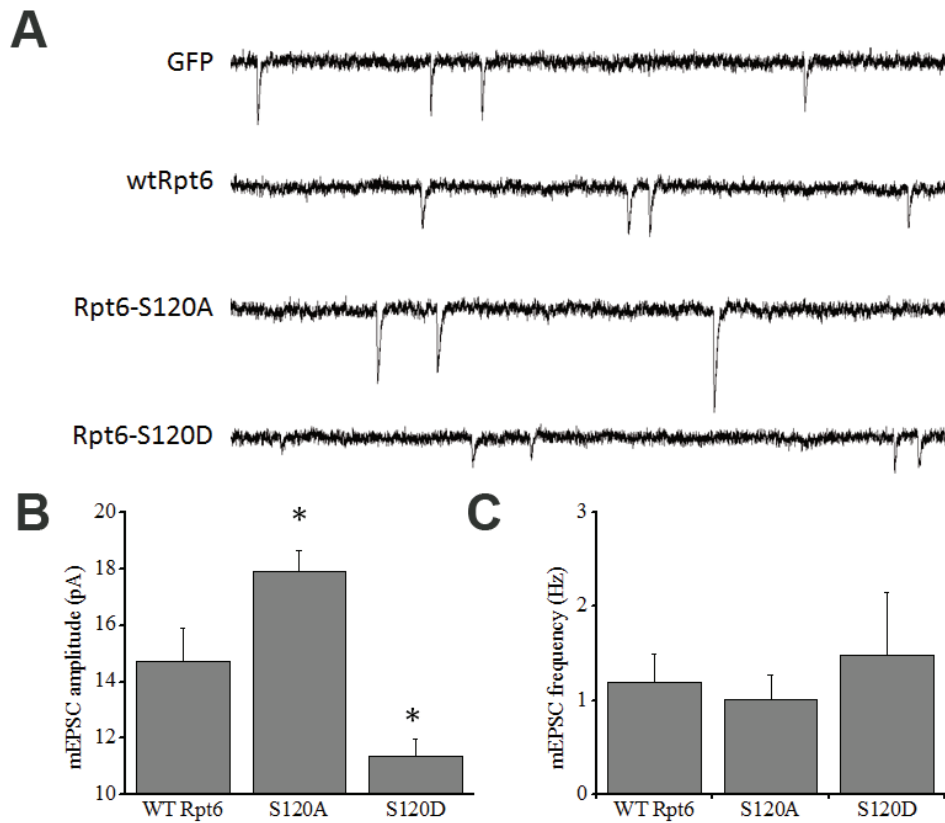


Figure 3-7: Phosphorylation of Rpt6 S120 regulates synaptic strength

A, Rat Hippocampal neurons were infected with Sindbis HA-Rpt6 (WT, S120A, S120D). Miniature excitatory post synaptic currents (mEPSCs) were recorded. *C*, S120A Rpt6 increased mEPSC amplitude relative to WT, while S120D decreased mEPSC amplitude relative to WT. No significant change to mEPSC frequency was observed ($n = 8, 12$ and 9 for WT, S120A and S120D respectively; *, $p < 0.05$).

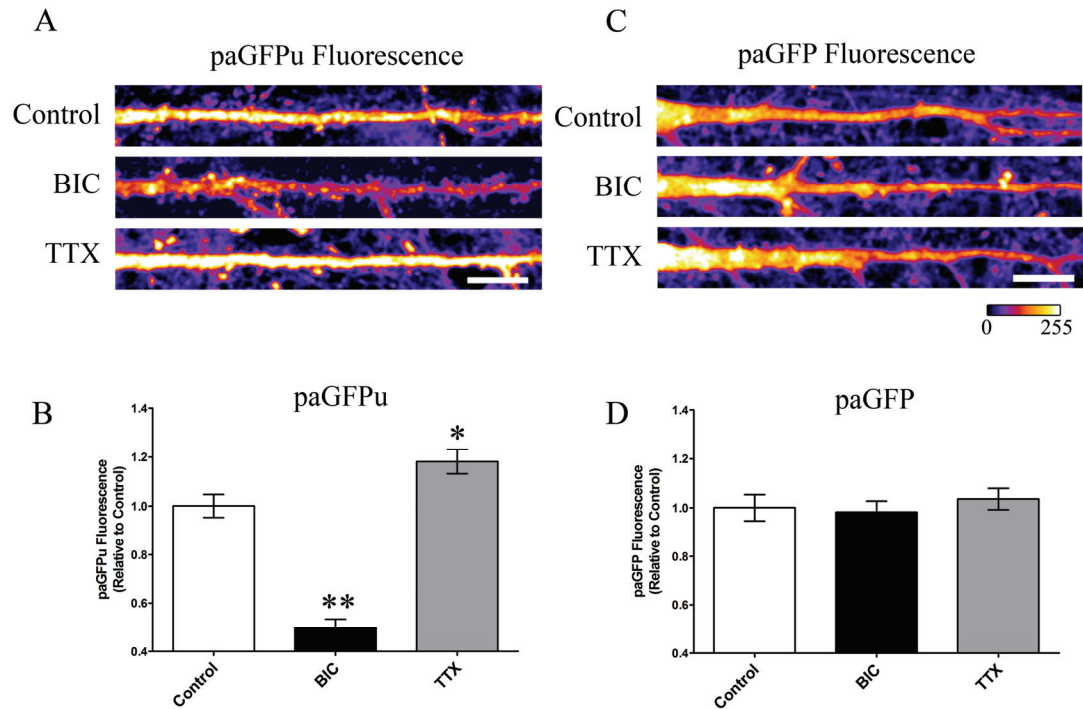


Figure 3-8: UPS activity is regulated during homeostatic plasticity

A, Representative straightened dendrites and somas of cultured hippocampal neurons expressing the UPS reporter paGFPu. Neurons were treated with TTX (2 μ M) or BIC (50 μ M) for 10 hours. Scale Bar = 10 microns. *B*, Bar graph depicting the total dendritic paGFPu fluorescence \pm SEM (AU) per treated group relative to control (untreated). BIC dramatically increased paGFPu degradation, while TTX blocked paGFPu degradation relative to Control. For statistical analysis, one-way ANOVA with *post hoc* Dunnett's multiple-comparison test was used. * $p < 0.01$; ** $p < 0.001$ (n=92, 77 and 92 imaged dendrites from 4 independent experiments for Control, BIC and TTX respectively). *A*, Representative straightened dendrites and somas of cultured hippocampal neurons expressing the control reporter paGFP. Neurons were treated with TTX (2 μ M) or BIC (50 μ M) for 10 hours. Scale Bar = 10 microns. *C*, Bar graph depicting the total dendritic paGFP fluorescence \pm SEM (AU) per treated group relative to control (untreated). Treatment with BIC or TTX did not affect the fluorescence levels of the paGFP no-degron control reporter (n=70, 65 and 71 imaged dendrites from 4 independent experiments for Control, BIC and TTX respectively).

Chapter IV

Conclusion

Summary

It has become increasingly evident that the UPS plays an essential role in neuronal function. Mechanisms of protein ubiquitination have been widely studied in neurons. Indeed, there has been extensive research on the role of E3 ligases such as E6-AP, Nedd4 and *Highwire* in neuronal function [63,164,165]. In contrast, relatively little is known about proteasome function in neurons. In my thesis work we aimed to elucidate mechanisms of proteasome function in neurons. Specifically we aimed to uncover how the proteasome is regulated by neuronal activity, and how this regulation would contribute to activity-dependent synaptic remodeling.

In chapter 2 we identified a rapid and dynamic regulation of proteasome function by neuronal activity. Interestingly, this regulation was bi-directional, with activity blockade inhibiting the proteasome and activity upregulation stimulating the proteasome. The activity-dependent stimulation of the proteasome was dependent on Ca²⁺ influx, which is in line with previous research reporting that UPS components may be regulated directly by Ca²⁺ [103,137,138,139,140]. We hypothesized that downstream calcium-dependent kinases may be involved in regulation of the proteasome. We identified CaMKII, a key kinase involved in many aspects of neuronal function, as a novel regulator of proteasome activity in neurons [128]. Additionally, we identified Rpt6, a 19S regulatory subunit of the proteasome, to be phosphorylated by CaMKII. While CaMKII is known to target many synaptic proteins for phosphorylation [166], prior to our studies, the proteasome has never been shown to be phosphorylated by CaMKII. Interestingly, CaMKII has been recently

been shown as scaffolding protein crucial for the translocation of the proteasome into synaptic spines [100]. This indicates that phosphorylation of Rpt6 by CaMKII may be required for the activity-dependent trafficking of the proteasome in neurons.

In Chapter 3 we aimed to further elucidate mechanisms of proteasome regulation in neurons. Specifically, we investigated how CaMKII-dependent phosphorylation of Rpt6 regulates proteasome function. We identified Serine 120 of Rpt6 as the CaMKII-dependent phosphorylation site on the proteasome. We showed that phosphorylation of Rpt6 S120 is important for regulation of proteasome function. Specifically it is involved in activity-dependent stimulation and actin-dependent sequestration of the proteasome. Indeed, the tethering of the proteasome to the actin cytoskeleton has been shown to be essential for its sequestration in synaptic spines [99]. Additionally we showed that genetic modification of Rpt6 phosphorylation leads to significant changes in synaptic strength. Overexpression of our phospho-mimetic or phospho-dead Rpt6 mutants caused significant changes to mEPSC amplitude. Chronic upregulation or downregulation of neuronal activity has also been shown to cause changes in synaptic strength in a process known as homeostatic plasticity [161]. Indeed, we also showed that chronic modifications in neuronal activity directly regulate the activity of the proteasome. We would hypothesize that phosphorylation of Rpt6 is a key regulatory mechanism in this process. Additionally we hypothesize that the proteasome itself may be a key mediator of homeostatic plasticity. Together, our results suggest that neuronal activity controls phosphorylation of Rpt6 at S120 to regulate proteasome function and synaptic strength.

Regulation of the proteasome

While the ubiquitination process has been extensively studied, much less is known about regulation of the proteasome. In our studies we have uncovered a novel mechanism for regulation of the proteasome. Phosphorylation has recently emerged as a potentially key regulatory mechanism. Indeed the proteasome function has been shown to be regulated by phosphorylation of both 20S and 19S subunits [112]. PKA is the protein kinase most often found to phosphorylate the proteasome.

Phosphorylation of 20S by PKA was shown to increase peptidase activity of individual β subunits [34]. Additionally, phosphorylation of 19S subunit Rpt6 at Serine 120 by PKA was shown to be required for forskolin-induced increase of proteasome activity [32]. We found Rpt6 to be phosphorylated by CaMKII at the same site, Serine 120. Interestingly, the sequence preceding S120 (R-N-D-S) matches the consensus sequence for CaMKII (R-x-x-S), but not PKA (R-R-x-S) [141]. The functional relevance of these post-translational modifications is still unclear.

Phosphorylation may regulate proteasome function by modulating catalytic activity. Serine 120 lies within a specific domain of Rpt6, the OB fold, that has been shown to be involved in chaperone-like activity of Rpt subunits [157,158]. Additionally, we hypothesize phosphorylation of S120 to be involved in trafficking or sequestration of the proteasome, most likely by controlling association with regulatory or scaffolding proteins. We have shown that CaMKII phosphorylates Rpt6. CaMKII has also been shown to act as a scaffold to sequester proteasomes at synapses in response to

neuronal activity [100]. It is plausible that phosphorylation of Rpt6 regulates association of the proteasome with CaMKII.

UPS and synaptic plasticity

Both UPS-dependent protein degradation and CaMKII activity have been implicated as key players in synaptic plasticity. For the first time, our studies link the function of the proteasome to CaMKII activity, providing further insight into molecular mechanisms of synaptic plasticity. CaMKII phosphorylates many key synaptic substrates such as Glur1 and SynGAP to promote synaptic plasticity [128]. Our work suggests that CaMKII further promotes synaptic plasticity by regulating the proteasome. Calcium influx through NMDA receptors activates Calmodulin and CaMKII. Activated CaMKII then phosphorylates the proteasome at 19S subunit Rpt6, inducing sequestration in synaptic spines. Activity of the proteasome is likely concomitantly increased to stimulate degradation of synaptic proteins (Figure 4-1). This degradation of synaptic substrates occurs in parallel with local protein synthesis to promote synaptic plasticity [3].

Interestingly, recent studies on fear memory in rodents indirectly support our hypothesis that CaMKII regulates activity-dependent proteasome function in neurons. Firstly, Lee et al. showed that infusion of a proteasome inhibitor into the CA1 region of the hippocampus immediately after memory retrieval prevented protein synthesis inhibition-induced memory impairment, as well as the extinction of fear memory [68]. This suggests proteasome-dependent protein degradation underlies the destabilization

processes after fear memory retrieval. Secondly, Cao et al. showed that transient CaMKII α overexpression at the time of recall impairs the retrieval of new and old fear memories. Their analysis suggested that excessive CaMKII α activity-induced recall deficits are caused by the active erasure of the stored memories rather than disrupting the retrieval access to the stored information [167]. Therefore proteasome inhibition and excessive CaMKII α activity produce opposite effects on retrieval and extinction of fear memory. In their discussion, Cao et al. postulate the involvement of the UPS. Indeed, our data suggest that CaMKII dependent regulation of the proteasome may play a key role in active erasure of stored memories. We are currently creating Rpt6 phospho-mutant transgenic mice to address this question. We hypothesize that in the fear conditioning paradigm, the S120D mice would behave similar to the CaMKII stimulated mice. Specifically there would likely be an accelerated erasure of fear memories. In contrast, the S120A mice may mimic proteasome inhibition treatments to cause stabilization of fear memories.

UPS and neurodegenerative disease

AD is commonly characterized by progressive memory loss and accumulation of neurofibrillary tangles (NFT) and extracellular senile plaques mainly consisting of A β peptides [85]. Recent evidence has implicated aberrant calcium signaling as a key mechanism in A β toxicity [168]. UPS dysfunction has also been widely considered a contributor to the pathophysiology of AD. A β oligomers or plaques increase basal levels of intracellular calcium, which activate protein phosphatases and induce long

term depression (LTD) and synaptic loss [169,170]. Interestingly, impairments in activity and trafficking of calcium activated kinases such as CaMKII has also been observed [171,172,173]. Since our data also implicates CaMKII as a key regulator of proteasome function, we hypothesize that the proteasome dysfunction observed in AD may be due to aberrant calcium signaling and CaMKII activity. Further studies are needed to determine if CaMKII-dependent regulation of proteasome function is impaired in AD. Specifically, it would be interesting to see if neurons expressing phospho-mimetic Rpt6 are protected from $\alpha\beta$ induced synaptic dysfunction. Additionally, in the future we can cross a phospho-mimetic Rpt6 S120D transgenic mouse with an AD mouse model. We predict that pathogenesis may be ameliorated in these mice.

PD is another neurodegenerative disease commonly associated with UPS dysfunction. Mutations in UCH-L1, a DUB, have been implicated in the pathogenesis of familial PD and mouse neurodegeneration models [81,84,174]. UCH-L1 is highly expressed in neurons and important for the maintenance of cellular mono-ubiquitin levels [175,176]. We hypothesized that loss of UCH-L1 function may lead to UPS dysfunction, which may be an underlying mechanism in the pathogenesis in PD. Although inhibition of UCH-L1 did not affect *in vitro* proteasome activity, a significant decline in ubiquitin-dependent degradation was observed [102]. Together these studies further solidify the importance of the UPS in neuronal function and dysfunction.

Synaptic substrates of the UPS

Our work in Chapter 4 suggests that genetic manipulation of proteasome activity is sufficient to regulate synaptic strength. These effects are most likely a result of altered degradation of synaptic UPS substrates. There exists a fine-tuned balance between protein de-ubiquitination, ubiquitination and proteolysis in the cell to control the stability substrates. Indeed, as we originally hypothesized, the proteasome is likely regulated in synergy with ubiquitination to allow for the efficient degradation of protein substrates. Modifying proteasome function by phosphorylation of Rpt6 tips this balance to support a more efficient stabilization or degradation of synaptic proteins. During periods of low neuronal activity, Rpt6 remains dephosphorylated and proteasome function is impaired. This allows for increased stabilization of synaptic substrates, and increased synaptic strength. In contrast, increased neuronal activity leads to upregulation of proteasome function, more efficient degradation of synaptic proteins, and a decrease in synaptic strength.

These results raise two important questions. Firstly, which synaptic proteins are substrates of the UPS? Secondly, and more importantly, which UPS-dependent synaptic substrates have their abundance dynamically controlled by neuronal activity to regulate synaptic remodeling? Mass spectrometry experiments by our laboratory have identified over 100 synaptic proteins that are ubiquitinated. Further proteomics studies need to be performed to identify which UPS substrates have their ubiquitination status modified during neuronal activity blockade or upregulation. The abundance of many synaptic proteins has been shown to be regulated by neuronal

activity [92]. Only a few of these proteins have been shown to be directly degraded by the UPS in an activity dependent manner. Among these are the scaffolding proteins PSD-95, Shank, GKAP, AKAP and GRIP1 [50,92,110]. It would be of great interest to determine if the abundance of these synaptic proteins is modified in neurons expressing our Rpt6 phospho-mutants.

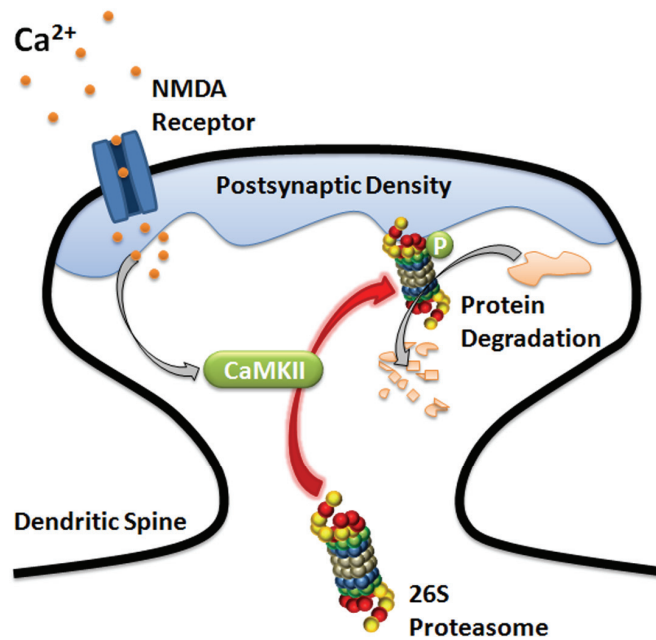


Figure 4-1: Model of CaMKII-dependent regulation of the proteasome

Neuronal activity induces calcium (Ca^{2+}) influx through NMDA receptors. Calcium binds and activates calmodulin. Activated calmodulin relieves CaMKII auto-inhibition, allowing CaMKII to phosphorylate and activate itself. Activated CaMKII then triggers translocation and sequestration of proteasome into synaptic spines, presumably by phosphorylation of subunit Rpt6 at Serine 120. Sequestered proteasomes are activated, stimulating degradation of synaptic substrates.

References

1. Sheng M, Kim MJ (2002) Postsynaptic signaling and plasticity mechanisms. *Science* 298: 776-780.
2. Martin KC, Zukin RS (2006) RNA trafficking and local protein synthesis in dendrites: an overview. *J Neurosci* 26: 7131-7134.
3. Sutton MA, Schuman EM (2006) Dendritic protein synthesis, synaptic plasticity, and memory. *Cell* 127: 49-58.
4. Patrick GN (2006) Synapse formation and plasticity: recent insights from the perspective of the ubiquitin proteasome system. *Curr Opin Neurobiol* 16: 90-94.
5. Hershko A, Ciechanover A (1998) The ubiquitin system. *Annu Rev Biochem* 67: 425-479.
6. Hicke L, Schubert HL, Hill CP (2005) Ubiquitin-binding domains. *Nat Rev Mol Cell Biol* 6: 610-621.
7. Reyes-Turcu FE, Ventii KH, Wilkinson KD (2009) Regulation and cellular roles of ubiquitin-specific deubiquitinating enzymes. *Annu Rev Biochem* 78: 363-397.
8. Schnell JD, Hicke L (2003) Non-traditional functions of ubiquitin and ubiquitin-binding proteins. *J Biol Chem* 278: 35857-35860.
9. Pickart CM, Cohen RE (2004) Proteasomes and their kin: proteases in the machine age. *Nat Rev Mol Cell Biol* 5: 177-187.
10. Marques AJ, Palanimurugan R, Matias AC, Ramos PC, Dohmen RJ (2009) Catalytic mechanism and assembly of the proteasome. *Chem Rev* 109: 1509-1536.
11. Glickman MH, Rubin DM, Coux O, Wefes I, Pfeifer G, et al. (1998) A subcomplex of the proteasome regulatory particle required for ubiquitin-conjugate degradation and related to the COP9-signalosome and eIF3. *Cell* 94: 615-623.

12. DeMartino GN, Slaughter CA (1999) The proteasome, a novel protease regulated by multiple mechanisms. *J Biol Chem* 274: 22123-22126.
13. Kaneko T, Hamazaki J, Iemura S, Sasaki K, Furuyama K, et al. (2009) Assembly pathway of the Mammalian proteasome base subcomplex is mediated by multiple specific chaperones. *Cell* 137: 914-925.
14. Funakoshi M, Tomko RJ, Jr., Kobayashi H, Hochstrasser M (2009) Multiple assembly chaperones govern biogenesis of the proteasome regulatory particle base. *Cell* 137: 887-899.
15. van Nocker S, Sadis S, Rubin DM, Glickman M, Fu H, et al. (1996) The multiubiquitin-chain-binding protein Mcb1 is a component of the 26S proteasome in *Saccharomyces cerevisiae* and plays a nonessential, substrate-specific role in protein turnover. *Mol Cell Biol* 16: 6020-6028.
16. Kraut DA, Prakash S, Matouschek A (2007) To degrade or release: ubiquitin-chain remodeling. *Trends Cell Biol* 17: 419-421.
17. Varshavsky A (2005) Regulated protein degradation. *Trends Biochem Sci* 30: 283-286.
18. Murata S, Yashiroda H, Tanaka K (2009) Molecular mechanisms of proteasome assembly. *Nat Rev Mol Cell Biol* 10: 104-115.
19. Besche HC, Peth A, Goldberg AL (2009) Getting to first base in proteasome assembly. *Cell* 138: 25-28.
20. Dubiel W, Pratt G, Ferrell K, Rechsteiner M (1992) Purification of an 11 S regulator of the multicatalytic protease. *J Biol Chem* 267: 22369-22377.
21. Rechsteiner M, Realini C, Ustrell V (2000) The proteasome activator 11 S REG (PA28) and class I antigen presentation. *Biochem J* 345 Pt 1: 1-15.
22. Ustrell V, Hoffman L, Pratt G, Rechsteiner M (2002) PA200, a nuclear proteasome activator involved in DNA repair. *EMBO J* 21: 3516-3525.

23. Kopp F, Dahlmann B, Kuehn L (2001) Reconstitution of hybrid proteasomes from purified PA700-20 S complexes and PA28 α activator: ultrastructure and peptidase activities. *J Mol Biol* 313: 465-471.
24. Blickwedehl J, Agarwal M, Seong C, Pandita RK, Melendy T, et al. (2008) Role for proteasome activator PA200 and postglutamyl proteasome activity in genomic stability. *Proc Natl Acad Sci U S A* 105: 16165-16170.
25. Hunter T (2007) The age of crosstalk: phosphorylation, ubiquitination, and beyond. *Mol Cell* 28: 730-738.
26. Bose S, Stratford FL, Broadfoot KI, Mason GG, Rivett AJ (2004) Phosphorylation of 20S proteasome α subunit C8 (α 7) stabilizes the 26S proteasome and plays a role in the regulation of proteasome complexes by gamma-interferon. *Biochem J* 378: 177-184.
27. Mason GG, Murray RZ, Pappin D, Rivett AJ (1998) Phosphorylation of ATPase subunits of the 26S proteasome. *FEBS Lett* 430: 269-274.
28. Rivett AJ, Bose S, Brooks P, Broadfoot KI (2001) Regulation of proteasome complexes by gamma-interferon and phosphorylation. *Biochimie* 83: 363-366.
29. Fernandez Murray P, Pardo PS, Zelada AM, Passeron S (2002) In vivo and in vitro phosphorylation of *Candida albicans* 20S proteasome. *Arch Biochem Biophys* 404: 116-125.
30. Lu H, Zong C, Wang Y, Young GW, Deng N, et al. (2008) Revealing the dynamics of 20S proteasome phosphoproteome: A combined CID and ETD approach. *Mol Cell Proteomics*.
31. Satoh K, Sasajima H, Nyomura KI, Yokosawa H, Sawada H (2001) Assembly of the 26S proteasome is regulated by phosphorylation of the p45/Rpt6 ATPase subunit. *Biochemistry* 40: 314-319.
32. Zhang F, Hu Y, Huang P, Toleman CA, Paterson AJ, et al. (2007) Proteasome function is regulated by cyclic AMP-dependent protein kinase through phosphorylation of Rpt6. *J Biol Chem* 282: 22460-22471.

33. Bardag-Gorce F, Venkatesh R, Li J, French BA, French SW (2004) Hyperphosphorylation of rat liver proteasome subunits: the effects of ethanol and okadaic acid are compared. *Life Sci* 75: 585-597.
34. Zong C, Gomes AV, Drews O, Li X, Young GW, et al. (2006) Regulation of murine cardiac 20S proteasomes: role of associating partners. *Circ Res* 99: 372-380.
35. Asai M, Tsukamoto O, Minamino T, Asanuma H, Fujita M, et al. (2009) PKA rapidly enhances proteasome assembly and activity in in vivo canine hearts. *J Mol Cell Cardiol* 46: 452-462.
36. Nguyen PV, Woo NH (2003) Regulation of hippocampal synaptic plasticity by cyclic AMP-dependent protein kinases. *Prog Neurobiol* 71: 401-437.
37. Sumegi M, Hunyadi-Gulyas E, Medzihradszky KF, Udvardy A (2003) 26S proteasome subunits are O-linked N-acetylglucosamine-modified in *Drosophila melanogaster*. *Biochem Biophys Res Commun* 312: 1284-1289.
38. Zhang F, Su K, Yang X, Bowe DB, Paterson AJ, et al. (2003) O-GlcNAc modification is an endogenous inhibitor of the proteasome. *Cell* 115: 715-725.
39. Ciechanover A, Brundin P (2003) The ubiquitin proteasome system in neurodegenerative diseases: sometimes the chicken, sometimes the egg. *Neuron* 40: 427-446.
40. Bock HH, Jossin Y, May P, Bergner O, Herz J (2004) Apolipoprotein E receptors are required for reelin-induced proteasomal degradation of the neuronal adaptor protein Disabled-1. *J Biol Chem* 279: 33471-33479.
41. Campbell DS, Holt CE (2001) Chemotropic responses of retinal growth cones mediated by rapid local protein synthesis and degradation. *Neuron* 32: 1013-1026.
42. DiAntonio A, Haghghi AP, Portman SL, Lee JD, Amaranto AM, et al. (2001) Ubiquitination-dependent mechanisms regulate synaptic growth and function. *Nature* 412: 449-452.

43. Chain DG, Schwartz JH, Hegde AN (1999) Ubiquitin-mediated proteolysis in learning and memory. *Mol Neurobiol* 20: 125-142.
44. Hegde AN, Goldberg AL, Schwartz JH (1993) Regulatory subunits of cAMP-dependent protein kinases are degraded after conjugation to ubiquitin: a molecular mechanism underlying long-term synaptic plasticity. *Proc Natl Acad Sci U S A* 90: 7436-7440.
45. Hegde AN, Inokuchi K, Pei W, Casadio A, Ghirardi M, et al. (1997) Ubiquitin C-terminal hydrolase is an immediate-early gene essential for long-term facilitation in *Aplysia*. *Cell* 89: 115-126.
46. Luscher C, Nicoll RA, Malenka RC, Muller D (2000) Synaptic plasticity and dynamic modulation of the postsynaptic membrane. *Nat Neurosci* 3: 545-550.
47. Shepherd JD, Huganir RL (2007) The cell biology of synaptic plasticity: AMPA receptor trafficking. *Annu Rev Cell Dev Biol* 23: 613-643.
48. Fonseca R, Vabulas RM, Hartl FU, Bonhoeffer T, Nagerl UV (2006) A balance of protein synthesis and proteasome-dependent degradation determines the maintenance of LTP. *Neuron* 52: 239-245.
49. Karpova A, Mikhaylova M, Thomas U, Knopfel T, Behnisch T (2006) Involvement of protein synthesis and degradation in long-term potentiation of Schaffer collateral CA1 synapses. *J Neurosci* 26: 4949-4955.
50. Colledge M, Snyder EM, Crozier RA, Soderling JA, Jin Y, et al. (2003) Ubiquitination regulates PSD-95 degradation and AMPA receptor surface expression. *Neuron* 40: 595-607.
51. Deng PY, Lei S (2007) Long-term depression in identified stellate neurons of juvenile rat entorhinal cortex. *J Neurophysiol* 97: 727-737.
52. Hou L, Antion MD, Hu D, Spencer CM, Paylor R, et al. (2006) Dynamic translational and proteasomal regulation of fragile X mental retardation protein controls mGluR-dependent long-term depression. *Neuron* 51: 441-454.

53. Zhao Y, Hegde AN, Martin KC (2003) The ubiquitin proteasome system functions as an inhibitory constraint on synaptic strengthening. *Curr Biol* 13: 887-898.
54. Willeumier K, Pulst SM, Schweizer FE (2006) Proteasome inhibition triggers activity-dependent increase in the size of the recycling vesicle pool in cultured hippocampal neurons. *J Neurosci* 26: 11333-11341.
55. Yao I, Takagi H, Ageta H, Kahyo T, Sato S, et al. (2007) SCRAPPER-dependent ubiquitination of active zone protein RIM1 regulates synaptic vesicle release. *Cell* 130: 943-957.
56. Burbea M, Dreier L, Dittman JS, Grunwald ME, Kaplan JM (2002) Ubiquitin and AP180 regulate the abundance of GLR-1 glutamate receptors at postsynaptic elements in *C. elegans*. *Neuron* 35: 107-120.
57. Juo P, Kaplan JM (2004) The anaphase-promoting complex regulates the abundance of GLR-1 glutamate receptors in the ventral nerve cord of *C. elegans*. *Curr Biol* 14: 2057-2062.
58. van Roessel P, Elliott DA, Robinson IM, Prokop A, Brand AH (2004) Independent regulation of synaptic size and activity by the anaphase-promoting complex. *Cell* 119: 707-718.
59. Patrick GN, Bingol B, Weld HA, Schuman EM (2003) Ubiquitin-mediated proteasome activity is required for agonist-induced endocytosis of GluRs. *Curr Biol* 13: 2073-2081.
60. Huibregtse JM, Scheffner M, Beaudenon S, Howley PM (1995) A family of proteins structurally and functionally related to the E6-AP ubiquitin-protein ligase. *Proc Natl Acad Sci U S A* 92: 5249.
61. Kishino T, Lalande M, Wagstaff J (1997) UBE3A/E6-AP mutations cause Angelman syndrome. *Nat Genet* 15: 70-73.
62. Jiang YH, Armstrong D, Albrecht U, Atkins CM, Noebels JL, et al. (1998) Mutation of the Angelman ubiquitin ligase in mice causes increased

cytoplasmic p53 and deficits of contextual learning and long-term potentiation. *Neuron* 21: 799-811.

63. Greer PL, Hanayama R, Bloodgood BL, Mardinly AR, Lipton DM, et al. (2010) The Angelman Syndrome protein Ube3A regulates synapse development by ubiquitinating arc. *Cell* 140: 704-716.
64. Davis HP, Squire LR (1984) Protein synthesis and memory: a review. *Psychol Bull* 96: 518-559.
65. Bourtchouladze R, Abel T, Berman N, Gordon R, Lapidus K, et al. (1998) Different training procedures recruit either one or two critical periods for contextual memory consolidation, each of which requires protein synthesis and PKA. *Learn Mem* 5: 365-374.
66. Nader K, Schafe GE, Le Doux JE (2000) Fear memories require protein synthesis in the amygdala for reconsolidation after retrieval. *Nature* 406: 722-726.
67. Vianna MR, Szapiro G, McGaugh JL, Medina JH, Izquierdo I (2001) Retrieval of memory for fear-motivated training initiates extinction requiring protein synthesis in the rat hippocampus. *Proc Natl Acad Sci U S A* 98: 12251-12254.
68. Lee SH, Choi JH, Lee N, Lee HR, Kim JI, et al. (2008) Synaptic protein degradation underlies destabilization of retrieved fear memory. *Science* 319: 1253-1256.
69. Chung KK, Dawson VL, Dawson TM (2001) The role of the ubiquitin-proteasomal pathway in Parkinson's disease and other neurodegenerative disorders. *Trends Neurosci* 24: S7-14.
70. Lowe J, Mayer RJ, Landon M (1993) Ubiquitin in neurodegenerative diseases. *Brain Pathol* 3: 55-65.
71. Ross CA, Poirier MA (2004) Protein aggregation and neurodegenerative disease. *Nat Med* 10 Suppl: S10-17.

72. Anderson JP, Walker DE, Goldstein JM, de Laat R, Banducci K, et al. (2006) Phosphorylation of Ser-129 is the dominant pathological modification of alpha-synuclein in familial and sporadic Lewy body disease. *J Biol Chem* 281: 29739-29752.
73. Dahlmann B (2007) Role of proteasomes in disease. *BMC Biochem* 8 Suppl 1: S3.
74. Bossy-Wetzell E, Schwarzenbacher R, Lipton SA (2004) Molecular pathways to neurodegeneration. *Nat Med* 10 Suppl: S2-9.
75. Dawson TM, Dawson VL (2003) Rare genetic mutations shed light on the pathogenesis of Parkinson disease. *J Clin Invest* 111: 145-151.
76. Shimura H, Hattori N, Kubo S, Mizuno Y, Asakawa S, et al. (2000) Familial Parkinson disease gene product, parkin, is a ubiquitin-protein ligase. *Nat Genet* 25: 302-305.
77. Zhang Y, Gao J, Chung KK, Huang H, Dawson VL, et al. (2000) Parkin functions as an E2-dependent ubiquitin- protein ligase and promotes the degradation of the synaptic vesicle-associated protein, CDCrel-1. *Proc Natl Acad Sci U S A* 97: 13354-13359.
78. Chin LS, Olzmann JA, Li L (2010) Parkin-mediated ubiquitin signalling in aggresome formation and autophagy. *Biochem Soc Trans* 38: 144-149.
79. Von Coelln R, Thomas B, Savitt JM, Lim KL, Sasaki M, et al. (2004) Loss of locus coeruleus neurons and reduced startle in parkin null mice. *Proc Natl Acad Sci U S A* 101: 10744-10749.
80. Pankratz N, Foroud T (2007) Genetics of Parkinson disease. *Genet Med* 9: 801-811.
81. Saigoh K, Wang YL, Suh JG, Yamanishi T, Sakai Y, et al. (1999) Intragenic deletion in the gene encoding ubiquitin carboxy-terminal hydrolase in gad mice. *Nat Genet* 23: 47-51.

82. Ichihara N, Wu J, Chui DH, Yamazaki K, Wakabayashi T, et al. (1995) Axonal degeneration promotes abnormal accumulation of amyloid beta-protein in ascending gracile tract of gracile axonal dystrophy (GAD) mouse. *Brain Res* 695: 173-178.
83. Case A, Stein RL (2006) Mechanistic studies of ubiquitin C-terminal hydrolase L1. *Biochemistry* 45: 2443-2452.
84. Setsuie R, Wada K (2007) The functions of UCH-L1 and its relation to neurodegenerative diseases. *Neurochem Int* 51: 105-111.
85. Walsh DM, Selkoe DJ (2004) Deciphering the molecular basis of memory failure in Alzheimer's disease. *Neuron* 44: 181-193.
86. Selkoe DJ (2002) Alzheimer's disease is a synaptic failure. *Science* 298: 789-791.
87. Hsieh H, Boehm J, Sato C, Iwatsubo T, Tomita T, et al. (2006) AMPAR removal underlies A β -induced synaptic depression and dendritic spine loss. *Neuron* 52: 831-843.
88. Almeida CG, Takahashi RH, Gouras GK (2006) Beta-amyloid accumulation impairs multivesicular body sorting by inhibiting the ubiquitin-proteasome system. *J Neurosci* 26: 4277-4288.
89. Lopez Salon M, Pasquini L, Besio Moreno M, Pasquini JM, Soto E (2003) Relationship between beta-amyloid degradation and the 26S proteasome in neural cells. *Exp Neurol* 180: 131-143.
90. Diaz-Hernandez M, Valera AG, Moran MA, Gomez-Ramos P, Alvarez-Castelao B, et al. (2006) Inhibition of 26S proteasome activity by huntingtin filaments but not inclusion bodies isolated from mouse and human brain. *J Neurochem* 98: 1585-1596.
91. Bence NF, Sampat RM, Kopito RR (2001) Impairment of the ubiquitin-proteasome system by protein aggregation. *Science* 292: 1552-1555.

92. Ehlers MD (2003) Activity level controls postsynaptic composition and signaling via the ubiquitin-proteasome system. *Nat Neurosci* 6: 231-242.
93. Piccoli G, Verpelli C, Tonna N, Romorini S, Alessio M, et al. (2007) Proteomic Analysis of Activity-Dependent Synaptic Plasticity in Hippocampal Neurons. *J Proteome Res*.
94. Ding M, Chao D, Wang G, Shen K (2007) Spatial Regulation of an E3 Ubiquitin Ligase Directs Selective Synapse Elimination. *Science*.
95. Schmidt M, Hanna J, Elsasser S, Finley D (2005) Proteasome-associated proteins: regulation of a proteolytic machine. *Biol Chem* 386: 725-737.
96. Wang X, Chen CF, Baker PR, Chen PL, Kaiser P, et al. (2007) Mass spectrometric characterization of the affinity-purified human 26S proteasome complex. *Biochemistry* 46: 3553-3565.
97. Wang X, Huang L (2008) Identifying dynamic interactors of protein complexes by quantitative mass spectrometry. *Mol Cell Proteomics* 7: 46-57.
98. Verma R, Chen S, Feldman R, Schieltz D, Yates J, et al. (2000) Proteasomal proteomics: identification of nucleotide-sensitive proteasome-interacting proteins by mass spectrometric analysis of affinity-purified proteasomes. *Mol Biol Cell* 11: 3425-3439.
99. Bingol B, Schuman EM (2006) Activity-dependent dynamics and sequestration of proteasomes in dendritic spines. *Nature* 441: 1144-1148.
100. Bingol B, Wang CF, Arnott D, Cheng D, Peng J, et al. (2010) Autophosphorylated CaMKIIalpha acts as a scaffold to recruit proteasomes to dendritic spines. *Cell* 140: 567-578.
101. Shen H, Korutla L, Champtiaux N, Toda S, LaLumiere R, et al. (2007) NAC1 regulates the recruitment of the proteasome complex into dendritic spines. *J Neurosci* 27: 8903-8913.

102. Cartier AE, Djakovic SN, Salehi A, Wilson SM, Masliah E, et al. (2009) Regulation of synaptic structure by ubiquitin C-terminal hydrolase L1. *J Neurosci* 29: 7857-7868.
103. Chen H, Polo S, Di Fiore PP, De Camilli PV (2003) Rapid Ca²⁺-dependent decrease of protein ubiquitination at synapses. *Proc Natl Acad Sci U S A* 100: 14908-14913.
104. DiAntonio A, Hicke L (2004) Ubiquitin-dependent regulation of the synapse. *Annu Rev Neurosci* 27: 223-246.
105. Hegde AN (2004) Ubiquitin-proteasome-mediated local protein degradation and synaptic plasticity. *Prog Neurobiol* 73: 311-357.
106. Yi JJ, Ehlers MD (2007) Emerging roles for ubiquitin and protein degradation in neuronal function. *Pharmacol Rev* 59: 14-39.
107. Speese SD, Trotta N, Rodesch CK, Aravamudan B, Broadie K (2003) The ubiquitin proteasome system acutely regulates presynaptic protein turnover and synaptic efficacy. *Curr Biol* 13: 899-910.
108. Haas KF, Miller SL, Friedman DB, Broadie K (2007) The ubiquitin-proteasome system postsynaptically regulates glutamatergic synaptic function. *Mol Cell Neurosci* 35: 64-75.
109. Pak DT, Sheng M (2003) Targeted protein degradation and synapse remodeling by an inducible protein kinase. *Science* 302: 1368-1373.
110. Guo L, Wang Y (2007) Glutamate stimulates glutamate receptor interacting protein 1 degradation by ubiquitin-proteasome system to regulate surface expression of GluR2. *Neuroscience* 145: 100-109.
111. Glickman MH, Raveh D (2005) Proteasome plasticity. *FEBS Lett* 579: 3214-3223.
112. Zhang F, Paterson AJ, Huang P, Wang K, Kudlow JE (2007) Metabolic control of proteasome function. *Physiology (Bethesda)* 22: 373-379.

113. Gilon T, Chomsky O, Kulka RG (1998) Degradation signals for ubiquitin system proteolysis in *Saccharomyces cerevisiae*. *Embo J* 17: 2759-2766.
114. Bence NF, Bennett EJ, Kopito RR (2005) Application and Analysis of the GFP(u) Family of Ubiquitin-Proteasome System Reporters. *Methods Enzymol* 399: 481-490.
115. Patterson GH, Lippincott-Schwartz J (2002) A photoactivatable GFP for selective photolabeling of proteins and cells. *Science* 297: 1873-1877.
116. Shaner NC, Campbell RE, Steinbach PA, Giepmans BN, Palmer AE, et al. (2004) Improved monomeric red, orange and yellow fluorescent proteins derived from *Discosoma* sp. red fluorescent protein. *Nat Biotechnol* 22: 1567-1572.
117. Murakami Y, Matsufuji S, Kameji T, Hayashi S, Igarashi K, et al. (1992) Ornithine decarboxylase is degraded by the 26S proteasome without ubiquitination. *Nature* 360: 597-599.
118. Hoyt MA, Zhang M, Coffino P (2003) Ubiquitin-independent mechanisms of mouse ornithine decarboxylase degradation are conserved between mammalian and fungal cells. *J Biol Chem* 278: 12135-12143.
119. Hoyt MA, Zhang M, Coffino P (2005) Probing the ubiquitin/proteasome system with ornithine decarboxylase, a ubiquitin-independent substrate. *Methods Enzymol* 398: 399-413.
120. Li X, Zhao X, Fang Y, Jiang X, Duong T, et al. (1998) Generation of destabilized green fluorescent protein as a transcription reporter. *J Biol Chem* 273: 34970-34975.
121. Sutton MA, Wall NR, Aakalu GN, Schuman EM (2004) Regulation of dendritic protein synthesis by miniature synaptic events. *Science* 304: 1979-1983.
122. Blackstone C, Sheng M (2002) Postsynaptic calcium signaling microdomains in neurons. *Front Biosci* 7: d872-885.

123. Cavazzini M, Bliss T, Emptage N (2005) Ca²⁺ and synaptic plasticity. *Cell Calcium* 38: 355-367.
124. Kennedy MB, Beale HC, Carlisle HJ, Washburn LR (2005) Integration of biochemical signalling in spines. *Nat Rev Neurosci* 6: 423-434.
125. Emptage N, Bliss TV, Fine A (1999) Single synaptic events evoke NMDA receptor-mediated release of calcium from internal stores in hippocampal dendritic spines. *Neuron* 22: 115-124.
126. Yuste R, Majewska A, Cash SS, Denk W (1999) Mechanisms of calcium influx into hippocampal spines: heterogeneity among spines, coincidence detection by NMDA receptors, and optical quantal analysis. *J Neurosci* 19: 1976-1987.
127. Mayford M (2007) Protein kinase signaling in synaptic plasticity and memory. *Curr Opin Neurobiol* 17: 313-317.
128. Wayman GA, Lee YS, Tokumitsu H, Silva A, Soderling TR (2008) Calmodulin-kinases: modulators of neuronal development and plasticity. *Neuron* 59: 914-931.
129. Ishida A, Kameshita I, Okuno S, Kitani T, Fujisawa H (1995) A novel highly specific and potent inhibitor of calmodulin-dependent protein kinase II. *Biochem Biophys Res Commun* 212: 806-812.
130. Fong YL, Taylor WL, Means AR, Soderling TR (1989) Studies of the regulatory mechanism of Ca²⁺/calmodulin-dependent protein kinase II. Mutation of threonine 286 to alanine and aspartate. *J Biol Chem* 264: 16759-16763.
131. Waldmann R, Hanson PI, Schulman H (1990) Multifunctional Ca²⁺/calmodulin-dependent protein kinase made Ca²⁺ independent for functional studies. *Biochemistry* 29: 1679-1684.
132. Ludemann R, Lerea KM, Etlinger JD (1993) Copurification of casein kinase II with 20 S proteasomes and phosphorylation of a 30-kDa proteasome subunit. *J Biol Chem* 268: 17413-17417.

133. Thompson D, Hakala K, Demartino GN (2009) Subcomplexes of PA700, the 19S regulator of the 26S proteasome, reveal relative roles of AAA subunits in 26S proteasome assembly, activation, and ATPase activity. *J Biol Chem*.
134. Hendil KB, Kristensen P, Uerkvitz W (1995) Human proteasomes analysed with monoclonal antibodies. *Biochem J* 305 (Pt 1): 245-252.
135. Marshall J, Dolan BM, Garcia EP, Sathe S, Tang X, et al. (2003) Calcium channel and NMDA receptor activities differentially regulate nuclear C/EBPbeta levels to control neuronal survival. *Neuron* 39: 625-639.
136. Lerea LS, Butler LS, McNamara JO (1992) NMDA and non-NMDA receptor-mediated increase of c-fos mRNA in dentate gyrus neurons involves calcium influx via different routes. *J Neurosci* 12: 2973-2981.
137. Realini C, Rechsteiner M (1995) A proteasome activator subunit binds calcium. *J Biol Chem* 270: 29664-29667.
138. Santella L, Ercolano E, Nusco GA (2005) The cell cycle: a new entry in the field of Ca²⁺ signaling. *Cell Mol Life Sci* 62: 2405-2413.
139. Santella L, Kyojuka K, De Riso L, Carafoli E (1998) Calcium, protease action, and the regulation of the cell cycle. *Cell Calcium* 23: 123-130.
140. Aizawa H, Kawahara H, Tanaka K, Yokosawa H (1996) Activation of the proteasome during *Xenopus* egg activation implies a link between proteasome activation and intracellular calcium release. *Biochem Biophys Res Commun* 218: 224-228.
141. Kemp BE, Pearson RB (1990) Protein kinase recognition sequence motifs. *Trends Biochem Sci* 15: 342-346.
142. Makhinson M, Chotiner JK, Watson JB, O'Dell TJ (1999) Adenylyl cyclase activation modulates activity-dependent changes in synaptic strength and Ca²⁺/calmodulin-dependent kinase II autophosphorylation. *J Neurosci* 19: 2500-2510.

143. Valverde RH, Tortelote GG, Lemos T, Mintz E, Vieyra A (2005) Ca²⁺/calmodulin-dependent protein kinase II is an essential mediator in the coordinated regulation of electrocyte Ca²⁺-ATPase by calmodulin and protein kinase A. *J Biol Chem* 280: 30611-30618.
144. Gillette TG, Kumar B, Thompson D, Slaughter CA, DeMartino GN (2008) Differential roles of the COOH termini of AAA subunits of PA700 (19 S regulator) in asymmetric assembly and activation of the 26 S proteasome. *J Biol Chem* 283: 31813-31822.
145. Ferrell K, Wilkinson CR, Dubiel W, Gordon C (2000) Regulatory subunit interactions of the 26S proteasome, a complex problem. *Trends Biochem Sci* 25: 83-88.
146. Rose J, Jin SX, Craig AM (2009) Heterosynaptic molecular dynamics: locally induced propagating synaptic accumulation of CaM kinase II. *Neuron* 61: 351-358.
147. Lee SJ, Escobedo-Lozoya Y, Szatmari EM, Yasuda R (2009) Activation of CaMKII in single dendritic spines during long-term potentiation. *Nature* 458: 299-304.
148. Dong C, Upadhya SC, Ding L, Smith TK, Hegde AN (2008) Proteasome inhibition enhances the induction and impairs the maintenance of late-phase long-term potentiation. *Learn Mem* 15: 335-347.
149. Artinian J, McGauran AM, De Jaeger X, Mouldous L, Frances B, et al. (2008) Protein degradation, as with protein synthesis, is required during not only long-term spatial memory consolidation but also reconsolidation. *Eur J Neurosci* 27: 3009-3019.
150. Bezprozvanny I, Mattson MP (2008) Neuronal calcium mishandling and the pathogenesis of Alzheimer's disease. *Trends Neurosci* 31: 454-463.
151. Kisselev AF, Goldberg AL (2005) Monitoring activity and inhibition of 26S proteasomes with fluorogenic peptide substrates. *Methods Enzymol* 398: 364-378.

152. Scholz WK, Palfrey HC (1991) Glutamate-stimulated protein phosphorylation in cultured hippocampal pyramidal neurons. *J Neurosci* 11: 2422-2432.
153. Ma CP, Slaughter CA, DeMartino GN (1992) Identification, purification, and characterization of a protein activator (PA28) of the 20 S proteasome (macropain). *J Biol Chem* 267: 10515-10523.
154. Liu CW, Li X, Thompson D, Wooding K, Chang TL, et al. (2006) ATP binding and ATP hydrolysis play distinct roles in the function of 26S proteasome. *Mol Cell* 24: 39-50.
155. DeMartino GN, Moomaw CR, Zagnitko OP, Proske RJ, Chu-Ping M, et al. (1994) PA700, an ATP-dependent activator of the 20 S proteasome, is an ATPase containing multiple members of a nucleotide-binding protein family. *J Biol Chem* 269: 20878-20884.
156. Djakovic SN, Schwarz LA, Barylko B, DeMartino GN, Patrick GN (2009) Regulation of the proteasome by neuronal activity and calcium/calmodulin-dependent protein kinase II. *J Biol Chem* 284: 26655-26665.
157. Zhang F, Wu Z, Zhang P, Tian G, Finley D, et al. (2009) Mechanism of substrate unfolding and translocation by the regulatory particle of the proteasome from *Methanocaldococcus jannaschii*. *Mol Cell* 34: 485-496.
158. Zhang F, Hu M, Tian G, Zhang P, Finley D, et al. (2009) Structural insights into the regulatory particle of the proteasome from *Methanocaldococcus jannaschii*. *Mol Cell* 34: 473-484.
159. Obenauer JC, Cantley LC, Yaffe MB (2003) Scansite 2.0: Proteome-wide prediction of cell signaling interactions using short sequence motifs. *Nucleic Acids Res* 31: 3635-3641.
160. Allison DW, Gelfand VI, Spector I, Craig AM (1998) Role of actin in anchoring postsynaptic receptors in cultured hippocampal neurons: differential attachment of NMDA versus AMPA receptors. *J Neurosci* 18: 2423-2436.

161. Turrigiano GG, Leslie KR, Desai NS, Rutherford LC, Nelson SB (1998) Activity-dependent scaling of quantal amplitude in neocortical neurons. *Nature* 391: 892-896.
162. Hung AY, Sung CC, Brito IL, Sheng M (2010) Degradation of postsynaptic scaffold GKAP and regulation of dendritic spine morphology by the TRIM3 ubiquitin ligase in rat hippocampal neurons. *PLoS One* 5: e9842.
163. Shen K, Meyer T (1999) Dynamic control of CaMKII translocation and localization in hippocampal neurons by NMDA receptor stimulation. *Science* 284: 162-166.
164. DiAntonio A (2010) Nedd4 branches out. *Neuron* 65: 293-294.
165. Fulga TA, Van Vactor D (2008) Synapses and growth cones on two sides of a highwire. *Neuron* 57: 339-344.
166. Yamauchi T (2002) Molecular constituents and phosphorylation-dependent regulation of the post-synaptic density. *Mass Spectrom Rev* 21: 266-286.
167. Cao X, Wang H, Mei B, An S, Yin L, et al. (2008) Inducible and selective erasure of memories in the mouse brain via chemical-genetic manipulation. *Neuron* 60: 353-366.
168. Xie CW (2004) Calcium-regulated signaling pathways: role in amyloid beta-induced synaptic dysfunction. *Neuromolecular Med* 6: 53-64.
169. Snyder EM, Nong Y, Almeida CG, Paul S, Moran T, et al. (2005) Regulation of NMDA receptor trafficking by amyloid-beta. *Nat Neurosci* 8: 1051-1058.
170. Knobloch M, Farinelli M, Konietzko U, Nitsch RM, Mansuy IM (2007) Abeta oligomer-mediated long-term potentiation impairment involves protein phosphatase 1-dependent mechanisms. *J Neurosci* 27: 7648-7653.
171. Zhao D, Watson JB, Xie CW (2004) Amyloid beta prevents activation of calcium/calmodulin-dependent protein kinase II and AMPA receptor

phosphorylation during hippocampal long-term potentiation. *J Neurophysiol* 92: 2853-2858.

172. Townsend M, Mehta T, Selkoe DJ (2007) Soluble A β inhibits specific signal transduction cascades common to the insulin receptor pathway. *J Biol Chem* 282: 33305-33312.
173. Gu Z, Liu W, Yan Z (2009) β -Amyloid impairs AMPA receptor trafficking and function by reducing Ca²⁺/calmodulin-dependent protein kinase II synaptic distribution. *J Biol Chem* 284: 10639-10649.
174. Leroy E, Boyer R, Auburger G, Leube B, Ulm G, et al. (1998) The ubiquitin pathway in Parkinson's disease. *Nature* 395: 451-452.
175. Wilkinson KD, Lee KM, Deshpande S, Duerksen-Hughes P, Boss JM, et al. (1989) The neuron-specific protein PGP 9.5 is a ubiquitin carboxyl-terminal hydrolase. *Science* 246: 670-673.
176. Finley D, Bartel B, Varshavsky A (1989) The tails of ubiquitin precursors are ribosomal proteins whose fusion to ubiquitin facilitates ribosome biogenesis. *Nature* 338: 394-401.